Université catholique de Louvain

Faculté des Sciences

Institut des Sciences de la Vie

Evolution of peroxiredoxin 5 mitochondrial targeting in mammals: molecular mechanism and functional consequences

Thèse présentée par Valérie Van der Eecken en vue de l'obtention du grade de docteur en sciences

Promoteur	Pr. Bernard Knoops
Membres du Jury	Pr. Thierry Arnould
	Pr. Marc Boutry
	Pr. Laurence Drouard
	Pr. René Rezsöhazy
Président du Jury	Pr. Claude Remacle

Novembre 2012

Au sens strict, ce manuscrit est le rapport précis d'un travail expérimental mené au sein d'un laboratoire. Il est également le dernier paragraphe d'une page qui se tourne. Si, dans ce cas-ci, l'écriture de la page a nécessité beaucoup de temps, cette page est néanmoins telle que je souhaitais qu'elle soit écrite : en deux colonnes. En effet, ces nombreuses années m'auront permis d'expérimenter l'aventure d'une thèse tout en ayant la chance d'enseigner. Alors que je m'apprête à réaliser un saut de page en chapitre inconnu, je souhaite terminer la page en cours en remerciant toutes les personnes qui ont contribué, de près ou de loin, à l'écriture de ces deux colonnes.

Je voudrais remercier en tout premier lieu mon promoteur de thèse, le professeur Bernard Knoops. Merci à toi Bernard pour m'avoir accueillie dans ton laboratoire. Merci pour ton encadrement, pour tes corrections (rapides !) et pour ton soutien durant toutes ces années. Travailler pour toi a toujours été très agréable !

Je remercie également le professeur Paul P. Van Veldhoven pour m'avoir permis de réaliser les fractionnements subcellulaires dans son laboratoire. Merci également à toutes les personnes qui m'ont aidée lors de la collecte d'échantillons de mammifères – et ils sont nombreux : Professeur R.K. Wayne pour l'ADN de loup à crinière et de renard gris, Professeur M.A.G. Van Der Heyden pour le tissu d'ours, Docteur J.C. Bertho pour le sang de loup, Professeur E. Le Boulengé pour le tissu de chien viverrin, Caroline Louis pour le sang de phoque et (mon) Bernard pour m'avoir accompagnée dans l'improbable chasse au renard sous la neige.

Mes remerciements vont également à Sophie et Dorothée. Votre travail aura apporté à ce projet une valeur inestimable. Vous encadrer a été un réel plaisir et m'a appris énormément.

Je remercie également tous les membres de mon jury pour le temps qu'ils ont consacré à la lecture de ce manuscrit et pour leurs remarques constructives qui m'ont permis de l'améliorer.

Le travail au labo n'aurait certainement pas été aussi agréable sans la présence de tous les Banissiens en blouse blanche. Merci à tous pour l'ambiance bon enfant qui a toujours régné sur le plateau. Julie, merci pour ton optimisme, ton sourire permanent et nos interminables discussions. Oksana, merci pour ton enthousiasme et ton étonnement perpétuel face aux expressions de la langue française. Un énorme merci à toi, André, de m'avoir encadrée lors de mon mémoire, de m'avoir aidée pour les clonages, ainsi que pour tes « clownages » qui m'auront toujours bien fait rire. Merci à Geoffroy d'avoir instauré une ambiance Tanuki – toujours une bonne raison de boire un verre, même si on ne la connait pas encore – au labo. Merci à Marc pour sa bonne humeur, son humour et ses coups de pouce bien utiles en Anglais. Je remercie également tous les anciens collègues : Elé, Dom, Stephanie et Cécile pour leurs précieux conseils en début de thèse et pour les sympathiques discussions dans le labo. Merci à toi Véro, pour ton écoute ainsi que pour toutes les choses que tu fais et qui nous facilitent la vie.

Puis, je voudrais remercier les personnes qui auront contribué à l'écriture de la seconde colonne, celle de l'assistanat. A tous les étudiants – les adorables BAC1, les BIR12 blagueurs et les BIOL13 travailleurs et intéressés – un énorme merci ! Vous enseigner la biologie a été un vrai plaisir. Un énorme merci à l'ensemble de l'équipe des « Invertépotes » – professeurs et assistants. A toi, Elé, avec qui j'ai passé des heures en salle de TP, merci pour les aventures extraordinaires que nous avons vécues ensemble. Merci à vous, Oksana et Delphine. Les dissections de moules, criquets, écrevisses et buccins ont été des moments incroyables, chaque année. Merci à vous, Marie-Thérèse, Daniel et Willy pour votre précieuse aide lors de l'organisation des TPs. Merci pour votre amabilité et votre bonne humeur que j'ai particulièrement appréciées et qui me manqueront très certainement. Merci également à tous les autres assistants de l'Ecole de Biologie pour leur dynamisme et pour la bonne entente qui règne au sein de l'équipe.

Je voudrais également remercier toutes les personnes extérieures au labo qui auront été essentielles durant ces nombreuses années. A mes amis, ma famille, ma belle-famille, qui m'ont soutenue tout au long de la thèse. Papa, Maman, merci de m'avoir toujours portée dans mes choix, d'avoir été à l'écoute à chaque moment de doute. Enfin, à toi Bernard. Merci pour ta présence, ton humour, ton soutien. Ta façon de voir la vie la rend si belle et si simple. Merci également au petit Guillaume qui m'a accompagnée en fin de rédaction et dont le sourire illumine désormais notre vie.

Contents

Summary

To scavenge reactive oxygen species and reactive nitrogen species, the mitochondrial matrix is equipped with antioxidant enzymes, amongst which peroxiredoxin 5 (PRDX5). Mitochondrial localization of this thiol-specific peroxidase results from the presence of an N-terminal mitochondrial targeting sequence (MTS). Human PRDX5 subcellular distribution is not restricted to mitochondria, as it is also found in the cytosol, the peroxisomes, and in a lesser extent, the nucleus. In human, PRDX5 subcellular targeting is dependent on the use of multiple alternative transcription start sites and two alternative in-frame translation initiation sites, which determine whether or not the region encoding the MTS is translated.

This work focuses on the interspecific variability of PRDX5 MTS in mammals. We found that, although mitochondrial PRDX5 is conserved in various vertebrate and invertebrate species, PRDX5 mitochondrial targeting has been lost in domestic pig and extant canids. Genomic sequence analyses revealed that the molecular mechanism underlying the abolition of PRDX5 MTS during canid evolution involves a mutation in the first PRDX5 translation initiation codon as well as the appearance of a STOP codon. Moreover, using domestic pig liver mitochondrial extracts, we show that the loss of mitochondrial PRDX5 correlates with high expressions of PRDX3 and glutathione peroxidase 4, suggesting the existence of compensatory mechanisms. However, our results indicate that higher expression of these other mitochondrial peroxidases is not sufficient to maintain high alkyl hydroperoxide reduction rates in pig liver mitochondrial extracts. Therefore, although PRDX5 appears to be dispensable in some mammalian species, we

cannot exclude that the abolition of mitochondrial PRDX5 results in a certain weakness at the cellular level under specific oxidative stress conditions. Finally, the functional consequences of the restoration of mitochondrial PRDX5 in Madin-Darby canine kidney (MDCK) cells were investigated. Unexpectedly, we show that the restoration of mitochondrial PRDX5 in MDCK cells provoked deleterious effects in cells exposed to acute oxidative stress conditions. Therefore, we propose that, although PRDX5 cytoprotective function is clearly demonstrated in human and rodents by several studies, the conservation of the mitochondrial isoform would not necessarily be an advantage in all mammalian species.

Abbreviations

AGT	alanine:glyoxylate aminotransferase
*Am*PRDX5	*Arenicola marina* peroxiredoxin 5
APP	aminopeptidase P
CHO	Chinese hamster ovary
Chr	chromosome
Cp	peroxidatic cysteine
Cr	resolving cysteine
DAPI	4′-6-diamidino-2-phenylindole
DTT	dithiothreitol
GFP	green fluorescent protein
GPX	glutathione peroxidase
GR	glutathione reductase
GRX	glutaredoxin
GSH	reduced glutathione
GSSG	oxidized glutathione
Hsp	heat shock protein
*Hs*PRDX5	*Homo sapiens* peroxiredoxin 5
Icp55	intermediate cleaving peptidase 55
JNK	c-*jun* N-terminal kinase
LDH	lactate dehydrogenase
l-GPX4	long form of glutathione peroxidase 4
L-PRDX5	long form of peroxiredoxin 5
LPS	lipopolysaccharide
MDCK	Madin-Darby canine kidney
MIP	mitochondrial intermediate peptidase
Mn-SOD	manganese superoxide dismutase
MPP	mitochondrial processing peptidase
MtHsp70	mitochondrial heat shock protein 70
MTS	mitochondrial targeting sequence
Mya	million years ago
NLS	nuclear localization signal
NOX	NADPH oxidase
NF-κB	nuclear factor-kappa B
Nrf2	transcription factor NF-E2-related factor

PAM	presequence-translocase associated motor
PDGF	platelet-derived growth factor
PDI	protein disulfide isomerase
PEX5	peroxin 5
PRDX	peroxiredoxin
PTS	peroxisomal targeting signal
RNS	reactive nitrogen species
ROOH	alkyl hydroperoxide
ROS	reactive oxygen species
Sec	selenocysteine
s-GPX4	short form of glutathione peroxidase 4
SNP	single nucleotide polymorphism
SOD	superoxide dismutase
S-PRDX5	short form of peroxiredoxin 5
Srx	sulfiredoxin
*Ss*PRDX5	*Sus scrofa* peroxiredoxin 5
t-BHP	*tert*-butyl hydroperoxide
TIM	translocase of the inner mitochondrial membrane
TNF- α	tumor necrosis factor-α
TOM	translocase of the outer mitochondrial membrane
TXN	thioredoxin
TXNRD	thioredoxin reductase
UTR	untranslated region

I. General introduction

1. Background

DIOXYGEN is essential to aerobic organism survival but is also inherently dangerous. This molecule is vital because its complete reduction to water during respiration results in ATP production, the main energy source for aerobic cells. In contrast, the dangerous property of dioxygen is due to the presence of two unpaired electrons with parallel spin configurations. Therefore, dioxygen cannot accept more than one electron at a time, generating highly reactive intermediate molecules. These reactive oxygen species (ROS) include both the non-radical oxygen derivates, such as hydrogen peroxide (H_2O_2), and the free radical oxygen derivates, i.e. containing one or more unpaired electrons, like the superoxide radical ($O_2^{\bullet -}$) and the hydroxyl radical ($OH^{\bullet}$). Free radical oxygen derivates can further react with nitric oxide ($NO^{\bullet}$), thereby producing various reactive nitrogen species (RNS) such as peroxynitrite ($ONOO^-$) (Halliwell and Gutteridge 2007).

ROS and RNS are continually generated from various endogenous and exogenous sources. An important endogenous ROS production site is the mitochondrial electron transport chain. Indeed, about 1 to 2% of the oxygen consumed by mitochondria during respiration is incompletely reduced (Halliwell and Gutteridge 2007). Also, ROS and RNS are produced by various enzymes including NADPH oxidases (NOXs), xanthine oxidase, Acyl-CoA oxidase and nitric oxide synthases (Halliwell and Gutteridge 2007; Angermuller et al. 2009). Moreover, ROS are produced in the endoplasmic reticulum during the process of protein folding and disulfide bond formation (Sevier and Kaiser 2008). External ROS and RNS sources are multiple and include ionizing radiations, ultraviolet radiation, cigarette smoke and the metabolism of drugs and xenobiotics (Halliwell and Gutteridge 2007).

Due to their high reactivity, excessive ROS and RNS concentrations can be harmful for the cells. Indeed, they are prone to oxidize and damage proteins, DNA and lipids. The importance of these damages can influence cell viability and trigger cell death (Halliwell and Gutteridge 2007). However, although ROS and RNS have been traditionally considered as toxic by-products of metabolism, these molecules exhibit also physiological beneficial functions. Indeed, ROS play a role in host defence systems, since plasma membrane oxidases in phagocytes generate free radicals to destroy invading pathogenic microorganisms (Nauseef 2007). In addition, it is clear now that low to moderate levels of ROS and RNS, especially hydrogen peroxide, are involved in cell signalling. For example, hydrogen peroxide is produced in response to various extracellular stimuli and mediates regulation of functions like cell growth, cell differentiation and gene expression through oxidation of cysteine residues from key signalling proteins like tyrosine kinases and phosphatases (Rhee 2006; Valko et al. 2007; Halliwell and Gutteridge 2007; Forman et al. 2010). Because of this dual role of ROS and RNS, one can easily understand the necessity to finely regulate their intracellular concentration. An imbalance between ROS/RNS production and removal leading to cellular damages is referred to as oxidative/nitrosative stress. Oxidative and nitrosative stresses are linked to aging and several human diseases, like cancer and cardiovascular, inflammatory and neurodegenerative diseases (Halliwell and Gutteridge 2007).

To regulate ROS and RNS intracellular levels, cells have developed enzymatic and non-enzymatic antioxidant systems. An antioxidant is defined as "a substance that delays, prevents or removes oxidative damages from a target molecule". Non-enzymatic defence systems include glutathione (GSH), metallothioneins, ascorbic acid, coenzyme Q or melatonin. Enzymatic antioxidant systems depend on the action of

superoxide dismutates (SODs), catalase, glutathione peroxidases (GPXs) and peroxiredoxins (PRDXs) (Halliwell and Gutteridge 2007).

This work is focused on mitochondrial targeting of PRDX5, the last mammalian PRDX member that has been discovered. Therefore, the following sections introduce the PRDX family, with emphasis on PRDX5. The mechanism of protein import into the mitochondrial matrix is also developed in this introduction. Finally, as this work highlights unusual features of pig and dog PRDX5 subcellular localization, the last section of this introduction is dedicated to these two species and their phylogenetic position within placental mammals.

2. Peroxiredoxins

In 1988, the first eukaryotic member of the PRDX superfamily was discovered as a 27-kDa protein in the yeast *Saccharomyces cerevisiae* (Kim et al. 1988). This enzyme, named thiol-specific antioxidant protein (TSA), was shown to protect against oxidation in a thiol-containing system. Since then, numerous PRDX members have been identified in many organisms, defining a superfamily which is highly conserved throughout evolution and represented in all kingdoms of life (Knoops et al. 2007). It appeared that PRDXs are highly expressed in virtually all living species. They are among the most abundant proteins in *Escherichia coli* and represent 0.1 to 0.8 % of total soluble proteins in mammalian cells (Link et al. 1997; Chae et al. 1999; Seo et al. 2000). The peroxiredoxin superfamily includes three isoforms in the bacterium *Escherichia coli*, five in the yeast *Saccharomyces cerevisiae*, nine in the plant *Arabidopsis thaliana* and six in mammals (Knoops et al. 2007).

PRDXs show no significant sequence homology with catalase, SODs or selenocysteine-containing GPXs. Their catalytic mechanism does not require any redox cofactors such as heme, flavin or metal ions (Knoops et al. 2007). PRDXs are thiol-dependent enzymes that reduce hydrogen peroxide, alkyl hydroperoxides and, for some of them, peroxynitrite with high catalytic rates (~10^7 $M^{-1}s^{-1}$) (Poole 2007). They use thioredoxins (TXNs or TRXs), sometimes glutaredoxins (GRXs) or cyclophilins as electron donors (see below).

2.1. Catalytic mechanism and classification of PRDXs

All PRDXs share a conserved and catalytically essential cysteine residue in their N-terminal domain, referred to as the peroxidatic cysteine (Cp). Peroxide reduction by PRDXs involves the three following steps: the peroxidation, resolution and recycling steps (Fig. 2.1). The peroxidation step is common to all PRDXs. In this reaction, the Cp attacks the oxygen atom of

the peroxide to form a cysteine sulfenic acid (Cp-SOH) and breaks the O—O bond of the peroxide. Once the O—O bond is broken, the hydroxide/alkoxide leaving group is protonated by a catalytic acid (which is presumed to be a water molecule), releasing the corresponding alcohol or a water molecule (Hall et al. 2010).

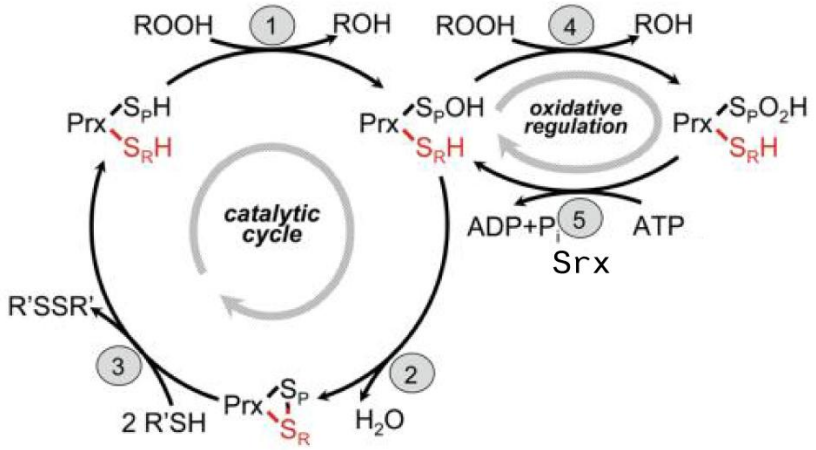

Fig. 2.1. Catalytic cycle of PRDXs (or Prxs in this scheme). Peroxide reduction involves a peroxidation step (1), a resolution step (2) and a recycling step (3). Sp and Sr (red) designate the sulphur atoms of the Cp and the Cr respectively. PRDXs can be inactivated by hyperoxidation (4). For several PRDXs, the sulfinic inactivated form (-O_2H) can be reduced by sulfiredoxin (Srx) in an ATP-dependent manner (5) [Adapted from Hall et al. (2009)].

The resolution (second step) consists in the reduction of the cysteine sulfenic acid (Cp-SOH). According to the resolution mechanism and the number of cysteine residues involved in catalysis, PRDXs are classified into three subfamilies (Fig. 2.2) (Wood et al. 2003; Hall et al. 2011):

i) **Typical 2-Cys PRDXs** contain a second cysteine residue in the C-terminal domain (Cr, resolving cysteine). The Cr from one unit attacks the Cp-SOH from a second subunit, yielding a stable intermolecular disulfide bridge. During the recycling step (step 3), the disulfide bridge is reduced by a thiol-dependent reductant. Mammalian typical 2-Cys PRDXs use TXN as reductant. Oxidized TXN is finally reduced by thioredoxin reductase (TXNRD) and NADPH is the final electron donor (Wood et al. 2003). Other enzymes were reported to be able to reduce typical 2-Cys PRDXs such as GRXs or cyclophilin A (Lee et al. 2001; Hanschmann et al. 2010). In mammals, four typical 2-Cys PRDXs exist (PRDX1-4).

ii) **Atypical 2-Cys PRDXs** function according to the same catalytic mechanism but are functionally monomeric. The Cr is located in the same polypeptide chain and the reaction with the Cp yields an intramolecular disulfide bond. In mammals, PRDX5 is the only atypical 2-Cys PRDX and uses TXN or cyclophilin A as electron donor (Seo et al. 2000; Lee et al. 2001).

iii) **1-Cys PRDXs** contain only the Cp. The Cp-SOH is reduced by an external thiol. PRDX6 is the unique member of the mammalian 1-Cys PRDXs subfamily. It uses GSH in the presence of glutathione S-transferase π as electron donor (Manevich et al. 2004; Ralat et al. 2006; Ralat et al. 2008). Also, ascorbate was reported to be a potential candidate to reduce mammalian PRDX6 (Monteiro et al. 2007; Fisher 2011).

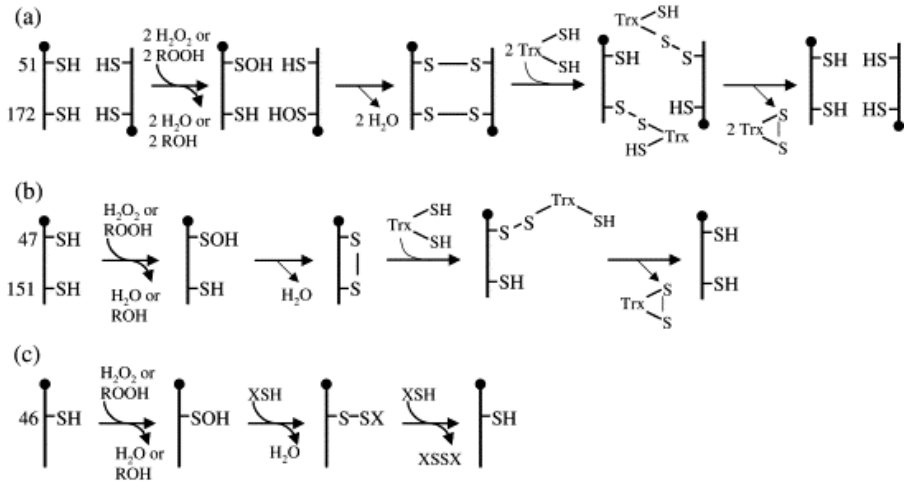

Fig. 2.2. Mechanisms of peroxidase reaction for (a) typical 2-Cys PRDXs, (b) atypical 2-Cys PRDXs and (c) 1-Cys PRDXs. The reduction of hydrogen peroxide (H_2O_2) or alkyl hydroperoxides (ROOH) to water or to the corresponding alcohol results in the oxidation of the peroxidatic cysteine into a sulfenic acid (-SOH). This leads to the formation of an intermolecular disulfide bond in typical 2-Cys PRDXs and an intramolecular disulfide bond in atypical 2-Cys PRDXs. Oxidized PRDXs are subsequently reduced by thiol-containing electron donors. The amino acid numbering refers to human proteins [From Leyens et al. (2003)].

In addition to this three-step catalytic mechanism, the Cp-OH can react with additional peroxides to form sulfinic acid (Cp-O_2H; Fig. 2.1) or, in some cases sulfonic acid (Cp-O_3H). Hyperoxidized Cp cannot react with the Cr to form the disulfide bridge. Consequently, the resolution step cannot occur and the enzyme remains inactive. The Cp-O_2H, but not the Cp-O_3H, can nevertheless be reduced in an ATP-dependent manner by sulfiredoxin (Srx) (Woo et al. 2003a). In this hyperoxidation-reduction cycle, the PRDX peroxidase activity is turned off reversibly. Hyperoxidation of the Cp is thought to rely on the presence of a C-terminal helix containing a conserved "YF" motif which induces a kinetic pause in disulfide bond formation. As a result, oxidative regulation occurs in some eukaryotic typical 2-Cys PRDXs, but is observed neither in prokaryotic PRDXs nor in mammalian PRDX5 (Hall et al. 2011).

2.2. PRDX functions

2.2.1. Antioxidant defence

PRDXs contribute to antioxidant defence through their ability to detoxify hydrogen peroxide, organic hydroperoxides and peroxynitrite. During their initial characterization, PRDXs were not recognized as a dominant player in cell protection against oxidative stress. Their ability to compete with the efficient heme- and selenium-containing peroxidases like catalase and GPXs was met with scepticism (Hofmann et al. 2002). Consequently, the protective antioxidant function of PRDXs was thought to be predominant only in prokaryotes, which often lack the heme- and selenoperoxidases. However, since then, kinetic and abundance data predicted that PRDXs would play an important role in peroxide detoxification, even in eukaryotic cells. According to these data, PRDXs would be responsible for the reduction of the major part of the mitochondrial and cytoplasmic hydrogen peroxide (Cox et al. 2010). It is also interesting to note that the ability of some PRDXs to decompose peroxynitrite with high efficiency could confer to this family a more specific function in antioxidant defence (Dubuisson et al. 2004; Trujillo et al. 2007). Finally, it was recently suggested that, in addition to their ability to reduce hydrogen peroxide, organic hydroperoxides and peroxynitrite, PRDX2 and PRDX3 could participate to detoxification of amino acid, peptide and protein hydroperoxides (Peskin et al. 2010). This novel substrate specifity would confer to the PRDXs a possible function in prevention of the accumulation of these reactive species which can provoke secondary damages to other targets.

2.2.2. Role of hyperoxidized typical 2-Cys-PRDX

It is now generally accepted that, in addition to their role in antioxidant defence systems, typical 2-Cys PRDXs are key actors in hydrogen peroxide-mediated cell signalling. This role emerged with the discovery of the

regulation of PRDXs through their hyperoxidation, leading to the reversible inactivation of their peroxidase activity (see before and Fig. 2.1). The mechanism by which hyperoxidation of typical 2-Cys PRDXs acts in cell signalling is still unclear. The floodgate model (Fig. 2.3), which is still speculative, predicts that, at low hydrogen peroxide concentrations, PRDXs exert their peroxidase activity, acting as a barrier. When a local peroxide burst occurs, the peroxidatic activity is switched off, allowing the hydrogen peroxide level to build up locally to concentrations leading to oxidation of specific downstream target proteins, thereby triggering signalling pathways (Hall et al. 2009; Rhee and Woo 2011).

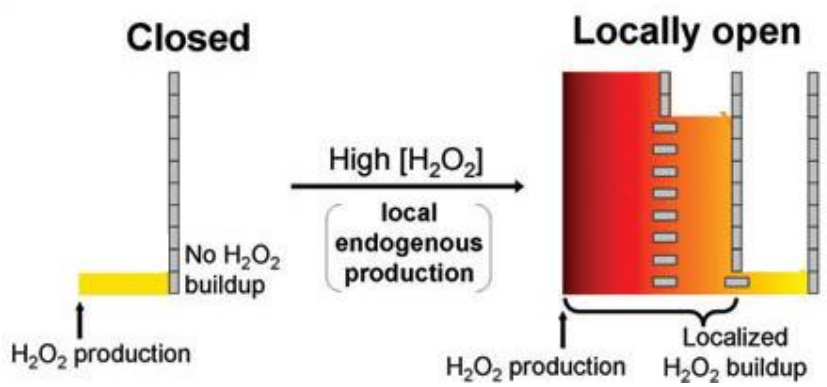

Fig. 2.3. Floodgate model. In the speculative floodgate model, active PRDXs act as a barrier at low hydrogen peroxide concentrations (represented by the vertical grey rectangles). When the peroxide level increases locally, PRDXs are inactivated (represented by the horizontal grey rectangles), allowing the hydrogen peroxide level to build up. The multiple barriers represent the cell-wide distribution of PRDXs. Only the PRDXs that are close to the hydrogen peroxide generation site are inactivated, whereas those at increasing distance remains activated. This allows the hydrogen peroxide increase to be a localized phenomenon. Hydrogen peroxide level is represented by both colour gradient and height. [Adapted from Hall et al. (2009)].

In addition to inactivating PRDX peroxidatic activity, it was shown that hyperoxidation results also in structural changes leading to gain of chaperone function (Fig. 2.4). Indeed, hyperoxidized PRDXs can form toroid decamers undergoing aggregation, allowing the formation of high molecular mass complexes exhibiting a chaperone activity. The chaperone activity of

typical 2-Cys was evidenced in several studies, as PRDXs from both yeast and humans have been demonstrated to inhibit thermal aggregation of substrates *in vitro* and to enhance heat shock resistance (Jang et al. 2004; Moon et al. 2005; Lee et al. 2007).

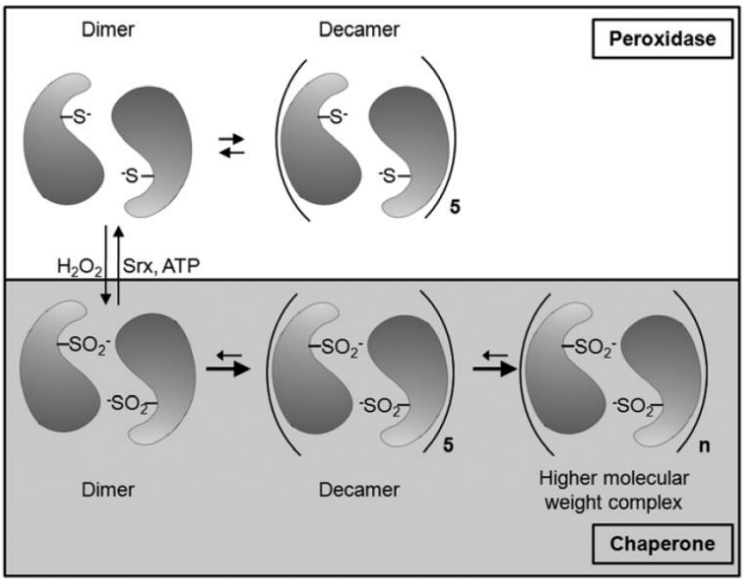

Fig. 2.4. Chaperone function of hyperoxidized PRDXs. At low hydrogen peroxide concentrations, 2-Cys PRDXs exist mostly as low molecular weight structures (dimers and decamers) that act as peroxidase and protect proteins from denaturation. Under oxidative stress conditions, 2-Cys PRDXs form high molecular weight complexes (aggregates) that exhibit much higher chaperone activity than dimers and decamers. [From Rhee and Woo (2011)].

Recently, a new role for PRDXs hyperoxidation was suggested. Indeed, using a yeast model, Day and co-workers proposed that the hyperoxidation-mediated PRDX inactivation would be important to maintain the activity of TXN, allowing this latter to act on other substrates. This would ensure the repair of oxidized proteins and cell survival during oxidative stress conditions (Day et al. 2012).

2.2.3. Other physiological functions linked to PRDX regulation mechanisms

It is interesting to note that other post-translational mechanisms in addition to hyperoxidation may regulate PRDX peroxidatic activity, and thereby may contribute to the role of PRDXs in cell signalling. Indeed, PRDXs can be redox-regulated by glutathionylation and S-nitrosylation (Sullivan et al. 2000; Fratelli et al. 2002; Fratelli et al. 2003; Fang et al. 2007; Park et al. 2009; Wu et al. 2010; Park et al. 2011). Also, acetylation and C-terminal truncation can modulate PRDX activity in a redox-independent manner (Koo et al. 2002; Sayed and Williams 2004; Parmigiani et al. 2008; Jara et al. 2008; Seo et al. 2009). Interestingly, C-terminal truncation of 2-Cys PRDXs eliminates the "YF" motif, rendering the PRDXs resistant to hyperoxidation. By this regulation mechanism, peroxidatic activity is maintained even during acute oxidative stress. Moreover, phosphorylation was also shown to inactivate the peroxidatic activity of typical 2-Cys PRDXs in a redox-independent manner, allowing transient accumulation of hydrogen peroxide for growth factor signalling. Interestingly, reversible inactivation of 2-Cys PRDXs via threonine phosphorylation appears to play a role in cell cycle progression (Chang et al. 2002; Qu et al. 2007; Rhee and Woo 2011).

2.2.4. PRDX functions linked to interactions with binding proteins and RNA

PRDXs were shown to interact with a large number of proteins. In this manner, PRDXs regulate the function of the binding partner in a redox-dependent manner or in a redox-independent manner. Accordingly, PRDXs are involved in various cellular functions such as apoptosis, differentiation, proliferation, oxidative protein folding and inflammation. An exhaustive list of PRDX binding proteins and the related functions is given in a recent review (Rhee and Woo 2011). One example is the role of PRDX4 in oxidative protein folding in the endoplasmic reticulum of mammalian cells by interaction with the protein disulfide isomerase (PDI) (Tavender et al. 2010;

Zito et al. 2010). Interestingly, in addition to their role related to interactions with binding proteins, it was recently suggested that PRDXs are implicated in RNA metabolism. Indeed, Kim and coworkers (2012) identified PRDX1 as an RNA-binding protein exhibiting RNA chaperone activity.

2.3. Subcellular localization of mammalian PRDXs

The number of PRDX isoforms increased during evolution, varying from three in bacteria to six in mammals and nine in plants. This evolution correlates with cell compartmentalization and allowed the existence of mitochondrial, nuclear, peroxisomal and chloroplast isoforms.

In mammals, PRDX1 and PRDX2 are mainly cytosolic but also nuclear (Plishker et al. 1992; Ishii et al. 1995; Iwahara et al. 1995; Kang et al. 1998; Cha et al. 2000; Oberley et al. 2001; Jin et al. 2009; Lee et al. 2011). PRDX3 is targeted to the mitochondria by its cleavable N-terminal mitochondrial targeting sequence (MTS) (Watabe et al. 1994; Araki et al. 1999; Oberley et al. 2001; Mowbray et al. 2008). PRDX4 exhibits a secretory N-terminal targeting sequence. This isoform is mainly retained in the endoplasmic reticulum but is also secreted (Tavender et al. 2008). Moreover, it was recently evidenced that an alternately transcribed PRDX4 form, lacking the secretory targeting signal, is localized in the cytosol of spermatids from postpubertal testis (Yim et al. 2011). PRDX5 possesses also a complex subcellular distribution, as it is found in the cytosol, the mitochondria, the peroxisomes and the nucleus (Yamashita et al. 1999; Kropotov et al. 1999; Knoops et al. 1999; Seo et al. 2000; Kropotov et al. 2004; Lu et al. 2006). This complex subcellular distribution is linked to the presence of an N-terminal MTS and a C-terminal peroxisomal targeting sequence (see point 3.3). Finally, PRDX6 is mainly cytosolic, but was also reported to be present in lysosomes and lamellar bodies of lung epithelial cells. Targeting to these compartments depends on ten residues near the N-

terminal region of the protein (Frank et al. 1997; Fujii et al. 2001; Wu et al. 2006; Sorokina et al. 2009; Fisher 2011; Sorokina et al. 2011).

2.4. Mammalian mitochondrial PRDXs

In mammals, PRDX3 and PRDX5 are located in the mitochondrial matrix. In this compartment, PRDX3 and PRDX5 coexist with other antioxidant enzymes, namely manganese-SOD (Box 1), GPX1 (Box 2) and GPX4 (Box 3). Together, these enzymes control ROS/RNS levels in mitochondria (Fig. 2.5).

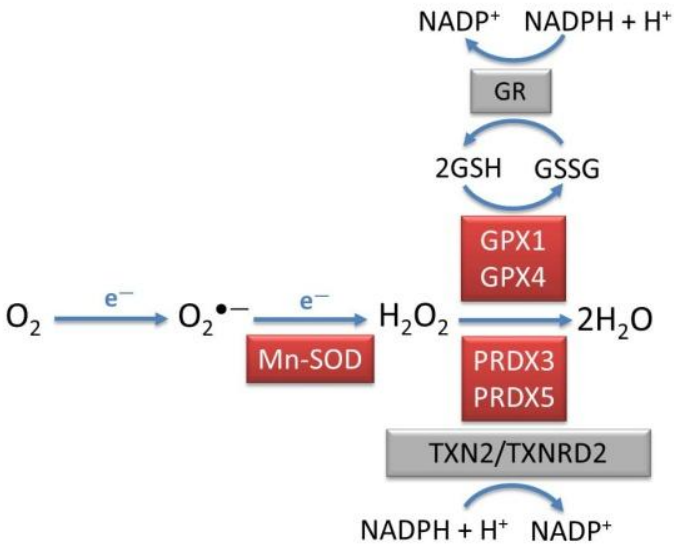

Fig. 2.5. Mitochondrial antioxidant enzymes. Manganese superoxide dismutase (Mn-SOD) is responsible for the dismutation of $O_2^{\bullet-}$ into H_2O_2. Glutathione peroxidases 1 and 4 (GPX1 and GPX4) catalyze the reduction of H_2O_2 to water, with glutathione (GSH) as electron donor. Oxidized glutathione (GSSG) is reduced by glutathione reductase (GR) at the expense of NADPH. H_2O_2 can also be reduced by PRDX3 and PRDX5, which depend on the TXN2/TXNRD2 system. NADPH is used as final electron donor.

Box 1 | **Manganese superoxide dismutase (Mn-SOD)**

Mn-SOD, also known as SOD2, catalyzes the dismutation of the superoxide radical with a high rate constant (1.8×10^9 $M^{-1}s^{-1}$; see Fig. 2.5). The catalytic activity of this homotetrameric enzyme depends on the presence of manganese (Halliwell and Gutteridge 2007). Mn-SOD is strictly localized in mitochondria. Mitochondrial localization results of the presence of an N-terminal mitochondrial targeting sequence (MTS). In human, the sequence of this MTS presents a Val16Ala genetic dimorphism, which was shown to improve mitochondrial uptake (Sutton et al. 2003). A number of epidemiological studies have been conducted to examine the association between the Val16Ala dimorphism and cancer susceptibility, but the results remain controversial (see Holley et al. (2011) for review).

The importance of Mn-SOD is illustrated by the pre- and neo-natal lethality in Mn-$SOD^{-/-}$ mice (Li et al. 1995; Lebovitz et al. 1996; Melov et al. 1999; Huang et al. 2001). Moreover, heterozygous Mn-$SOD^{+/-}$ mice exhibit increased mitochondrial damage and susceptibility to oxidative stress, alterations in mitochondrial function and enhanced cancer incidence (Williams et al. 1998; Kokoszka et al. 2001; Van Remmen et al. 2001; Van Remmen et al. 2003). Conversely, overexpression of Mn-SOD in mice has been shown to protect against oxidative damage without altering life span (Silva et al. 2005; Jang et al. 2009).

2.4.1 PRDX3

PRDX3 was originally identified in murine erythroleukemia cells and was thought to play a role in erythrocyte differentiation (Yamamoto et al. 1989; Nemoto et al. 1990). A few years later, Watabe *et al*. isolated bovine PRDX3 in adrenal cortex as a highly abundant mitochondrial matrix protein used as substrate by the Lon protease (Watabe et al. 1994). PRDX3 protein contains 256 amino acids, among which the 61 N-terminal residues form a mitochondrial targeting sequence (MTS). This MTS is cleaved upon mitochondrial import, releasing a mature protein of 21.5 kDa (Cox et al. 2010).

PRDX3 was shown to react efficiently with hydrogen peroxide with a rate constant of 2×10^7 $M^{-1}s^{-1}$ (Cox et al. 2009b). Given this high reaction rate and the high abundance of the protein in the mitochondrial matrix, it

was suggested that PRDX3 is responsible for 90% of mitochondrial hydrogen peroxide decomposition (Cox et al. 2010). PRDX3 is also able to reduce organic peroxides and amino acid, peptide and protein hydroperoxides (Peskin et al. 2010). Its peroxynitrite reductase activity has never been measured so far. PRDX3 uses mitochondrial TXN2 as electron donor. The oxidized form of TXN2 is reduced by mitochondrial TXNRD2 in a NADPH-dependent manner. Recently, Hanschmann *et al.* showed that GRX2 also contributes to the reduction of PRDX3 (Hanschmann et al. 2010). In turn, GRX2 can be reduced by either GSH/GSSH or TXNRD2 (see Fig. 2.6).

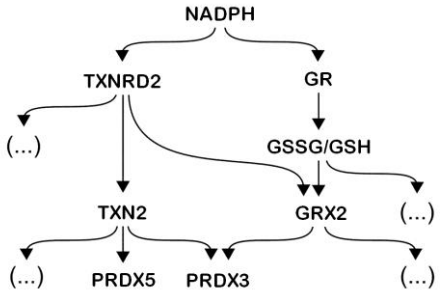

Fig. 2.6. PRDX3 reduction by thioredoxin 2 (TXN2) and glutaredoxin 2 (GRX2). PRDX3 can be reduced by the thioredoxin (TXN) system, in which TXN2 reduces PRDX3 and is subsequently reduced by thioredoxin reductase 2 (TXNRD2) at the expense of NADPH. Additionally, PRDX3 can be reduced by GRX2, which uses electrons from either TXNRD2 or glutathione (GSH). Oxidized glutathione (GSSG) is reduced by glutathione reductase (GR), which uses electrons from NADPH. [Adapted from Hanschmann et al. (2010)].

The role of PRDX3 in antioxidant defence was investigated by studying the effects of a modulation of PRDX3 expression in cultured cells and *in vivo*. Overexpression of PRDX3 in cells increases resistance to exposure to various apoptosis inducers (Shih et al. 2001; Nonn et al. 2003; Godoy et al. 2011) and decreases ROS production (Nonn et al. 2003). Silencing of PRDX3 in cells was shown to enhance protein carbonylation (De Simoni et al. 2008), alter mitochondrial morphology (Wonsey et al. 2002) and

increase sensitivity to cell death (Araki et al. 1999; Chang et al. 2004; Mukhopadhyay et al. 2006; De Simoni et al. 2008). PRDX3 knockout mice exhibit a hypersensitivity to lipopolysaccharide-induced lung inflammation (Li et al. 2007) and a higher frequency of stillbirths, which are associated to an increased oxidative stress in placenta (Li et al. 2008). Also, macrophages derived from these mice display an increased sensitivity to oxidative stress (Li et al. 2009). Overexpression of PRDX3 in transgenic mice prevents left ventricular remodeling and failure after myocardial infarction (Matsushima et al. 2006) and protects against paraquat-induced cognition impairment and amyloidogenesis (Chen et al. 2012). Moreover, hippocampal neurons from mice overexpressing PRDX3 are protected from excitotoxic injury (Hattori et al. 2003). Finally, glucose tolerance is improved in transgenic mice overexpressing PRDX3 through reduction of mitochondrial hydrogen peroxide (Chen et al. 2008).

PRDX3 was found to be ~30 fold more abundant in the mitochondria of Hela cells than GPX1 (Chang et al. 2004). PRDX3 is overexpressed in lung (Park et al. 2006) and prostate (Basu et al. 2011) cancer as well as in hepatocellular (Choi et al. 2002; Qiao et al. 2012) and breast carcinomas (Noh et al. 2001; Karihtala et al. 2003). A decreased PRDX3 expression was observed in neurodegenerative disorders such as amyotrophic lateral sclerosis (Wood-Allum et al. 2006), Down syndrome and Pick's disease (Krapfenbauer et al. 2003). Finally, Fanconi anemia was shown to be associated with a deregulation of PRDX3, including cleavage and mislocalization (Mukhopadhyay et al. 2006). All these diseases were shown to be linked to oxidative stress.

Box 2 | **Glutathione peroxidase 1 (GPX1)**

GPX1, also termed cytosolic GPX (c-GPX), is a member of the GPX family of peroxidases. GPX1 is tetrameric, each subunit bearing a catalytic selenocysteine (Sec) residue. The presence of selenium (Se) lowers the pKa of the Sec, conferring a high reactivity towards peroxides (Halliwell and Gutteridge 2007). GPX1 detoxifies efficiently hydrogen peroxide (rate constant ~ 1-5 x 10^7 $M^{-1}s^{-1}$) and various organic hydroperoxides (rate constant ~ 2 x 10^6 to 4 x 10^7 $M^{-1}s^{-1}$) and requires two equivalents of glutathione (GSH) as co-substrate (Fig. 2.5) (Toppo et al. 2009; Flohe et al. 2011). GPX1 is ubiquitously distributed and, consistent with the antioxidant function of the enzyme, particularly high levels are found in tissues with high rates of peroxide production, such as erythrocytes, liver, kidney or lung (Brigelius-Flohe 1999). However, GPX1 biosynthesis relies on the availability of diet-supplied Se and is thus ceased rapidly in Se-deprived animals. Interestingly, recent studies on human isolated blood cells evidenced that, like some PRDXs, GPX1 activity may be inactivated by hydrogen peroxide. This irreversible inactivation involves the overoxidation of Se-OH to SeO_2H (Cho et al. 2010). GPX1 is predominantly localized in the cytosol, but a small proportion of GPX1 is also present in mitochondria (Panfili et al. 1991; Utsunomiya et al. 1991; Asayama et al. 1994; Esworthy et al. 1997). Also, peroxisomal localization of GPX1 was described in rat hepatocytes in several studies (Asayama et al. 1994; Singh et al. 1994).

Overwhelming evidence has demonstrated the protective function of GPX1 against oxidative stress. Indeed, overexpression or downregulation of GPX1 was shown to affect resistance to ROS-induced cell death (Mirault et al. 1991; Taylor et al. 1993). Also, $GPX1^{-/-}$ mice develop normally and tolerate moderate oxidative stress but are highly sensitive to severe oxidative challenges (Ho et al. 1997; Cheng et al. 1998; de Haan et al. 1998; Fu et al. 1999a; Fu et al. 1999b; Esposito et al. 2000). Conversely, transgenic mice overexpressing GPX1 exhibit a decreased ROS-induced lethality (Cheng et al. 1998). Surprisingly, GPX1 appears to exert a dual role in mice by protecting against oxidative stress but promoting nitrosative stress, since $GPX1^{-/-}$ mice were shown to be more resistant to RNS-induced cell death (Jiang et al. 2000; Fu et al. 2001). Finally, it is interesting to note that altered GPX1 expression was found in various human diseases like cancer, cardiovascular disease, neurodegenerative diseases and diabetes (Lei et al. 2007; Lubos et al. 2011).

As a member of the typical 2-Cys PRDX group, PRDX3 can undergo inactivation by hyperoxidation of the Cp. Although PRDX3 was reported to be more resistant to hyperoxidation than cytosolic PRDX1 and PRDX2 (Cox et al. 2009a), PRDX3 hyperoxidation has been observed in liver of aged rats and in cultured cells following exposure to hydrogen peroxide or drugs generating hydrogen peroxide (Chevallet et al. 2003; Woo et al. 2003b; Saito

et al. 2007; Musicco et al. 2009). Hyperoxidized PRDX3 is reduced by Srx, which is translocated from the cytosol to the mitochondria by a yet unknown mechanism (Noh et al. 2009). Interestingly, Srx reduces hyperoxidized PRDX3 more slowly than hyperoxidized PRDX1 and PRDX2 (Chevallet et al. 2003; Woo et al. 2003b). Therefore, despite the fact that PRDX3 is more resistant to hyperoxidation, its slow reduction by Srx would allow an accumulation of inactivated PRDX3 under certain conditions. This would permit a local increase in mitochondrial hydrogen peroxide levels for cell signalling (Cox et al. 2010). Thus, in addition to its role as protective antioxidant, PRDX3 may potentially play a role in mitochondrial redox signalling, albeit this role remains speculative. Moreover, since PRDX3 can undergo hyperoxidation, this protein might form high molecular weight complexes displaying chaperone activity. However, so far, there is no direct evidence of chaperone activity linked to PRDX3 hyperoxidation.

2.4.2 PRDX5

A detailed description of PRDX5 is given in the next chapter of this introduction.

Box 3 | **Glutathione peroxidase 4 (GPX4)**

GPX4, or phospholipid hydroperoxide GPX (PHGPX), is the fourth selenium-containing GPX member that has been characterized. GPX4 differs from the other GPXs in many points. Indeed, GPX4 is a monomer whereas the other GPXs exhibit a tetrameric structure. Moreover, in addition to reduce hydrogen peroxide, GPX4 is able to reduce phospholipid hydroperoxides and a wide range of other lipid peroxides (Imai and Nakagawa 2003). In contrast to GPX1, GPX4 exhibits a limited specifity for GSH and can alternatively use protein-thiol groups as reducing substrates (Toppo et al. 2009). Finally, GPX4 presents an unusual tissue distribution, as its activity is lower than that of GPX1 in all organs except in testis, where GPX4 is highly abundant. Interestingly, unlike for GPX1, GPX4 expression is maintained even in selenium-depleted animals (Brigelius-Flohe 1999).

GPX4 is localized in the mitochondria, the cytosol and the nucleus. This complex subcellular distribution is a consequence of the existence of three GPX4 isoforms which derive from a single gene. The long form (l-GPX4), or mitochondrial form, is identical to the short form (s-GPX4) but contains an additional N-terminal mitochondrial targeting sequence (MTS). This MTS is processed after mitochondrial import, yielding a mature l-GPX4 which is indistinguishable in size from s-GPX4. Because of the lack of an MTS, s-GPX4 is found in the cytosol, but also in the nucleus. The start codons of both l-GPX4 and s-GPX4 as well as the MTS are encoded by the first exon of the *GPX4* gene (Pushpa-Rekha et al. 1995; Arai et al. 1996). Expression of the third GPX4 isoform involves the transcription of an alternative first exon encoding a nuclear localization signal (NLS) (Pfeifer et al. 2001). This isoform is found in the nucleus.

Due to its ability to detoxify membrane-integrated lipid hydroperoxides, GPX4 is generally considered as a primary defence system against oxidative damages to cellular membranes. Furthermore, Seiler and co-workers showed that GPX4 is a key regulator of apoptosis through the regulation of 12/15-lipoxygenase-dependent lipid peroxidation in mitochondria (Seiler et al. 2008). Consistent with this important function, knocking out GPX4 results in prenatal lethality, while mice deficient in other GPXs are viable (Imai et al. 2003; Yant et al. 2003). Moreover, GPX4 ablation in adult mice results in lethality within two weeks, indicating that GPX4 is also essential for survival of adult mice (Yoo et al. 2012). A multitude of other *in vitro* and *in vivo* studies support the antioxidant role of GPX4 (Yagi et al. 1996; Ran et al. 2004). Finally, in addition to its antioxidant function, GPX4 was shown to be implicated in spermatogenesis and sperm function (Conrad et al. 2005; Imai et al. 2009; Schneider et al. 2009; Liang et al. 2009; Puglisi et al. 2012).

3. Peroxiredoxin 5

PRDX5 is the last member of the mammalian PRDX family that has been identified and characterized (Wattiez et al. 1999; Knoops et al. 1999; Kropotov et al. 1999; Yamashita et al. 1999) (Fig 3.1). Mature human PRDX5 shares only 28 to 30% sequence identity with human PRDX1-4 and PRDX6, indicating that PRDX5 is the most divergent isoform in the mammalian PRDX family (Leyens et al. 2003; Rhee et al. 2005). As mentioned before, PRDX5 is the only atypical 2-Cys PRDX in mammals.

3.1. Human PRDX5 gene and genomic context

Human *PRDX5* is localized on chromosome 11q13 and is composed of six exons and five introns spanning ~3.7 kb (Fig 3.2A). The number of exons and introns as well as the size of the protein-encoding exons appears to be conserved among chordates (Nguyen-Nhu et al. 2007). In mammals, *PRDX5* is in very close proximity with the *HSPC152/TRMT112* gene, which is positioned in the opposite direction (Fig. 3.2A) and which encodes a small accessory protein required in some methyltransferase complexes (Figaro et al. 2008; Songe-Moller et al. 2010). Only 689 bp separate the two first translation initiation codons of the two genes in human. Consequently, it is likely that *PRDX5* and *HSPC152/TRM112* share regulating sequences (Nguyen-Nhu et al. 2007; Knoops et al. 2011).

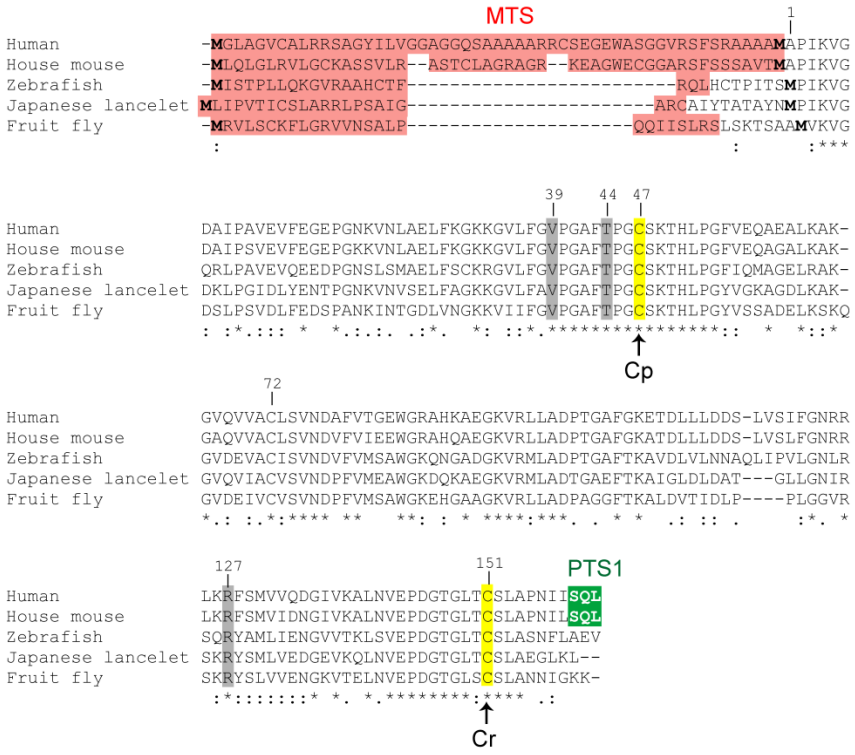

Fig. 3.1. **Amino acid sequence alignment of human PRDX5 and animal orthologs**. The alignment was generated by ClustalX 2.0.7 (Larkin et al. 2007) program. Asterisks indicate identities, dots and double dots indicate conservative and highly conservative substitutions, respectively. Amino acid numbering refers to mature human PRDX5 (Declercq et al. 2001). Methionines encoded by the two alternative translation initiation sites are indicated in bold type. Confirmed (human) and predicted (TargetP v1.1) (Nielsen et al. 1997; Emanuelsson et al. 2000) mitochondrial targeting sequences (MTS) are highlighted in red. Peroxidatic (Cp) and resolving (Cr) Cys implicated in catalysis are highlighted in yellow. The peroxisomal targeting signal type I (PTS1) is highlighted in green. Residues involved in the stabilization of the catalytic site are in grey. GenBank accession numbers are as follows: NP_036226 (Human, *Homo sapiens*); NP_036151 (House mouse, *Mus musculus*); CN508467 (Zebrafish, *Danio rerio*); AF498232 (Japanese lancelet, *Branchiostoma belcheri tsingtaunese*); NP_650679 (Fruit fly, *Drosophila melanogaster*). [From Knoops et al. (2011)].

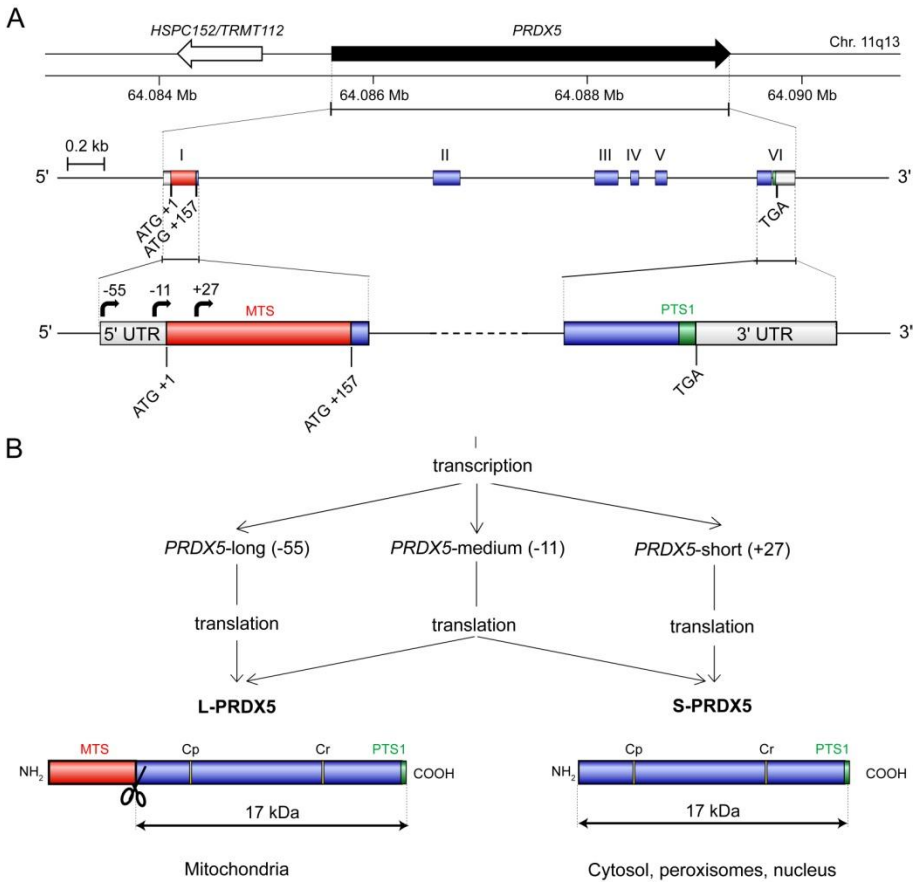

Fig. 3.2. Human *PRDX5* gene organisation and protein isoforms. (A) Human *PRDX5* gene is located on chromosome 11q13 and is flanked by *HSPC152/TRMT112* gene. Human *PRDX5* gene contains six exons (boxes) and five introns. 5′- and 3′-untranslated regions (UTRs) are indicated by open boxes. In human liver, three alternative transcription initiation sites were identified (black arrows)(Nguyen-Nhu et al. 2007). Exon I contains also two in-frame ATG initiation codons. The regions encoding the mitochondrial targeting sequence (MTS) and peroxisomal targeting signal type I (PTS1) are in red and green respectively. **(B)** The presence of alternative transcription and translation start sites in human *PRDX5* gene results in the production of a long PRDX5 form (L-PRDX5) and a short PRDX5 form (S-PRDX5). L-PRDX5 contains a cleavable N-terminal MTS (red) and is therefore imported into mitochondria. S-PRDX5 contains a weak C-terminal PTS1 signal and is targeted to the cytosol, the peroxisomes and the nucleus. Peroxidatic (Cp) and resolving (Cr) Cys implicated in catalysis are indicated. [Adapted from Nguyen-Nhu et al. (2007) and Knoops et al. (2011)].

3.2. *PRDX5 expression*

Analysis of the 5'-flanking region of human *PRDX5* reveals features of a housekeeping gene, i.e. CpG islands, no TATA- and CAAT-boxes as well as multiple transcription start sites (see point 3.3). PRDX5 is constitutively expressed in virtually all mammalian tissues, with the highest expression in tissues that are particularly exposed to oxidative stress such as thyroid gland, lung or kidney (Knoops et al., 1999). The amounts of PRDX5 were estimated between 0.2 and 1.3 µg/mg of soluble proteins in rat tissues (Seo et al. 2000). However, the expression level is variable between cell types and can also be regulated in pathophysiological conditions or in response to stress. For example, PRDX5 expression is upregulated in degenerative human tendons (Wang et al. 2001), in breast carcinoma (Karihtala et al. 2009), in human hypertensive kidney cortex (Marques et al. 2011) and in different thyroid pathologies (Gerard et al. 2005; Poncin et al. 2008; Senou et al. 2010). On the opposite, downregulation of PRDX5 was observed in corticobasal neurodegeneration (Chen et al. 2005) and in adrenocortical carcinoma (Fernandez-Ranvier et al. 2008).

Little is known about the mechanisms involved in the regulation of *PRDX5* expression. Albeit their implication in *PRDX5* regulation is not clear, several putative response elements for transcription factors involved in the response to oxidative stress, such as Nrf2 or Nf-κB, are present in the 5'-flanking region of human *PRDX5* (Kropotov et al. 2006b; Nguyen-Nhu et al. 2007; Kropotov et al. 2007). Moreover, it was demonstrated that transcription factors such as Foxo3a, GATA1, GABP and NeuroD6 can regulate *PRDX5* expression (Uittenbogaard and Chiaramello 2002; Olmos et al. 2009; Usmanova et al. 2011; Seo et al. 2012).

3.3. Subcellular distribution of PRDX5

As mentioned before (see point 2.3), PRDX5 exhibits the widest subcellular distribution among the PRDX members. Indeed, it can be localized in the cytosol (Yamashita et al. 1999; Seo et al. 2000; Kinnula et al. 2002; Banmeyer et al. 2004), the mitochondria (Knoops et al. 1999; Oberley et al. 2001; Banmeyer et al. 2004; Leyens et al. 2004; Pagliarini et al. 2008; Radyuk et al. 2009), the peroxisomes (Yamashita et al. 1999; Seo et al. 2000; Schluter et al. 2010) and, in several situations, in the nucleus (Kropotov et al. 1999; Oberley et al. 2001; Kinnula et al. 2002; Gerard et al. 2005; Lu et al. 2006; Poncin et al. 2008).

This wide subcellular localization is permitted by a complex gene organization (Fig. 3.2.A). Indeed, human *PRDX5* gene presents two alternative in-frame translation initiation codons, both present on the first exon. To our knowledge, the relative efficiencies of these two translation initiation sites, depending on the respect of the Kozak consensus, were not investigated yet. Moreover, several alternative transcription start sites were identified from transcripts issued from liver, brain and lung. These transcription initiation sites are positioned upstream and downstream of the more 5′ translation start site (Nguyen-Nhu et al. 2007). In human, the presence of these alternative transcription and translation start sites results in the synthesis of either a short PRDX5 form (S-PRDX5), or a long PRDX5 form (L-PRDX5) containing 52 additional residues at the N-terminal terminus (Figs. 3.1 and 3.2B). S-PRDX5 is located in the cytosol, the nucleus and the peroxisomes. Peroxisomal distribution is a consequence of the presence of a weak C-terminal peroxisomal targeting signal (PTS1), which is encoded by the sixth exon. On the other hand, the N-terminal extension present in L-PRDX5 was shown to correspond to a mitochondrial targeting sequence (MTS), as it is able to target the green fluorescent reporter protein into mitochondria (Knoops et al. 1999). Therefore, L-PRDX5 is imported as a

precursor into the mitochondrial matrix where the MTS is cleaved off, releasing a mature protein which is indistinguishable in size from S-PRDX5 (Seo et al. 2000; Banmeyer et al. 2004). Although the exact cleavage site was never experimentally demonstrated, it is generally assumed that the first amino acid downstream of the cleavage site corresponds exactly to the first amino acid of S-PRDX5 after the cleavage of its first methionine (Knoops et al. 2011). Finally, it is worthwhile to note that L-PRDX5 also exhibits the C-terminal peroxisomal targeting signal. However, because the MTS is a stronger targeting signal compared to the PTS1, it appeared that when both targeting sequences coexist, PRDX5 is preferentially imported into mitochondria (Banmeyer et al. 2004; Banmeyer et al. 2005).

3.4. Kinetics

PRDX5 is able to react with hydrogen peroxide, organic peroxides and peroxynitrite. Human PRDX5 reacts with hydrogen peroxide more slowly (~10^5 $M^{-1}s^{-1}$) than with organic peroxides (~10^6 $M^{-1}s^{-1}$) or peroxynitrite (~10^7 $M^{-1}s^{-1}$). This suggests that, in subcellular compartments where PRDX5 coexists with other PRDXs (cytosol, nucleus, mitochondria), PRDX5 could be involved more specifically in the reduction of peroxynitrite or organic peroxides rather than hydrogen peroxide (Trujillo et al. 2007; Cox et al. 2010).

The reduction of oxidized PRDX5 is performed by cytosolic or mitochondrial TXNs (TXN1 and TXN2, respectively). TXNs are then reduced by cytosolic or mitochondrial TXNRDs (TXNRD1 and TXNRD2, respectively) at the expense of NADPH (Seo et al. 2000; Zhou et al. 2000; Dubuisson et al. 2004; Trujillo et al. 2007). Cyclophilin A was also reported to potentially reduce PRDX5 (Lee et al. 2001). Noteworthy, PRDX5 reductant in peroxisomes remains unknown and is still to be identified (Knoops et al. 2011).

Although the enzymatic activities of typical 2-Cys PRDXs may be modulated by different posttranslational modifications (see point 2.2.3), little is known about such modifications on PRDX5. Interestingly, PRDX5 can undergo glutathionylation in rat exposed to oxidative stress, but the functional significance of this modification remains unknown yet (Fratelli et al. 2003). Furthermore, PRDX5 is not likely to undergo hyperoxidation since it lacks the C-terminal helix with the conserved "YF" motif (see point 2.1). Accordingly, it appears that mammalian PRDX5 is more resistant to sulfinylation than the typical 2-Cys-PRDXs (Woo and Rhee 2010) and that sulfiredoxin does not interact with PRDX5 (Woo et al. 2005).

3.5. Functions

The cytoprotective antioxidant role of PRDX5 has been abundantly investigated in various cellular models. Indeed, it was reported that PRDX5 overexpression protects cell lines against nitro-oxidative stresses (Seo et al. 2000; Zhou et al. 2000; Nguyen-Nhu and Knoops 2003; Banmeyer et al. 2004; Zitzler et al. 2004; Yuan et al. 2004; Peng et al. 2004a; Peng et al. 2004b; Radyuk et al. 2009), whereas PRDX5 silencing makes the cells more vulnerable (Serikov et al. 2006; Kropotov et al. 2006a; Avila et al. 2008; De Simoni et al. 2008; Gao et al. 2011). Furthermore, PRDX5 has been shown to exert an antioxidant protective function in tissues, as exogenous administration of recombinant human PRDX5 protects mouse brain against ibotenate-induced excitotoxic stress (Plaisant et al. 2003). Recently, the antioxidant function of PRDX5 was investigated in transgenic mice with PRDX5 downregulation in kidney, lung and liver. PRDX5 knock-down had no physiological effects under basal conditions, but proteomic analysis after hypoxia revealed altered expression of renal proteins, among which proteins involved in antioxidant protection (Yang et al. 2010).

As mentioned before (see point 1), hydrogen peroxide is a key molecule involved in cell signalling (Rhee 2006; Valko et al. 2007; Halliwell and Gutteridge 2007; Forman et al. 2010). Initially, PRDX5 was shown to modulate peroxide levels produced in cells stimulated with PDGF, TNF-α, or p53 (Seo et al. 2000; Zhou et al. 2000). Therefore, PRDX5 could potentially play a role in peroxide-dependent signal transduction. Also, since PRDX5 was reported to be translocated to the nucleus under oxidative stress (Gerard et al. 2005; Poncin et al. 2008), one could hypothesize that PRDX5 is involved in redox-dependent transcription regulation. However, in contrast to the cytoprotective function of PRDX5 which is well documented, little is known about the possible function of PRDX5 in redox signalling. Also, PRDX5 lacks characteristics to be a good candidate for this function, as it is not prone to undergo hyperoxidation (see point 3.4) or phosphorylation by kinases, like typical 2-Cys PRDXs (Chang et al. 2002; Woo et al. 2010). However, a recent study reported that PRDX5 can play a role in LPS-induced microglial activation through modulation of ROS levels and signalling cascades dependent on c-*jun* N-terminal kinase (JNK) (Sun et al. 2010). Moreover, it was shown that *Drospohila* PRDX5 plays an important modulatory role in immune signalling, by regulating negatively specific immune pathways (Radyuk et al. 2010).

It is important to emphasize that PRDX5 coexists in subcellular compartments with different peroxide-detoxifying enzymes. In the mitochondria, PRDX5 coexists with GPX1, GPX4 and PRDX3. The mitochondrial localization of PRDX5 seems to be a conserved feature as this protein was detected in mitochondria of various animal species, i.e. human, rat, mouse, hamster, bovine and fruitfly (Knoops et al. 1999; Oberley et al. 2001; Banmeyer et al. 2004; Leyens et al. 2004; Pagliarini et al. 2008; Radyuk et al. 2009). Recent reports based on rate constants and enzyme abundance suggest that mitochondrial PRDX5 would play a minor role in hydrogen peroxide reduction compared with PRDX3 and GPX1, but would possess a

more specific function through its high reactivity towards alkyl hydroperoxides (~ 10^6 $M^{-1}s^{-1}$) and peroxynitrite (~ 10^7 $M^{-1}s^{-1}$) (Cox et al., 2010; Trujillo et al., 2007). However, this proposed kinetic hierarchy has to be qualified with respect to the cell type and the availability of physiological reductants. Moreover, *in vivo*, mitochondrial peroxidases are likely to be heterogeneously distributed in some niches and display also different susceptibilities to inactivation (Knoops et al. 2011).

In the cytosol, mammalian PRDX5 coexists with PRDX1, PRDX2 and PRDX6. In this compartment, it was proposed that PRDX1 and PRDX2 should rather be involved in hydrogen peroxide signalling, while PRDX5 and PRDX6 should rather be implicated in antioxidant defence (Knoops et al. 2011).

In the peroxisomes, PRDX5 coexists with catalase, which is a very efficient hydrogen peroxide scavenger. In this organelle, PRDX5 could be involved in antioxidant defence through the reduction of alkyl hydroperoxides and peroxynitrite. However, the specific function of PRDX5 in this subcellular compartment remains unclear. Indeed, until now, no physiological reductant has been described for peroxisomal PRDX5. Moreover, to our knowledge, no study has yet investigated the effect of the overexpression/silencing of PRDX5 in the peroxisomal matrix itself (Knoops et al. 2011).

The function of PRDX5 in the nucleus is still a matter of debate. PRDX5 is not expressed in the nucleus at high levels and in all mammalian cell types. PRDX5 was first described as a DNA-binding protein repressing the transcription of the Alu-family of retroposons (Kropotov et al. 1999). Furthermore, it was shown that PRDX5 overexpression in the nucleus protects DNA from peroxide-induced oxidative damages (Banmeyer et al. 2004) while PRDX5 silencing stimulates etoposide-induced double-strand

DNA breaks (Kropotov et al. 2004), suggesting a protective antioxidant function in the nucleus. Interestingly, it was reported that PRDX5 is translocated into the nucleus under pathophysiological situations in some cell types, like thyrocytes (Gerard et al. 2005; Poncin et al. 2008). This suggests that PRDX5 may function in the nucleus either as a DNA-protective enzyme or as a redox-dependent signalling molecule (Knoops et al. 2011).

Furthermore, an unexpected role of PRDX5 in immunogenicity was described. Indeed, a point mutation in *PRDX5* gene identified in human metastatic melanoma was shown to yield a tumor antigen targeted by cytotoxic T lymphocytes (Sensi et al. 2005). Moreover, two other short peptides coded by *PRDX5* gene were also shown to contribute to immunogenicity (Sensi et al. 2009). These two antigenic nonapeptides were shown to derive from two distinct alternative splicing variants of *PRDX5*, widely expressed in neoplastic and normal tissues. These alternative splicing variants are unstable at the protein level as they are detectable only after inhibition of proteosomal degradation. It was proposed that the antigenic nonapeptides are involved in an immune-mediated response to stress contributing to the detection and elimination of damaged or neoplastic cells (Sensi et al. 2009).

Recently, a new function for PRDX5 in the initiation of post-ischemic inflammation in the brain emerged. Indeed, Shichita and coworkers (2012) showed that PRDX5 is released extracellularly from necrotic brain cells. This induces the expression of proinflammatory cytotokines in infiltrating macrophages, thereby triggering a destructive inflammatory response. This new function contrasts with the antioxidant protective function of intracellular PRDX5.

4. Mitochondrial protein import

Cell compartmentalization appeared during eukaryotic evolution and allowed a physical separation of incompatible biochemical reactions. Consequently, each organelle needs to be equipped with a distinct set of proteins to carry out the various metabolic pathways. Mitochondria contain more than thousand different proteins. However, the coding capacity of the mitochondrial DNA is restricted to a few polypeptides, i.e. thirteen in human. All other proteins are encoded by nuclear DNA, synthetized at cytosolic ribosomes and subsequently imported into the mitochondria (van der Laan et al. 2010). Protein import into the mitochondria requires the existence of both:

i) signal sequences containing targeting information and

ii) sophisticated translocation machineries allowing signal sequence recognition and protein translocation across the mitochondrial double-membrane system.

Most of our knowledge on mitochondrial protein import derives from studies on *Neurospora crassa* and *Saccharomyces cerevisiae*. However, despite the existence of some species-specificities like in some parasitic trypanosomatids (Singha et al. 2012), the mitochondrial import machinery appears to be well conserved throughout eukaryotes, including in mammalian mitochondria.

4.1. Mitochondrial translocation pathways: an overview

For most precursor proteins, the common entry gate to the mitochondria is the translocase of the outer membrane (TOM) complex. After passing through the TOM complex, precursors are sorted to different mitochondrial subcompartments. Currently, five different protein import pathways are characterized (Fig. 4.1.) (for review see Becker et al. (2012)).

i) The presequence pathway concerns precursors carrying positively charged N-terminal presequences (see point 4.2.1). After crossing the outer membrane, preproteins are transferred to the presequence translocase of the inner membrane (TIM23) complex. Precursors are then either imported into the matrix with the help of the presequence translocase-associated motor (PAM) or laterally inserted into the inner membrane. Other presequence-containing precursors are first completely translocated into the matrix and subsequently inserted into the inner membrane with the help of the oxidase assembly (OXA) machinery.

ii) The carrier pathway imports proteins from the carrier family into the inner membrane. These hydrophobic proteins contain multiple transmembrane segments and carry internal targeting signals. They are imported with the help of the TOM complex, the small TIM chaperone complex of the intermembrane space and the carrier translocase (TIM22) complex.

iii) The oxidative folding pathway is responsible for the transport of cysteine-containing proteins to the intermembrane space. The precursors are synthesized with internal signal sequences and use the TOM complex as well as the mitochondrial intermembrane space assembly (MIA) machinery, which oxidizes the Cys residues.

iv) The β-barrel pathway transports the precursors of pore-forming proteins of the outer membrane that are composed of multiple

transmembrane β-strands. Translocation of the precursors involves the TOM complex and the small TIM chaperone complex of the inner membrane space. Insertion into the outer membrane is mediated by the sorting and assembly machinery (SAM) complex.

v) The α-helical insertion pathway is the last discovered import pathway and concerns proteins anchored in the outer membrane by one or more transmembrane α-helical segments. Precursors are recognized by receptors of the TOM complex but do probably not cross the TOM channel. Thus, these precursors do not use the main translocation route across the outer membrane common to the other import pathways. Instead, they are transferred to the Mim1 complex for membrane insertion.

As this work deals with PRDX5, which is located in the mitochondrial matrix, the next section focuses on signal sequences and translocation machineries permitting protein import into this subcompartment. The other import patways are not detailed in this introduction (for review see Becker et al. (2012), Schmidt et al (2010) and Mokranjac and Neupert, (2009)).

Fig. 4.1. Overview of import pathways into mitochondria (facing page). The presequence pathway (red) imports presequence-containing precursors into the matrix or the inner membrane with the help of the translocase of the outer membrane (TOM) and the presequence translocase of the inner membrane (TIM23) complexes. Full translocation of precursors destined to the matrix is completed by the presequence-associated motor (PAM). The OXA complex is also involved in the insertion of some presequence-containing precursors into the inner membrane. The carrier pathway (green) inserts hydrophobic proteins into the inner membrane and involves the cooperation of TOM, small TIM and TIM22 complexes. The oxidative folding pathway (purple) drives the import and oxidative folding of intermembrane proteins and involves the TOM and mitochondrial intermembrane assembly (MIA) machinery. The β-barrel pathway (blue) leads to the insertion of β-barrel proteins into the outer membrane and is dependent on TOM, small TIM, as well as the sorting and assembly machinery (SAM) complexes. The α-helical insertion pathway (orange) inserts α-helical proteins into the outer membrane with the help of TOM receptors and Mim1. [Adapted from Becker et al. (2012)].

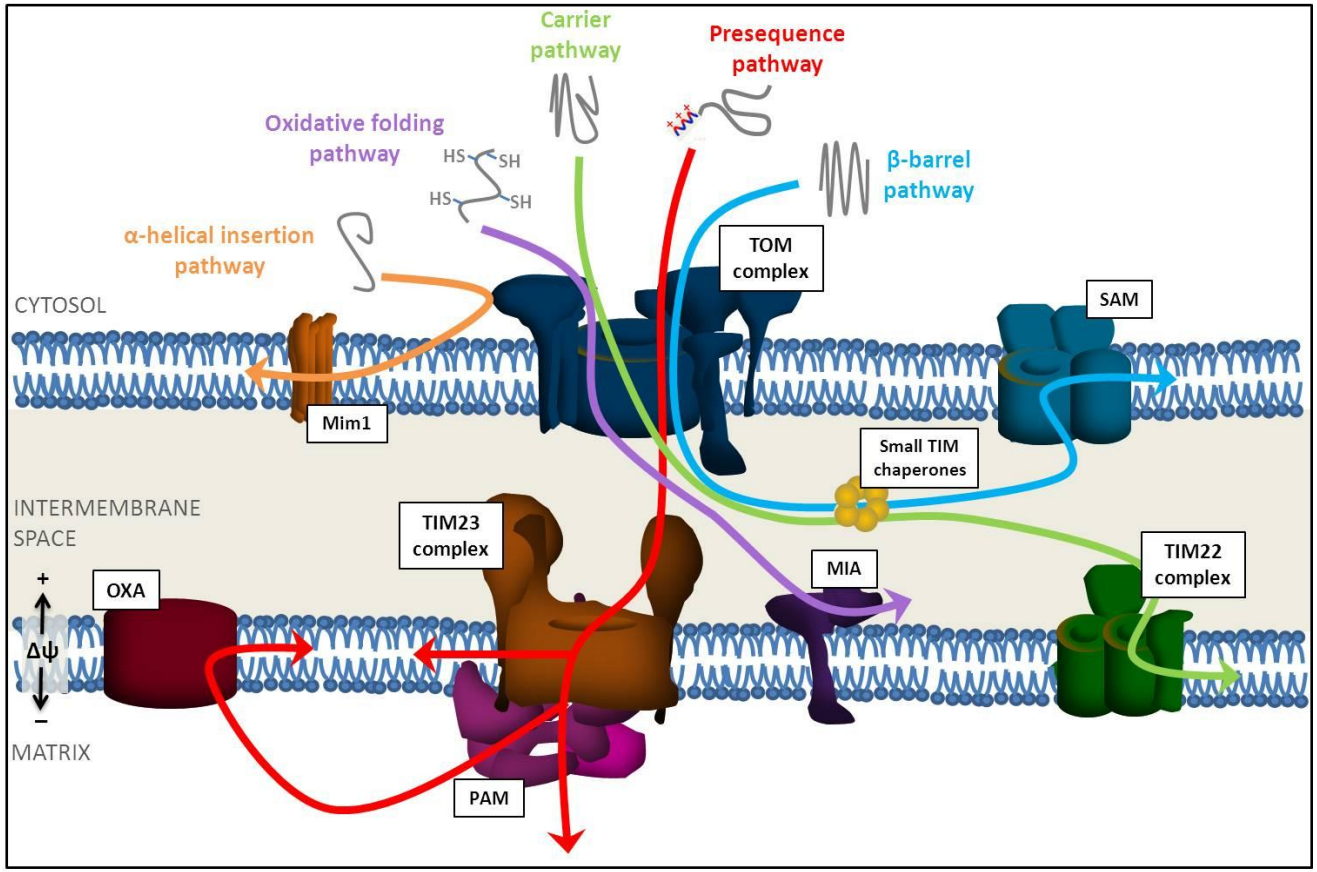
Carrier pathway
Presequence pathway
Oxidative folding pathway
HS
SH
HS
SH
β-barrel pathway
α-helical insertion pathway
TOM complex
CYTOSOL
SAM
Mim1
Small TIM chaperones
INTERMEMBRANE SPACE
TIM23 complex
MIA
TIM22 complex
OXA
+
Δψ
−
MATRIX
PAM

4.2. Protein import into the mitochondrial matrix

4.2.1. Presequences

Mitochondrial proteins are synthesized in the cytosol as precursor preproteins containing specific signal sequences which are both necessary and sufficient to direct them from the cytosol into mitochondria. In the case of proteins imported into the mitochondrial matrix, the signal sequence corresponds to a cleavable N-terminal mitochondrial targeting sequence (MTS), also called presequence (Neupert and Herrmann 2007; Chacinska et al. 2009). Presequences have a length of typically 15-50 residues, although presequences shorter than 10 and up to 100 residues were described. Their secondary structure is well conserved, as presequences adopt an amphipathic α-helical conformation, i.e. with one positively charged face and one hydrophobic face. These two faces are recognized by distinct binding sites on the outer membrane translocase (see below). Moreover, the positive charge of the presequence is critical for the electrophoretic effect of the membrane potential ($\Delta\psi$), which, together with ATP hydrolysis, constitutes the driving force for protein transport across the inner membrane (Chacinska et al. 2009). In contrast with the secondary structure, the primary structure of the presequence is not conserved, and varies even considerably between closely related orthologs (Neupert and Herrmann 2007).

It is important to note that, in some cases, protein import into the mitochondrial matrix can occur without presequence. This is the case of the nuclearly encoded mitochondrial transcription factor Mtf1p, which uses alternative internal import signals (Biswas and Getz, 2002; Biswas and Getz, 2004).

4.2.2. Protein translocation into the mitochondrial matrix

4.2.2.1. Crossing the outer membrane

A prerequisite for mitochondrial membrane translocation is that the newborn presequence-containing precursors are in a loosely-folded, translocation-competent state. Consequently, several cytosolic factors are involved in chaperoning precursors from their site of synthesis to the mitochondrial outer membrane. Mammalian cells use both Hsp90 and Hsp70 for preprotein transfer from the ribosome to the mitochondrial outer membrane receptors (Young et al. 2003). It was recently suggested that these two chaperones are a part of a large cytosolic complex containing other cochaperones, namely Hop, Tom34 and Cdc37 (Faou and Hoogenraad 2012).

The precursors enter into the mitochondria via the translocase of the outer mitochondrial membrane (TOM complex) (Neupert and Herrmann 2007). The yeast TOM complex is formed by seven subunits termed "Tom" followed by a number indicating their molecular mass (Fig. 4.1). By now, mammalian counterparts for all of the components have been identified. Preproteins cross the outer membrane through sequential binding to the different Tom subunits. The TOM complex contains two primary surface receptors, i.e. Tom20 and Tom70, which differ by their substrate specificity. Tom20 is typically involved in the recognition of N-terminal presequences, while Tom70 recognizes internal hydrophobic signal sequences of precursors which are not destined to the mitochondrial matrix (Hoogenraad et al. 2002; Neupert and Herrmann 2007). Nonetheless, in addition to its role in signal recognition for non matricial preproteins, Tom70 was shown to act as chaperone docking site. Therefore, both Tom70 and Tom20 would be implicated in presequence-containing protein import (Young et al. 2003; Yamamoto et al. 2009; Fan et al. 2011). Tom20 binds presequences by interacting with the hydrophobic face of the amphipathic α-helix (Abe et al. 2000). The preprotein is subsequently transferred to the protein-conducting

pore with the help of Tom5 and Tom22, which interacts with the positively charged face of the α -helix. The conducting channel of the TOM complex is formed by the β-barrel protein Tom40. Moreover, the general import pore is formed by the three small Tom proteins Tom5, Tom6 and Tom7, which are involved in the assembly and the dynamics of TOM complex. The precursor crosses the channel as an unfolded linear polypeptide chain with its N-terminus ahead. At the *trans* side of the outer membrane, the preprotein binds to the intermembrane space domain of Tom22 and eventually to Tom7. At this stage of import, the precursor is transferred to the translocase of the inner membrane, the TIM23 complex. (Johnston et al. 2002; Hoogenraad et al. 2002; Neupert and Herrmann 2007; Kato and Mihara 2008; Chacinska et al. 2009; Endo et al. 2011).

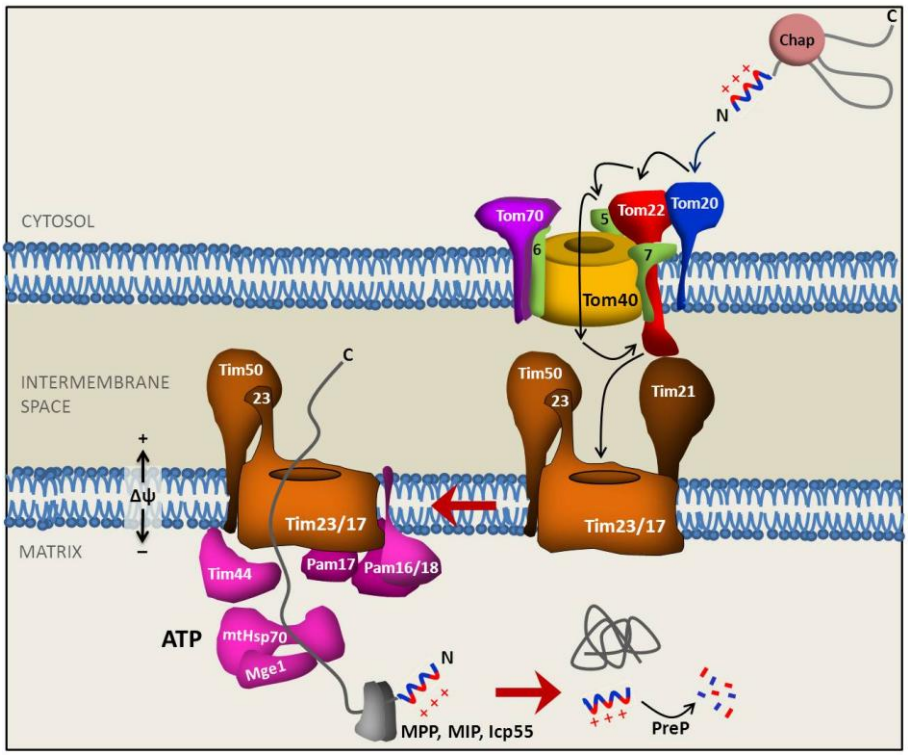

Fig. 4.2. Translocation of presequence-containing precursors across the double mitochondrial membrane (facing page). The outer mitochondrial membrane translocase (TOM complex) is composed of seven subunits. The receptor Tom20 recognizes the precursor and transfers them to the channel formed by Tom40 with the help of Tom22 and Tom5. The small Tom proteins, Tom5, Tom6 and Tom7 are involved in the stabilization of the TOM complex. Upon passage through the Tom40 channel, the precursor binds to the intermembrane space domain of Tom22 and is subsequently transferred to the inner mitochondrial membrane translocase (TIM23 complex) with the help of Tim21 and Tim50. The precursor is directed through the Tim23 channel by the $\Delta\psi$. The presequence-translocase associated motor (PAM, pink) fulfills the matrix translocation in an ATP-dependent manner. In the matrix, the presequence is cleaved from the precursor by the mitochondrial processing peptidase (MPP), and potentially by the mitochondrial intermediate peptidase (MIP) or the intermediate cleaving peptidase (Icp55). The free targeting peptides are subsequently degraded by presequence proteases (PreP). [Adapted from van der Laan et al. (2010)].

4.2.2.2. Crossing the inner membrane

The TIM23 complex is responsible for the translocation of presequence-containing precursors across the mitochondrial inner membrane. In yeast, the TIM23 complex is formed by four subunits forming the conducting channel, namely Tim17, Tim21, Tim23 and Tim50, as well as subunits constituting the presequence translocase-associated motor (PAM), i.e. Tim44, Pam16, Pam17, Pam18, mtHsp70 and Mge1 (Fig. 4.1) (Chacinska et al. 2009; van der Laan et al. 2010; Marom et al. 2011).

The presequence-containing precursor is handled over from Tom22 to the TIM23 complex with the help of the intermembrane-spanning domains of Tim50 and Tim21. Tim50 would act as the primary presequence receptor of the TIM23 complex (Schulz et al. 2011). The presence of the presequence and $\Delta\psi$ across the inner membrane triggers the opening of the translocation channel, which is formed by Tim23 and possibly Tim17. The precursor is inserted into the protein-conducting pore and is driven towards the matrix by the $\Delta\psi$, which exerts an electrophoretic force on the positively charged presequence. Full translocation of preprotein into the matrix requires an additional driving force, provided by the ATP-driven import motor, PAM. The recruitment of PAM by the TIM23 complex is accompanied by the release of Tim21. The central component of PAM is the mitochondrial chaperone Hsp70 (mtHsp70), which binds to the incoming precursor and finalizes matrix translocation using ATP. PAM comprises further five co-chaperones, i.e. Tim44, Mge1, Pam16, Pam17 and Pam18 that provide a membrane anchor for mt-Hsp70 and regulate the mt-Hsp70 ATPase activity (see Fig. 4.1) (Chacinska et al. 2009; van der Laan et al. 2010; Marom et al. 2011). Furthermore, Zim17/Tim15, which was also shown to bind mt-Hsp70, would be implicated in the maintenance of the solubility of the aggregate-prone mt-Hsp70 (Momose et al. 2007). The precise mechanism by which the PAM complex operates during protein translocation is still

under debate. In the "Brownian ratchet model" the mtHsp70 molecule binds to the incoming precursor and prevents its backsliding. By random diffusion, short segments of the polypeptide enter temporally into the matrix. Then, an additional mt-Hsp70 molecule binds to these segments, preventing again retrograde movement. In this process, ATP hydrolysis by mt-Hsp70 is enhanced by preprotein binding. Repeated cycles finally result in the full translocation of the precursor. On the other hand, the "pulling or power-stroke model" proposes that the ATP hydrolysis by the precursor-bound mt-Hsp70 induces a conformational change of mt-Hsp70, resulting in an active pulling of the precursor into the matrix. Moreover, in addition to these two models, modified versions have been proposed over the years. Additional studies will be required to settle this long standing dispute (Chacinska et al. 2009; van der Laan et al. 2010; Marom et al. 2011). Following translocation into the matrix, the presequence is removed from the precursor by specific mitochondrial proteases to release a mature protein (see point 4.1). Finally, the protein is folded and assembled with the help of mitochondrial chaperones, resulting in the completion of a mature and functionally active protein in the mitochondrial matrix (Hoogenraad et al. 2002).

Mammalian orthologs of the yeast TIM23 subunits forming the conducting channel, i.e. Tim50, Tim23, Tim17 and Tim44, have been identified. Moreover, mammalian homologues of the PAM members mt-Hsp70, Mge1 (mtGrpE), Pam16 (Magmas) and Pam18 (DNAJC19) are characterized. In addition, mammalian Hsp40 isoforms (Tid-1 proteins) are also reported to be a component of the PAM import motor in mammals (Hoogenraad et al. 2002; Goswami et al. 2010; Sinha et al. 2010; Marom et al. 2011).

4.2.2.3. Presequence processing

Once the precursor has been translocated, the presequence is no longer necessary and may hamper protein folding and assembly. Therefore, the presequence is proteolytically removed from the precursor upon translocation, releasing a mature protein in the mitochondrial matrix (Chacinska et al. 2009). The major presequence protease in the matrix is the heterodimeric mitochondrial processing peptidase (MPP). This metalloprotease typically cleaves presequences with an arginine residue at the -2 position ("R-2 motif") (Vogtle et al. 2009). It was also demonstrated that the cleavage of the presequence can occur in a two-step mechanism. Indeed, the mitochondrial intermediate peptidase (MIP) catalyzes preprotein maturation by removing an octapeptide after MPP processing. In this case, the presequence presents an "R-10 motif", with the arginine residue at position -2 from the MPP cleavage site and -10 from the MIP cleavage site (Gakh et al. 2002). Recently, a second two-step presequence processing, involving the intermediate cleaving peptidase Icp55, was evidenced in the yeast *Saccharomyces cerevisiae*. Icp55, a member of the aminopeptidase P (APP) family of metalloproteases, was shown to remove single amino acids from MPP-generated N-termini (Vogtle et al. 2009). Consequently, presequences which are sequentially cleaved by MPP and Icp55 exhibit an "R-3 motif". Until now, the two-step processing of presequences by MPP and Icp55 has never been demonstrated in mammals, although the mitochondrial form of mammalian APP3 should be a good candidate for sequential processing of MPP-generated termini (Vogtle et al. 2009). Finally, in a few cases, other proteases, like the less specific mAAA protease, were also shown to be involved in presequence processing (Nolden et al. 2005).

5. Pigs and dogs: species and phylogenetic relationships

5.1. Phylogeny of placental mammals

Mammalian phylogeny has been debated for more than a century. Recent molecular studies have unambiguously established that the eighteen orders of extant placental mammals can be grouped into three major clades: Afrotheria, Xenarthra and Boreoeutheria (Fig. 5.1). The clade Boreoeutheria is further divided in two major mammalian groups, Laurasiatheria and Euarchontoglires. Despite large-scale molecular phylogenetic analyses, the relationships between the three major clades remain unresolved. Also, many of the interordinal relationships (i.e. among the orders) within the four major mammalian groups remain unclear (Murphy et al. 2007; Wildman et al. 2007; Nishihara et al. 2009; Murphy and Eizirik 2009; Hallstrom and Janke 2010; McCormack et al. 2012). Therefore, no unambiguous phylogenic tree of placental mammals at the level of the order can be presented in this introduction. Instead, table 1.1 lists the eighteen orders of placental mammals and their affiliation to the major clades (Springer and Murphy 2007). Moreover, domestic pig (*Sus scrofa domesticus*) and dog (*Canis lupus familiaris*) belong both to the Laurasiatheria group. Pig is a member of the order Cetartiodactyla, while dog is a member of the order Carnivora.

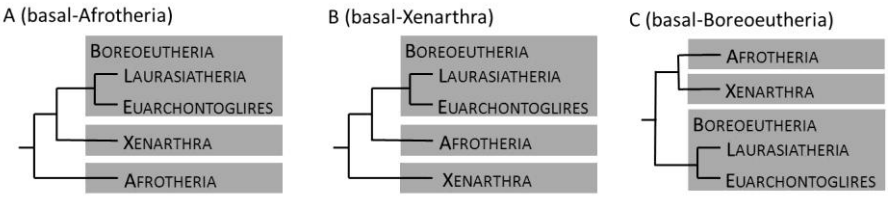

Fig. 5.1. Unresolved placental mammalian tree. Three competing hypotheses exist, predicting (A) a basal position of Afrotheria (B) a basal position of Xenarthra (C) a basal position of Boreoeutheria. [Adapted from Murphy et al. (2007) and Nishihara et al. (2009)].

Table 1.1. **Eighteen living orders in Placental mammals**

Boreoeutheria	
Laurasiatheria	
	Order Cetartiodactyla (cows*, pigs*, camels, hippos, whales, porpoises)
	Order Carnivora (dogs*, bears*, seals*, cats)
	Order Chiroptera (bats)
	Order Pholidota (pangolins)
	Order Eulipotyphla (moles, shrews, hedgehogs, solenodons)
	Order Perissodactyla (horses, rhinos, tapirs)
Euarchontoglires	
	Order Primates (humans*, monkeys*, lemurs, tarsiers)
	Order Dermoptera (flying lemurs)
	Order Scandentia (tree shrews)
	Order Rodentia (rats*, mice*, capybaras, squirrels)
	Order Lagomorpha (rabbits, hares, pikas)
Xenarthra	
	Order Xenarthra (sloths, armadillos, anteaters)
Afrotheria	
	Order Proboscidea (elephants)
	Order Sirenia (dugong, manatee)
	Order Hyracoidea (hyraxes)
	Order Tubulidentata (aardvark)
	Order Afrosoricida (golden moles, tenrecs, otter shrews)
	Order Macroscelidea (elephant shrews)

* Species which are studied/mentioned in this work

5.2. *Pig, a member of Cetartiodactyla*

According to the current classification, pigs belong to the order Cetartiodactyla, which diverged from other placental mammals approximately 84.6 million years ago (mya) (Murphy and Eizirik 2009). Cetardiodactyla are composed of four suborders, i.e. Tylopoda (camels and llamas), Suiformes (pigs and peccaries), Ruminantia (bovids, deer, tragulids and giraffes) and Cetancodonta (hippos, dolphins and whales). Phylogenetic relationships within Cetartiodactyla, and particularly the position of Suiformes, remain controversial (Fig. 5.2).

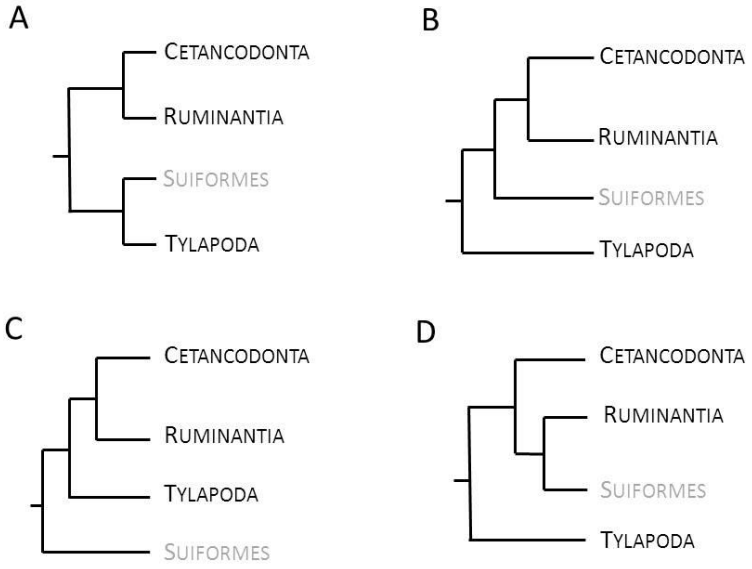

Fig. 5.2. Phylogeny of the Cetartiodactyls: a selection of hypotheses. It was proposed that **(A)** the Suiformes and Tylapoda cluster together as a sister clade of the Cetruminantia (Cetancodonta + Ruminantia) (Gatesy et al. 2002); **(B)** the Suiformes are a sister clade of the Cetruminantia (Price et al. 2005; O'Leary and Gatesy 2008; Zhou et al. 2011); **(C)** the Suiformes are the basal clade of the Cetartiodactyla (Marcot 2007; Hassanin et al. 2012); **(D)** the Suiformes and Ruminantia cluster together as a sister clade of the Cetancodonta (Agnarsson and May-Collado 2008). [Adapted from Boisserie et al. (2011)].

The suborder Suiformes consists of two living families: the Tasyassuidae (peccaries) and Suidae (pigs). The divergence of Suidae and Tayassuidae from their common ancestor would have occurred 33.8 − 37.2 mya (Orliac et al. 2010). According to our current knowledge, the extant Suidae family would comprise five genera, including *Sus*. The genus *Sus* appeared at least 3 − 5 mya in Europe and Indonesia, and is represented by seven species, among which *Sus scrofa*. The species *Sus scrofa* is geographically widespread, as it has spread naturally through Europe and Asia, and has been introduced into North and South America, Australia and Oceania (Ruvinsky et al. 2011). *Sus scrofa* diversified into numerous regionally distinct populations (subspecies), and several of them are likely to have been independently domesticated, or have contributed genes to domestic pigs through hybridization. The domestication process is thought to have begun over 10.000 years ago (Larson et al. 2011).

5.3. Dog, a member of Carnivora

5.3.1. Order Carnivora

The order Carnivora consists of about 286 living species and appeared around 63 mya. Early in the history of Carnivora, the order split into two suborders, the Caniformia (dog-like carnivores) and Feliformia (cat-like carnivores). Each of these groups diversified to form 16 extant families (Fig. 5.3). The suborder Caniformia further split into two groups: (i) the Cynoidea, comprising the Canidae family (dogs and relatives) which is thought to be the deepest divergence in the Caniformia, (ii) the Arctoidea, comprising the families Ursidae (bears), Procyonidae (raccoons, kinkajou and coatis), Mephitidae (skunks), Mustelidae (weasels and otters), Ailuridae (red panda), Otariidae (fur seals), Odobenidae (walrus) and Phocidae ('true seals') (Van Valkenburgh and Wayne 2010; Eizirik et al. 2010). Despite some controversy persists concerning the phylogenetic relationships among Caniformia families, several portions of the tree have been clarified and are well supported by numerous molecular analyses (reviewed in Eizirik and Murphy (2009) and Flynn et al. (2010)):

i) Skunks do not belong to the Mustelidae and form a distinct arctoid clade, i.e. Mephididea.
ii) Mustelidae and Procyonidae are sister taxa.
iii) Odobenidae are more closely related to Otariidae than to Phocidae. These three families form together the Pinnipedia clade, which is most closely related to the Musteloidea clade (Mustelidea + Procyonidae + Ailuridae + Mephitidae).
iv) The red panda (*Ailurus fulgens*) is the unique living member of the family Ailuridae. The phylogenetic position of Ailuridae within Musteloidea remains unresolved, being continuously disputed with each new phylogenetic study.

v) Giant panda (*Ailuropoda melanoleuca*) is a member of the Ursidae family. Its phylogenetic position is basal to all other living ursids.

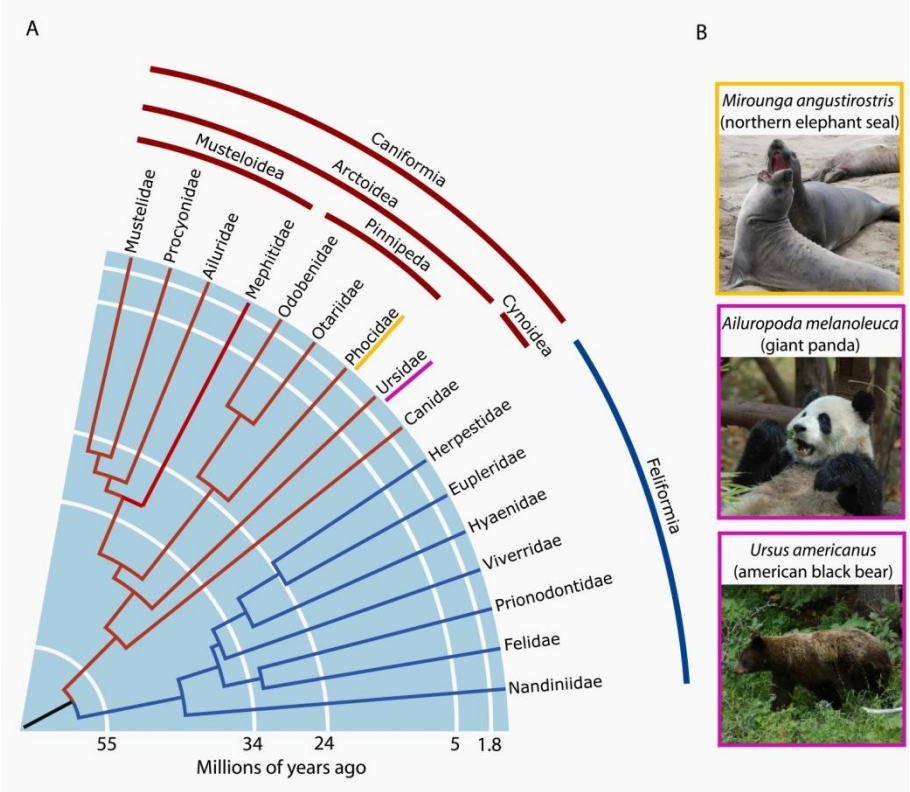

Fig. 5.3. Time-calibrated phylogeny of the order Carnivora. (A) The phylogeny of Carnvivora is currently not completely stabilized, e.g. concerning the position of Ailuridae. The presented phylogenetic tree is based on 14 nuclear gene sequences from 50 different genera representing all carnivoran families (Eizirik et al. 2010). [Adapted from Van Valkenburgh and Wayne (2010)]. **(B)** Non-canid carnivoran species which are studied in this work are represented. Pictures are from Myers et al. (2012).

5.3.2. Family Canidae

The family Canidae diverged from other Carnivora about 50 mya, but extant canids have diverged from a common ancestor within the last 10 million years. As a consequence, the 35 living canid species are genetically very similar (Ostrander and Wayne 2005). The Canidae family comprises three major phylogenetic groups: the fox-like canids, the wolf-like canids and the South American canids (Fig. 5.4). Additionally, several canids do not belong to any of the three main clades, such as the gray fox (*Urocyon cinereoargenteus*). The gray fox lineage was shown to be the most primitive among canids (Lindblad-Toh et al. 2005; Wayne and Ostrander 2007). The wolf-like canids, which have origins more than 6 mya, are more closely related to South American canids than to fox-like canids. Among wolf-like canids, dog (*Canis lupus familiaris*) is most closely related to gray wolf (*Canis lupus*), followed by coyote (*Canis latrans*), golden jackal (*Canis aureus*) and Ethiopian wolf (*Canis simensis*). African jackals (*Canis mesomelas* and *Canis adustus*) are the most basal members. The South American canids are rooted by the bush dog (*Speothos venaticus*) and the maned wolf (*Chrysocyon brachyurus*). Bat-eared fox (*Otocyon megalotis*) and the raccoon dog (*Nyctereutes procyonoides*) root the red fox-like canids (Lindblad-Toh et al. 2005).

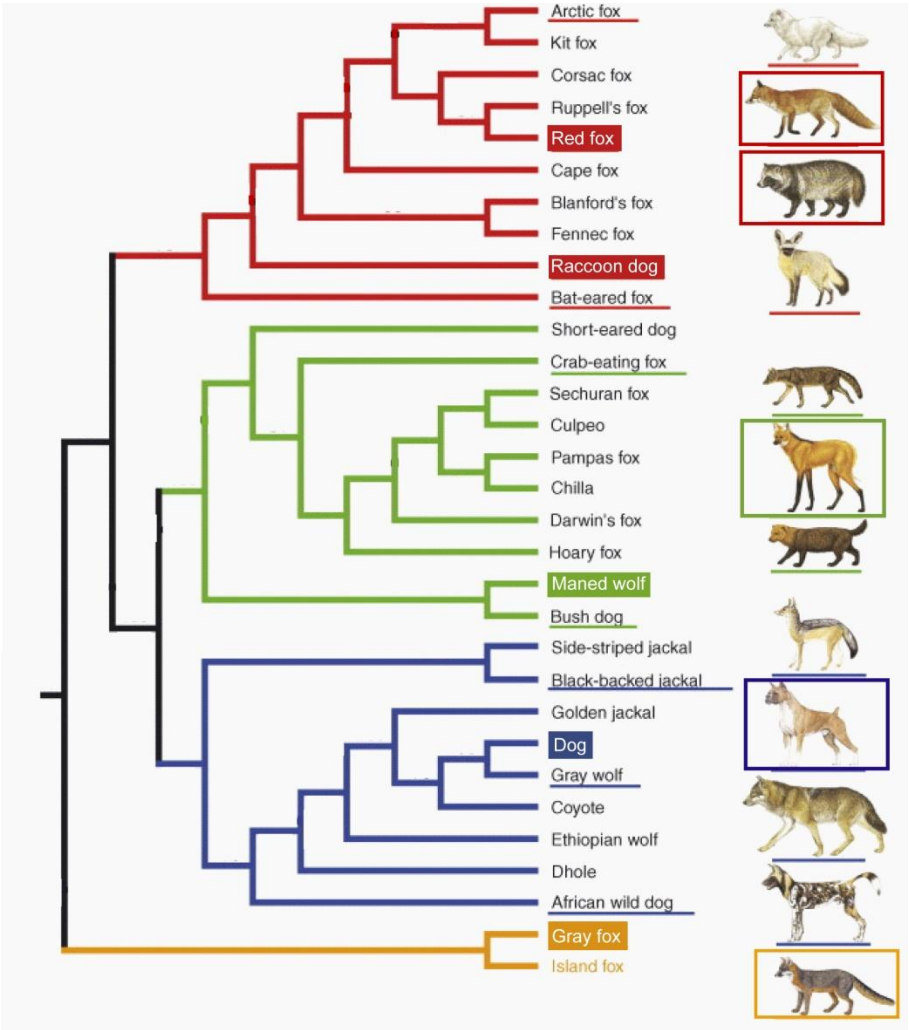

Fig. 5.4. Phylogeny of canid species. The phylogenetic tree is based on ~15kb from 12 exons and 4 introns. The three major phylogenetic groups are indicated in red for the fox-like canids, in green for the South American canids and in blue for the wolf-like canids. The gray fox and the island fox indicated in orange do not belong to a major clade. Underlined species names are represented with corresponding illustrations. Species which are studied in this work are boxed. [Adapted from Lindblad-Toh et al. (2005)].

5.3.3. Domestic dogs

Dogs are the first domesticated species in human history. Extensive molecular analyses clearly demonstrate that the domestic dog is derived from gray wolves only, rather than other wolf-like canids (Ostrander and Wayne 2005). Accordingly, domestic dog and gray wolf are extremely close relatives, differing by only ~0.04% and 0.21% in ~15 kb nuclear exon and intron sequences, respectively (Lindblad-Toh et al. 2005). The process by which domestication took place is poorly understood and involves most likely multiple domestication and backcrossing events (Leonard et al. 2002; Savolainen et al. 2002; Vila et al. 2005). Dogs would have evolved first through a progressive adaptation to the human presence, sharing living space and food sources. Later, humans have selectively bred dogs, creating more than 400 breeds exhibiting large behavioral and morphological variation (Lindblad-Toh et al. 2005). To date, the oldest fossil evidence which places dogs in close proximity with humans is 31.000 years old and was discovered in the Condroz, a region in the south of Belgium (Germonpre et al. 2009). However, whether these fossils represent the earliest domestic dogs or extinct varieties of wolves remains a matter of debate. Moreover, estimations regarding the time since domestication based on molecular studies vary greatly. Overall, domestication is thought to have originated at least 15.000, and possibly as far back as >100.000 years ago (Parker et al. 2010). Also, the geographical origin of dog domestication remains elusive. Indeed, albeit domestication was thought to have taken place in East Asia, recent mtDNA sequence analyses of African village dogs called this theory into question (Boyko et al. 2009).

II. Aim of the study

To regulate intracellular levels of ROS and RNS, mammalian cells are equipped with antioxidant enzymes, amongst which PRDX5. This peroxidase exhibits a remarkably wide subcellular distribution. Indeed, in human, PRDX5 was shown to be targeted to the mitochondria, the cytosol, the peroxisomes and in several cases, the nucleus. In this work, we studied the interspecific variability of PRDX5 mitochondrial targeting. Our work is based on the hypothesis that, although mitochondrial localization of PRDX5 is conserved amongst most animals, mitochondrial targeting of PRDX5 is absent in domestic pig and domestic dog.

In the first part of this study, the existence of interspecific variability in PRDX5 mitochondrial targeting was investigated. To this end, we examined the existence of a functional mitochondrial targeting sequence in lugworm PRDX5 and we compared PRDX5 subcellular distribution in domestic pig and rat. Afterward, the existence of compensatory mechanisms counterbalancing the absence of mitochondrial PRDX5 was investigated in pig liver mitochondrial extracts.

The second and third parts focused on the absence of mitochondrial PRDX5 in domestic dog. We assessed the absence of PRDX5 in dog mitochondria and examined the molecular evolution of PRDX5 mitochondrial targeting sequence in Caniformia. Moreover, we studied the functional consequences of the restoration of mitochondrial PRDX5 in dog cells, by expressing mitochondrial PRDX5 in Madin-Darby canine kidney (MDCK) cells.

During this thesis, we contributed to the following publications:

i) Knoops, B., Loumaye, E., and Van der Eecken, V. (2007) Evolution of the peroxiredoxins. *Subcell Biochem* 44: 27-40 (see provided CD-ROM).
ii) Knoops, B., Goemaere, J., Van der Eecken, V., and Declercq, J.P. (2011) Peroxiredoxin 5: Structure, mechanism and function of the mammalian

atypical 2-Cys peroxiredoxin. *Antioxid Redox Signal* 15: 817-829 (see provided CD-ROM).

iii) Nguyen-Nhu, N.T., Berck, J., Clippe, A., Duconseille, E., Cherif, H., Boone, C. Van der Eecken, V., Bernard, A., Banmeyer, I., and Knoops B. (2007) Human peroxiredoxin 5 gene organization, initial characterization of its promoter and identification of alternative forms of mRNA. *Biochim Biophys Acta* 1769: 472-483 (see provided CD-ROM).

iv) Van der Eecken, V., Clippe, A., Van Veldhoven, P.P., and Knoops, B. (2011) Mitochondrial targeting of peroxiredoxin 5 is preserved from annelids to mammals but is absent in pig *Sus scrofa domesticus*. *Mitochondrion* 11: 973-81.

III. Results

MITOCHONDRION
Volume 11, Number 6, Pages 973-81, 2011

doi:10.1016/j.mito.2011.06.013

6. Mitochondrial targeting of peroxiredoxin 5 is preserved from annelids to mammals but is absent in pig *Sus scrofa domesticus*

Valérie Van der Eecken[a], André Clippe[a], Paul P. Van Veldhoven[b] and Bernard Knoops[a,]

[a] Université catholique de Louvain, Institut des Sciences de la Vie (ISV), 4-5 place Croix du Sud, B-1348 Louvain-la-Neuve, Belgium.
[b] Katholieke Universiteit Leuven, Department of Molecular Cell Biology, LIPIT, Campus Gasthuisberg, Herestraat, 3000 Leuven, Belgium.

Address correspondence to:
Prof. Bernard Knoops
Institut des Sciences de la Vie
Université catholique de Louvain
place Croix du Sud, 4-5 bte 2
B-1348 Louvain-la-Neuve
Belgium
E-mail: bernard.knoops@uclouvain.be

Received 7 December 2010;
Received in revised form 13 May 2011;
Accepted 29 June 2011.

Abstract

Peroxiredoxin 5 (PRDX5) is a thioredoxin peroxidase able to reduce hydrogen peroxide, alkyl hydroperoxides and peroxynitrite. In human, PRDX5 was reported to be localized in the cytosol, the mitochondria, the peroxisomes and the nucleus. Mitochondrial localization results from the presence of an N-terminal mitochondrial targeting sequence (MTS). Here,

we examined the conservation of mitochondrial localization of PRDX5 in animal species. We found that PRDX5 MTS is present and functional in the annelid lugworm *Arenicola marina*. Surprisingly, although mitochondrial targeting is well conserved among animals, PRDX5 is missing in mitochondria of domestic pig. Thus, it appears that mitochondrial targeting of PRDX5 may have been lost throughout evolution in animal species, including pig, with unknown functional consequences.

***Keywords*:** Peroxiredoxin, Subcellular targeting, Mitochondrion, Annelids, Mammals

Abbreviations used: *Am*PRDX5: *Arenicola marina* peroxiredoxin 5; DTT: dithiothreitol; GFP: Green Fluorescent Protein; GPX: glutathione peroxidase; *Hs*PRDX5: *Homo sapiens* peroxiredoxin 5; L-PRDX5: long form of peroxiredoxin 5; MTS: mitochondrial targeting sequence; PRDX: peroxiredoxin; RNS: reactive nitrogen species; ROS: reactive oxygen species; S-PRDX5: short form of peroxiredoxin 5; *Ss*PRDX5: *Sus scrofa* peroxiredoxin 5; *t*-BHP: *tert*-butyl hydroperoxide

6.1. Introduction

To avoid oxidative and nitrosative damage caused by reactive oxygen species (ROS) and reactive nitrogen species (RNS), cells have developed enzymatic antioxidant defence systems including peroxiredoxins (PRDXs) (Wood et al. 2003; Rhee et al. 2005). Among the six isoforms of mammalian PRDXs (PRDX1-6), PRDX5 is the last member that has been characterized (Knoops et al. 1999; Kropotov et al. 1999; Yamashita et al. 1999). PRDX5 is able to reduce hydrogen peroxide, alkyl hydroperoxides or peroxynitrite and uses cytosolic and mitochondrial thioredoxins as physiological electron donors (Knoops et al. 1999; Seo et al. 2000; Dubuisson et al. 2004; Trujillo et

al. 2007). Moreover, the cytoprotective role of PRDX5 has been well documented as reviewed recently (Knoops et al. 2011).

Human PRDX5 can be localized in the cytosol, the mitochondria, the peroxisomes and the nucleus (Knoops et al. 1999; Kropotov et al. 1999; Yamashita et al. 1999; Seo et al. 2000; Kinnula et al. 2002; Lu et al. 2006). Intracellular targeting in human cells appears to depend on the use of multiple transcription start sites and two alternative translation initiation sites (Nguyen-Nhu et al. 2007). Indeed, translation initiating at the second site produces a short form (S-PRDX5) which is found in the cytosol, the peroxisomes and the nucleus (Knoops et al. 1999; Kropotov et al. 1999; Yamashita et al. 1999; Seo et al. 2000). If translation initiates at the first AUG codon, a long PRDX5 form (L-PRDX5) containing an additional N-terminal mitochondrial targeting sequence (MTS) is expressed (Nguyen-Nhu et al. 2007). L-PRDX5 is imported into the mitochondrial matrix where the MTS is cleaved, releasing a mature form which is indistinguishable from S-PRDX5 (Knoops et al. 1999; Wattiez et al. 1999; Seo et al. 2000; Banmeyer et al. 2004). Moreover, based on MTS identification in databases, mitochondrial localization of PRDX5 seems to be well conserved in animal kingdom (Zhang et al. 2003; Dubuisson et al. 2004; Nguyen-Nhu et al. 2007; Li et al. 2011) (see also Fig. 6.1 and annex 1). Accordingly, the presence of PRDX5 in mitochondria was experimentally demonstrated in human, rat, mouse, hamster, bovine and fruitfly (Knoops et al. 1999; Oberley et al. 2001; Banmeyer et al. 2004; Leyens et al. 2004; Pagliarini et al. 2008; Radyuk et al. 2009).


MTS
Human #
House mouse #
Norway rat #
Dog
Giant panda
Pig
Cattle #
Zebrafish
Japanese lancelet
Fruitfly #
Bay scallop
Lugworm
PTS1

Fig 6.1 (facing page). ClustalX 2.0.7 amino acid sequence alignment of human PRDX5 and animal orthologs. Dots (.) and double dots (:) indicate conservative substitutions, asterisks (*) indicate identities. Conservative cysteines, peroxisomal targeting sequences (PTS1) and TargetP v1.1 predicted MTS are highlighted in yellow, blue and red respectively. Methionines (bold) encoded by the two alternative initiation codons are indicated. Species names are written in blue for mammals, green for teleosteans (fishes), pink for cephalochordates, black for arthropods, grey for mollusks and red for annelids. The names of the species for which mitochondrial PRDX5 localization was experimentally evidenced are followed by a hash (#). GenBank accession numbers are as follows: NP_036226 (Human, *Homo sapiens*); NP_036151 (House mouse, *Mus musculus*); NP_446062 (Norway rat, *Rattus norvegicus*); XP_533241 (Dog, *Canis lupus familiaris*); XM_002916664 (Giant panda, *Ailuropoda melanoleuca*); NP_999309 (Pig, *Sus scrofa*); NP_777174 (Cattle, *Bos taurus*); CN508467 (Zebrafish, *Danio rerio*); AF498232 (Japanese lancelet, *Branchiostoma belcheri tsingtaunese*); NP_650679 (Fruit fly, *Drosophila melanogaster*); HM461987 (Bay scallop, *Argopecten irradians*); AAY96293 (Lugworm, *Arenicola marina*).

Here, we show that, while mitochondrial targeting of PRDX5 is widely conserved from annelids to mammals, this subcellular localization has been lost in some species including domestic pig *Sus scrofa domesticus*.

6.2. *Materials and methods*

6.2.1. Reagents and antibodies

Dulbecco's Modified Eagle medium (DMEM), F-12K medium, foetal calf serum (FCS), GlutaMAX, streptomycin, penicillin, pcDNA3.1/CT-GFP-TOPO vector and Mitotracker Red were obtained from Invitrogen. FuGENE-6 reagent was purchased from Roche. H_2O_2, *tert*-butyl hydroperoxide (*t*-BHP), Ponceau S, glutathione peroxidase (GPX) from bovine erythrocytes, mouse anti-β-actin monoclonal antibody and FITC-conjugated donkey anti-sheep IgG were purchased from Sigma. Polyclonal rabbit anti-PRDX3 and rabbit anti-PRDX5 antibodies, raised against recombinant human proteins, were obtained previously (Wang et al. 2001; De Simoni et al. 2008). Sheep anti-human catalase polyclonal antibody was obtained from SanBio and is raised against purified catalase from erythrocytes. Rabbit anti-GPX1 and rabbit anti-GPX4 polyclonal antibodies were obtained from AbFrontier and

are raised against recombinant human protein. Rat GPX4 monoclonal antibody raised against a peptide from murine GPX4 was kindly given by Professor M. Conrad (Helmholtz Zentrum München-German Research Center for Environmental Health) and is described in Seiler et al. (2008). FITC-conjugated donkey anti-rabbit IgG and TRITC-conjugated donkey anti-rabbit IgG were purchased from Jackson ImmunoResearch Laboratories, Inc. Peroxidase-conjugated goat anti-rabbit IgG, rabbit anti-rat IgG and goat anti-mouse IgG were obtained from Dako. Western Lightning Chemiluminescence kit was purchased from Perkin Elmer. Human recombinant PRDX5 was obtained as described previously (Wang et al. 2001).

6.2.2. Computer analysis

Multiple sequence alignments were performed with ClustalX 2.0.7 software (Larkin et al. 2007). TargetP 1.1 was used for MTS prediction (Nielsen et al. 1997; Emanuelsson et al. 2000).

6.2.3. Cell culture

COS-7 (green monkey kidney) and SAOS-2 (human primary osteogenic sarcoma) cell lines were cultured in DMEM 4.5g D-glucose/L with GlutaMAX, supplemented with 10% FCS. LLC-PK10 (porcine kidney) cells were cultured in DMEM/F12 (1:1) with GlutaMAX, supplemented with 10% FCS. C6 (rat gliome) cells were cultured in F-12K Medium, supplemented with 2,5% FCS and 15% horse serum. Cell lines were maintained at 37°C in 5% CO_2 in the presence of 100 U/ml streptomycin and 100 U/ml penicillin.

6.2.4. Expression of Homo sapiens and Arenicola marina PRDX5 MTS in fusion with Green Fluorescent Protein in COS-7 cells

The sequence encoding the MTS of human PRDX5 (*Hs*PRDX5) was PCR-amplified from human *PRDX5* cDNA (Knoops et al., 1999) using primers 5′-GGTTATGGGACTAGCTGGCG-3′ and 5′-TGATTGGGGCCATGGCTGCAGCG-3′. The sequence encoding the potential MTS of *Arenicola marina* PRDX5 (*Am*PRDX5) was amplified from *Arenicola marina PRDX5* cDNA (GenBank ID: DQ059566) using primers 5′-CACGATGCTGTCTCTGCGTT-3′ and 5′-CCTTGATCGGCATTCTGCGA-3′. PCR products were cloned into pcDNA3.1/CT-GFP-TOPO vector and the resulting plasmids were sequenced. COS-7 cells cultured on coverslips were transiently transfected using FuGENE-6 reagent according to manufacturer's instructions. 48 hours after transfection, cells were incubated with 100 nM Mitotracker Red and fixed with 4% formaldehyde. The coverslips were mounted in Mowiol containing 50 µg/ml 4′, 6-diamidino-2-phenylindole dihydrochloride (DAPI).

6.2.5. Purification of liver mitochondria

Pig and rat livers were homogenized and centrifuged to obtain nuclear fractions (N) and postnuclear supernatants (E). E-fractions were subfractionated into heavy mitochondrial (M), light mitochondrial (L), microsomal (P) and cytosolic (S) fractions by differential centrifugation. The L-fraction was further subfractionated on a Percoll gradient. Marker enzymes and protein content were measured in each fraction. Experimental procedures have been described previously (Declercq et al. 1984; Van Veldhoven et al. 1996).

6.2.6. Western blotting

Western blotting was performed as described previously (Banmeyer et al. 2004). Blots were probed with 1:4000 rabbit anti-human PRDX5 and 1:4000 rabbit anti-human PRDX3 polyclonal antibodies. PRDX3 protein levels were normalized to actin levels using 1:5000 mouse anti-β-actin monoclonal antibody. GPX1 detection was performed using 1:2000 rabbit anti-human GPX1 polyclonal antibody. For the determination of the subcellular distribution of GPX4, blots were probed with 1:5 rat anti-GPX4 monoclonal antibody (Fig. 6.7.D) and 1:2000 rabbit anti-human GPX4 polyclonal antibody. GPX4 protein level measurement was performed with rabbit anti-human GPX4 polyclonal antibody (Fig. 6.7.E). After incubation with the primary antibody, nitrocellulose membranes were washed in TTBS, followed by incubation with the HRP-conjugated secondary antibody. Blots were developed with the Western Lightning Chemiluminescence kit according to manufacturer's instructions. Proteins transferred to the blots were stained by incubating the nitrocellulose membrane with 0.5% (w/v) Ponceau S in 1% (v/v) acetic acid. Statistical analysis was carried out on the means of triplicates using a Student's t-test.

6.2.7. Immunostaining

Cells cultured on coverslips were stained with 100 nM Mitotracker Red prior to fixation. Immunostaining was performed as described previously (Knoops et al. 1999) using 1:200 rabbit anti-human PRDX5 polyclonal antibody and 1:50 FITC-conjugated donkey anti-rabbit IgG. Co-localization experiments with catalase were performed with 1:200 rabbit anti-human PRDX5 polyclonal antibody, 1:100 sheep anti-human catalase polyclonal antibody, 1:50 TRITC-conjugated donkey anti-rabbit IgG and 1:50 FITC-conjugated donkey anti-sheep IgG.

6.2.8. Peroxidase assay

Peroxidase activity was measured as described by Knoops et al. (1999) with minor modifications. The Percoll fractions 1 to 3 were pooled and incubated at 37°C in PBS containing 0.5 mM dithiothreitol (DTT). The reaction was initiated with the addition of 0.5 mM H_2O_2 or 0.3 mM *tert*-butyl hydroperoxide (*t*-BHP). Every 5 min, remaining H_2O_2 or *t*-BHP was measured by addition of ferrous ammonium sulfate and potassium thiocyanate to 25 µl of reaction mixture and compared with standards. Peroxidase activity of recombinant human PRDX5 and GPX from bovine erythrocytes was measured according to the same protocol. Statistical analysis was carried out on the means of triplicates using a Student's t-test.

6.3. Results

6.3.1. A functional MTS is present in AmPRDX5

To demonstrate the presence and the functionality of an MTS in *Am*PRDX5, a pcDNA3.1 plasmid containing the sequence encoding the 31 N-terminal residues of *Am*PRDX5 fused with the Green Fluorescent Protein (GFP) was generated (Fig. 6.2.E). After transient transfection of COS-7 cells with this vector, the reporter protein was detected in mitochondria, as demonstrated by colocalization with Mitotracker Red (Fig. 6.2. F-H). Human PRDX5 (*Hs*PRDX5) MTS constituted the positive control for MTS functionality (Fig. 6.2. A-D).

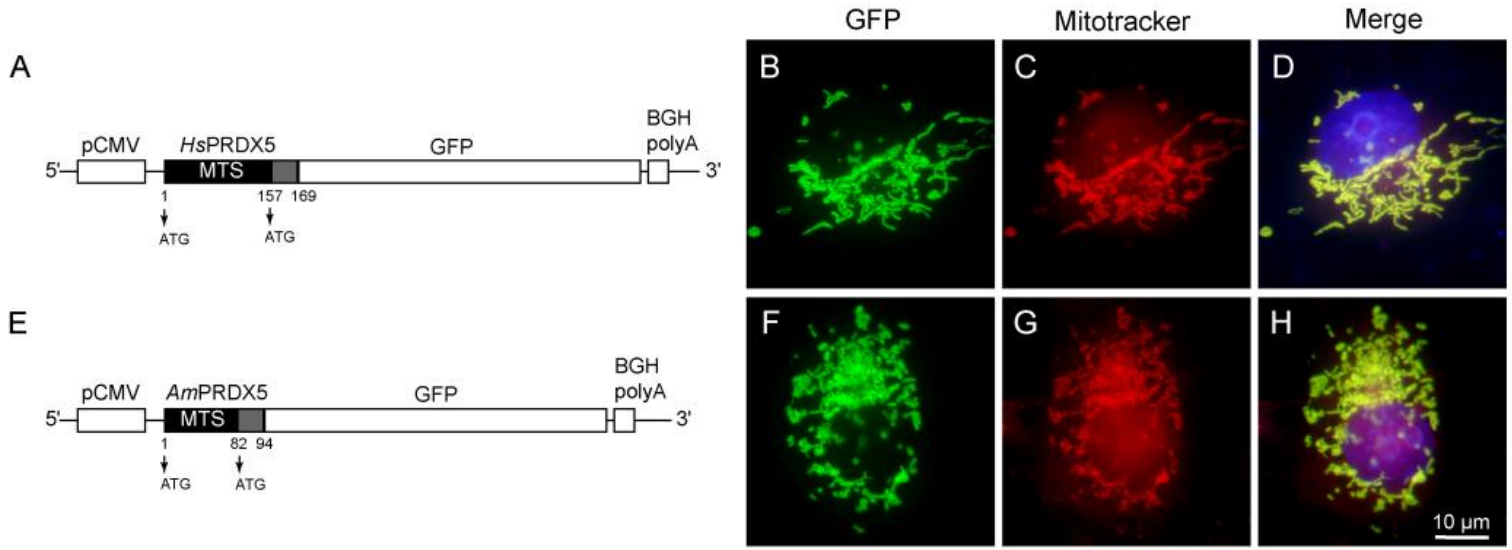

Fig. 6.2. Subcellular localization of *Homo sapiens* (A-D) and *Arenicola marina* (E-H) PRDX5 mitochondrial targeting sequences expressed in fusion with GFP. A and E, structure of the constructs cloned into mammalian expression vector pcDNA3.1 and transfected in COS-7 cells. Both alternative ATG initiation codons are indicated (arrows). Transfected cells were examined for GFP fusion expression (B and F). Mitochondria were stained with Mitotracker Red (C and G) and nuclei were counterstained with DAPI. *Am*PRDX5, *Arenicola marina* PRDX5; BGH polyA, bovine growth hormone polyadenylation signal; *Hs*PRDX5, *Homo sapiens* PRDX5; MTS, mitochondrial targeting sequence; pCMV, promoter of cytomegalovirus.

6.3.2. PRDX5 is absent in domestic pig mitochondria

Analysis of pig PRDX5 (*Ss*PRDX5) sequences from GenBank databases revealed the presence of a unique translation initiation codon for *SsPRDX5* corresponding to the second translation initiation site of *HsPRDX5* that produces the short form of the protein (S-PRDX5). The first AUG initiation codon enabling the translation of the long form of PRDX5 (L-PRDX5) is not present in pig (GenBank ID: NM_214144 and CU861533).

Absence of mitochondrial PRDX5 (L-PRDX5) in domestic pig tissue was confirmed by subcellular fractionation. Firstly, fractions resulting from the differential centrifugation of liver homogenate were analyzed for enzyme markers (see annex 2). Western blotting analysis of PRDX5 revealed that the enzyme was mainly present in the cytosolic (S) fraction (see annex 2). Secondly, in order to analyse PRDX5 localization in both peroxisomes and mitochondria, the light mitochondrial fraction (L) was further subfractionated on a Percoll gradient. PRDX5 was detected in the peroxisome-enriched fractions but not in fractions containing mitochondria (Fig. 6.3.A and C). When applying a similar approach to rat liver, rat PRDX5, used as positive control, was detected in both peroxisomal and mitochondrial fractions (Fig. 6.3.B and D).

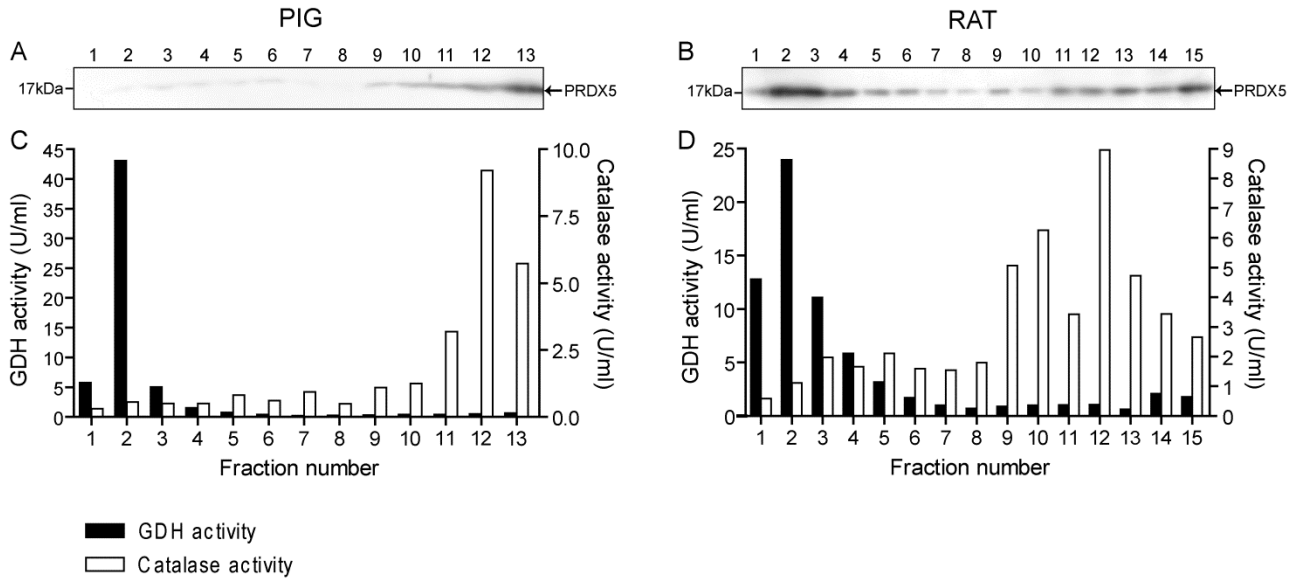

Fig. 6.3. Subcellular fractionation of pig and rat liver. Fractions obtained by separation of the light mitochondrial fraction (L) on a self-generating Percoll gradient were analyzed for GDH (mitochondrial marker) and catalase (peroxisomal marker) activities (C and D). Analysis of pig (A) and rat (B) PRDX5 content was performed by Western Blotting.

To confirm the absence of pig PRDX5 in mitochondria, PRDX5 expression was examined using immunofluorescence in the LLC-PK10 (pig) cell line. PRDX5 was detected in the cytosol and in organelles with granular patterns, but no colocalization with the mitochondrial marker was observed (Fig. 6.4. A-C). SAOS-2 and C6 cell lines were used as a positive control for the presence of PRDX5 in mitochondria of human and rat cells respectively (Fig. 6.4. D-I).

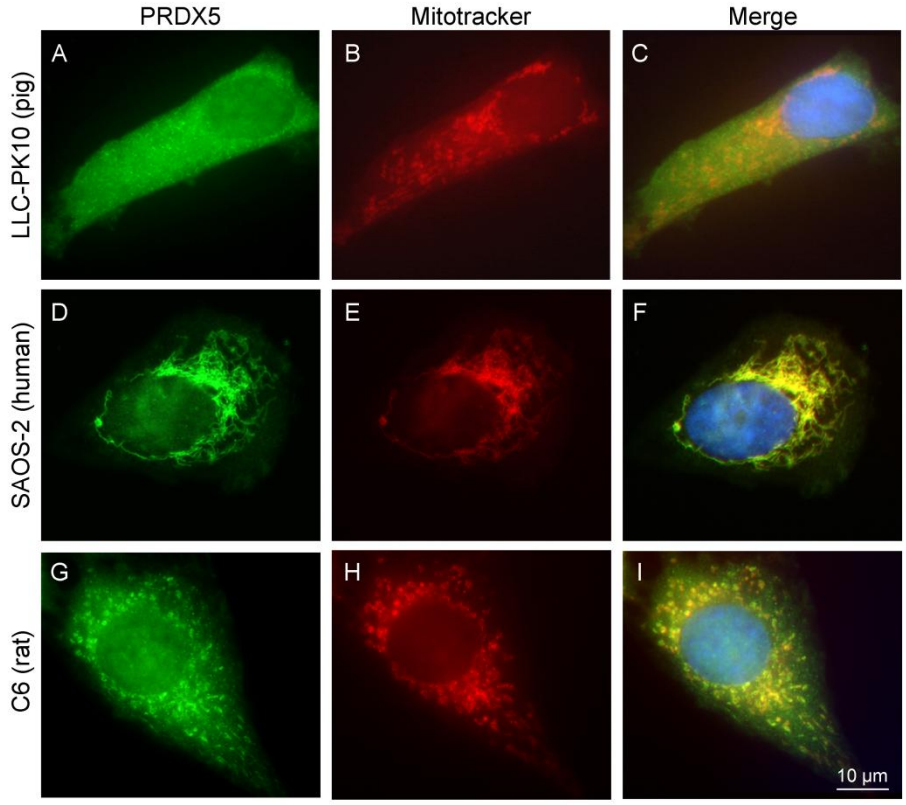

Fig. 6.4. Subcellular localization of PRDX5 in pig LLC-PK10 (A-C), human SAOS-2 (D-F) and rat C6 (G-I) cells. PRDX5 immunofluorescence detection (A, D and G) was performed, mitochondria were stained with Mitotracker Red (B, E and H) and nuclei were labelled with DAPI.

PRDX5 detection by immunofluorescence evidenced also the peroxisomal localization of the protein, as shown by co-localization with peroxisomal catalase (Fig. 6.5). In the LLC-PK10 and SAOS-2 cell lines,

PRDX5 was detected in almost all peroxisomes. In the C6 cell line, PRDX5 signal was detected in only several peroxisomes.

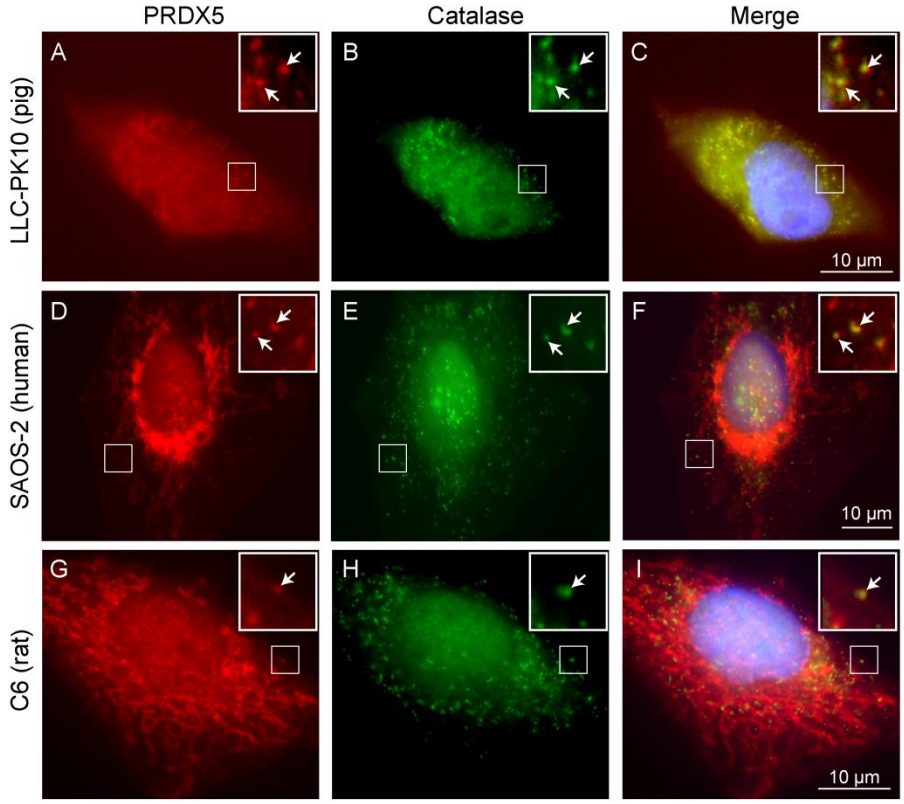

Fig. 6.5. Peroxisomal localization of PRDX5 in pig LLC-PK10 (A-C), human SAOS-2 (D-F) and rat C6 (G-I) cells. Detection of PRDX5 (A, D and G) and peroxisomal catalase (B, E and H) was performed by immunofluorescence. Nuclei were labelled with DAPI. Arrows indicate peroxisomes. Insets on the right corner represent magnification of outlined areas.

6.3.3. PRDX3, GPX1 and GPX4 expression in pig mitochondria

In human, PRDX5 coexists in mitochondria with other peroxidases, i. e. PRDX3, GPX1 and GPX4 (Cox et al. 2010). To confirm the presence of PRDX3 in pig mitochondria, the fractions obtained by subcellular fractionation of the liver were analyzed for PRDX3 content (Fig. 6.6.A). The results indicated that, like rat PRDX3, pig PRDX3 is present in mitochondria-enriched

fractions. To compare PRDX3 protein levels in pig and rat liver, PRDX3 was analyzed by Western blotting in postnuclear (E) fractions and normalized to actin levels (Fig. 6.6.B). The results indicated that PRDX3 protein content was ~4.5 fold higher in pig compared to rat (Fig. 6.6.C).

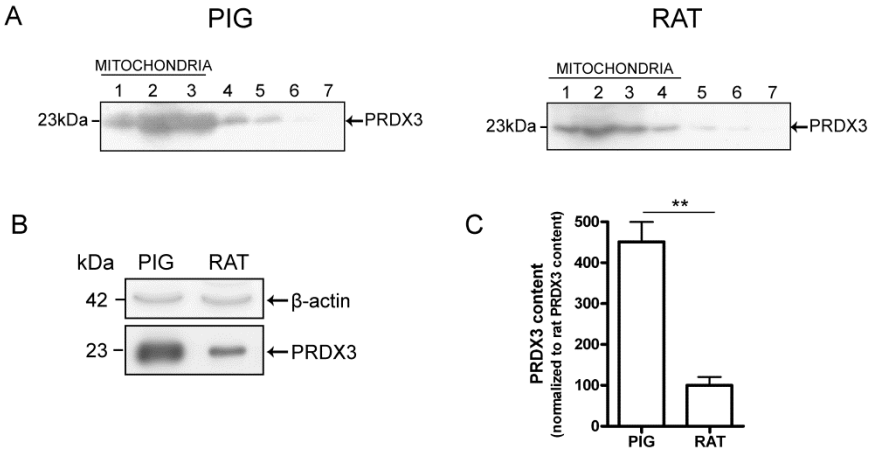

Fig. 6.6. Expression of PRDX3 in pig and rat liver mitochondria. Mitochondrial distribution of PRDX3 was assessed by Western blotting in the seven first fractions obtained by separation of the pig and rat liver light mitochondrial (L) fraction on a self-generating Percoll gradient (A). PRDX3 protein level was evaluated by Western blotting on pig and rat postnuclear (E) fractions (B). PRDX3 protein levels were normalized to β-actin and were expressed in relative percentage of PRDX3 content in rat liver (C). Values represent means ± S.E.M. from triplicates. Significance is designed as ** $p < 0.01$.

GPX1 and GPX4 localization in pig mitochondria was also examined by Western blotting on the fractions issued from liver subcellular fractionation (Fig. 6.7.A and 6.7.D). GPX1 and GPX4 were detected in mitochondrial fractions. Since GPX1 and GPX4 are not exclusively localized in mitochondria (Herbette et al. 2007), the comparison of GPX1 and GPX4 protein levels in pig and rat mitochondria was performed on the fractions containing these purified organelles. Therefore, the three first fractions obtained by separation on Percoll gradient were pooled and the GPX1 and GPX4 protein levels were analyzed by Western blotting. The values were normalized to the total transferred protein levels evaluated by Ponceau S staining. No difference of mitochondrial GPX1 content was detected

between rat and pig, while GPX4 content in mitochondria was ~2.7 fold higher in pig compared to rat (Fig. 6.7. C and F).

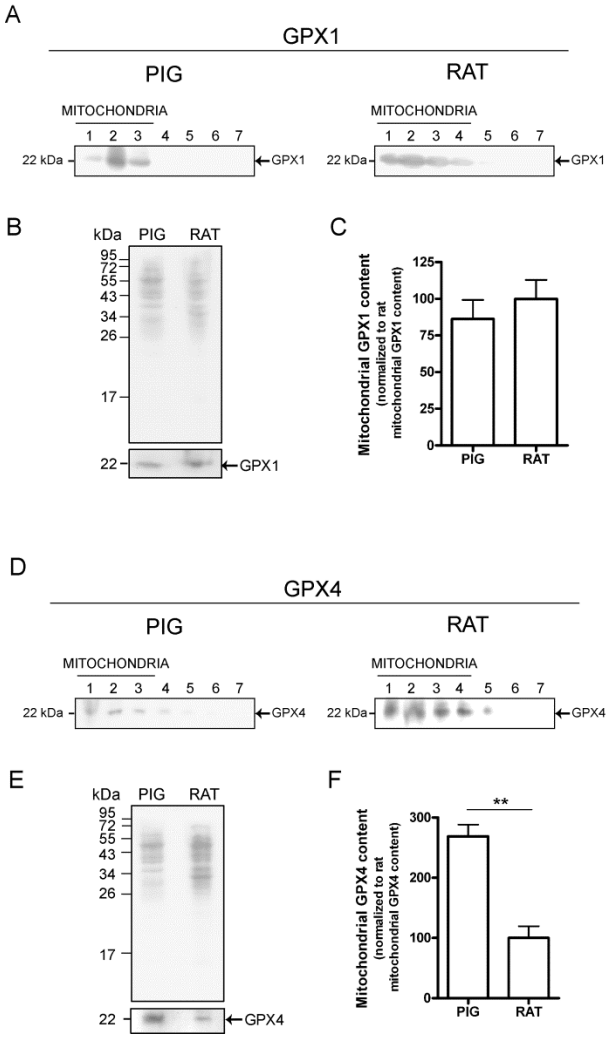

Fig. 6.7. Expression of GPX1 and GPX4 in pig and rat liver mitochondria. Mitochondrial distribution of GPX1 (A) and GPX4 (D) was assessed by Western blotting in the seven first fractions obtained by subcellular fractionation of pig and rat liver on a self-generating Percoll gradient. Mitochondrial GPX1 (B) and GPX4 (E) protein levels in pig and rat liver were evaluated by Western blotting on mitochondrial protein extracts deriving from the pooled three first Percoll fractions containing purified mitochondria. GPX1 and GPX4 protein levels were normalized to the total transferred protein level evaluated by Ponceau S staining and were expressed in relative percentage of GPX1 and GPX4 content in rat liver mitochondria (C and F). Values represent means ± S.E.M. from triplicates. Significance is designed as ** $p < 0.01$.

6.3.4. Comparison of peroxidase activity in pig and rat mitochondria

To examine the consequences of the absence of L-PRDX5 on peroxidase activity in porcine mitochondria, the global peroxidase activity was compared in pig and rat mitochondrial extracts. Peroxidase activity was evaluated by detecting the time-dependent consumption of H_2O_2 or *t*-BHP in presence of DTT as reductant. Human recombinant PRDX5 and purified GPX from bovine erythrocytes were used as positive controls. Recombinant PRDX5 exhibited peroxidase activity of 0.134 ± 0.032 nmol H_2O_2 / min x µg proteins and 0.177 ± 0.024 nmol *t*-BHP / min x µg proteins. Purified GPX exhibited peroxidase activities of 45.778 ± 7.129 nmol H_2O_2 / min x µg proteins and 82.901 ± 4.711 nmol *t*-BHP / min x µg proteins. These results indicate that DTT is able to reduce and regenerate both PRDXs and GPXs. Therefore, the peroxidase activity assay performed on mitochondrial extracts measures the peroxidase activities of both mitochondrial PRDXs and GPXs. No significant differences were detected between pig and rat peroxidase activities against H_2O_2 in liver mitochondrial extracts (Fig. 6.8). However, peroxidase activity against *t*-BHP was significantly lower in pig mitochondria than in rat mitochondria ($p < 0.001$).

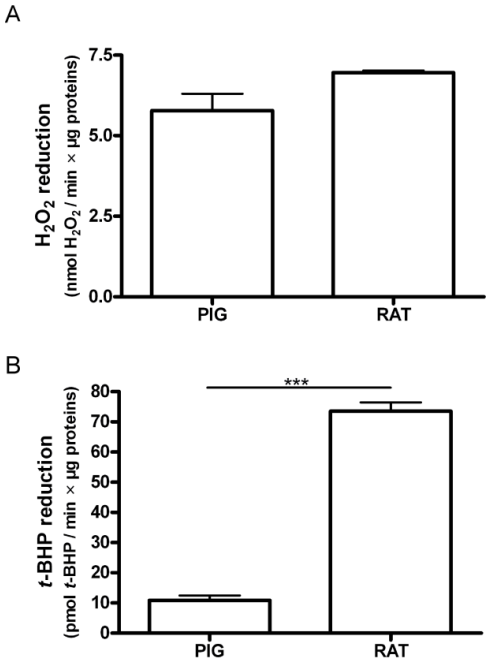

Fig. 6.8. Peroxidase activity in pig and rat mitochondrial protein extracts. Peroxidase activity was measured in the presence of DTT and H_2O_2 (A) or *t*-BHP (B). Proteins from the pooled three first fractions obtained by separation of the liver light mitochondrial fraction (L) on Percoll gradient were used. Results are the means ± S.E.M. of triplicate experiments. Significance is designed as *** $p < 0.001$.

6.4. Discussion

In this work, we first demonstrate the presence of a functional MTS in the annelid *Am*PRDX5, since the 31 N-terminal residues of the protein are sufficient to target the GFP reporter protein into mitochondria. Phylogenetically, the annelid *Arenicola marina* is the most distant animal species from human, for which a PRDX5 MTS has been functionally characterized. As mentioned before, PRDX5 mitochondrial targeting was also demonstrated in human, rodents, bovine and fruitfly (Knoops et al. 1999; Oberley et al. 2001; Banmeyer et al. 2004; Leyens et al. 2004; Pagliarini et al. 2008; Radyuk et al. 2009). Furthermore, based on MTS identification in databases, it appears that mitochondrial localization of PRDX5 is conserved in mollusks, arthropods, cephalochordates and vertebrates (see Fig. 6.1 and

Zhang et al. (2003), Li et al. (2011)). Taken together, these data suggest that mitochondrial targeting of PRDX5 is widely conserved from invertebrates to mammals. However, here, we show that mitochondrial PRDX5 (L-PRDX5) is missing in domestic pig although cytosolic/peroxisomal PRDX5 (S-PRDX5) appears to be conserved. The abolition of PRDX5 targeting to mitochondria is unexpected since this organelle is a major source of hydrogen peroxide and peroxynitrite in mammalian cells (Jezek and Hlavata 2005). Moreover, the cytoprotective function of PRDX5 in mitochondria was supported by several studies. Indeed, it has been shown previously that L-PRDX5 overexpression may prevent peroxide or drug-induced cell death and DNA damage (Nguyen-Nhu and Knoops 2003; Banmeyer et al. 2004; Peng et al. 2004a; Peng et al. 2004b; Banmeyer et al. 2005).

In domestic pig, the lack of L-PRDX5 could have been counterbalanced by higher expression of other mitochondrial peroxidases, i.e. PRDX3 (Watabe et al. 1994; Araki et al. 1999; Oberley et al. 2001; Mowbray et al. 2008), GPX1 (Panfili et al. 1991; Utsunomiya et al. 1991; Asayama et al. 1994; Esworthy et al. 1997; Legault et al. 2000) and GPX4 (Arai et al. 1996; Ursini et al. 1999; Schneider et al. 2009). In the present study, mitochondrial localization of pig PRDX3, GPX1 and GPX4 was confirmed experimentally (see Fig. 6.6 and 6.7). Moreover, in this work, PRDX3 and GPX4 were shown to be more abundant in pig liver mitochondria compared to rat liver mitochondria (see Fig. 6.6.C and 6.7.F), suggesting the existence of compensatory mechanisms counterbalancing the absence of PRDX5 in mitochondria of pig liver. To confirm these results, in addition to the use of Ponceau S-staining for protein loading estimation, GPX1 and GPX4 protein levels could be normalized using mitochondrial markers like Tom20 and Tim23. It would be interesting to compare pig and rat PRDX3, GPX1 and GPX4 expression in more tissues to support this hypothesis at the level of the whole organism. Tissues like thyroid gland, lung and kidney, in which PRDX5 is especially highly expressed (Knoops et

al. 1999), would be of particular interest. It would be also useful to evaluate PRDX3, GPX1 and GPX4 expression in pig and other mammals having maintained L-PRDX5. Furthermore, to study the consequences of the absence of L-PRDX5 on peroxidase activity in pig mitochondria, the global peroxidase activity was compared in pig and rat liver mitochondrial extracts. Our results indicate that peroxidase activity in presence of H_2O_2 is not different in pig and rat liver mitochondria (see Fig. 6.8.A). On the other hand, *t*-BHP reduction by liver mitochondrial extracts is significantly lower in pig compared to rat (Fig. 6.8.B). These results suggest that the expression of PRDX3, GPX1 and GPX4 in pig liver mitochondria is sufficient to maintain comparable H_2O_2 reduction rates, but is not sufficient to maintain similar alkyl hydroperoxide reduction rates compared to rat liver mitochondria. Different substrate specificities of mitochondrial peroxidases could account for the dissimilarities obtained between pig and rat H_2O_2 and *t*-BHP reduction rates. Indeed, PRDX3 is highly reactive towards H_2O_2 (k_2 = 2 x 10^7 M^{-1} s^{-1}) and is thought to be a more efficient H_2O_2 scavenger (Cox et al. 2010). Therefore, a higher PRDX3 expression in pig compared to rat liver mitochondria would enable the maintenance of H_2O_2 reduction rates but not alkyl hydroperoxide reduction rates. It is important to note that, *in vivo*, mitochondrial peroxidase activity relies on recycling by physiological reductants. The availability of these reductants is thus likely to modulate the contribution of PRDX3, PRDX5, GPX1 and GPX4 to mitochondrial peroxide removal. Moreover, recent reports based on rate constants and enzyme abundance suggest that PRDX5 possesses a specific function in mitochondria through its high reactivity towards alkyl hydroperoxides and peroxynitrite (k_2 ~ 10^7 $M^{-1}s^{-1}$) (Trujillo et al. 2007; Cox et al. 2010). So far, PRDX5 is the only mitochondrial peroxidase for which a peroxynitrite reductase activity was demonstrated. Because PRDX5 is absent in pig mitochondria, further studies would be necessary to measure peroxidase activity of pig mitochondrial extracts in presence of peroxynitrite. Also, it

would be of interest to determine whether other peroxidases are able to reduce peroxynitrite with similar rate constants.

Strikingly, according to sequence analysis, we reported also previously that PRDX5 should be absent in dog mitochondria (Nguyen-Nhu et al. 2007) (see also Fig. 6.1). While the present work was being finalized, the absence of dog L-PRDX5 was evidenced (Usmanova et al. 2011). Thus, mitochondrial PRDX5 has been lost in at least one caniformia (dog) and one artiodactyla (pig). It is interesting to note that bovine (artiodactyla) (Leyens et al. 2004) and giant panda (caniformia) have maintained a PRDX5 MTS (see Fig. 6.1). Taken together, these data suggest that the loss of PRDX5 MTS results from at least two separate and recent events during evolution. Moreover, it appears that mitochondrial PRDX5 is not essential in dog and pig. However, the reproductive occurrences in these two domesticated species were finely regulated by human intervention, biasing the natural selection process. Therefore, one cannot conclude that the abolition of mitochondrial PRDX5 has occurred without any consequences on evolutionary success in dog and pig.

Finally, a sequence comparison of the 5′ region of the *PRDX5* gene from different animal species revealed that the abolition of L-PRDX5 in pig involves a mutation of the first ATG initiation codon. This impedes the synthesis of the L-PRDX5. Interestingly, subcellular distribution of the intermediary metabolic enzyme alanine:glyoxylate aminotransferase (AGT) was reported to change at many occasions during mammalian evolution according to a similar molecular basis (Holbrook et al. 2000; Birdsey et al. 2004). Moreover, the abolition of mitochondrial localization of AGT was found to be an adaptation to herbivory. In the case of PRDX5, it is difficult to correlate its variable subcellular distribution to a phenotypic trait or to positive selection pressures. In this context, it should be noted that *PRDX5* and *HSPC152/TRM112* genes closely coexist and are positioned in opposite

orientations (Nguyen-Nhu et al. 2007). This feature appears to be conserved in mammals and is thus also present in pig (Genbank accession numbers XM_003122572.3 and NM_214144.1). Therefore, the 5′ region of *PRDX5* is likely to coincide with *HSPC152/TRM112* promoter and is thereby possibly exposed to selection pressures linked to both PRDX5 and HSPC152/TRM112 functions.

To conclude, the present study demonstrates the abolition of mitochondrial PRDX5 in domestic pig, while PRDX5 MTS functionality is maintained in numerous species between annelids and mammals. Further studies will be necessary to determine the functional consequences of this loss although our work suggests that some compensatory mechanisms may have occurred.

6.5. Acknowledgements

We thank Prof. S.J. Atkinson (Indiana University School of medicine), Prof. E. Hermans (Université catholique de Louvain) and Prof. P. Dumont (Université catholique de Louvain) for providing LLC-PK10, C6 and SAOS-2 cell lines respectively. Professor M. Conrad (Helmholtz Zentrum München-German Research Center for Environmental Health) is also acknowledged for providing monoclonal anti-GPX4 antibody. We thank K. Doshishti-Agolli, M. Pirson and Dr. E. Loumaye for critical reading. This work was supported by grants from the National Fund for Scientific Research (FRFC N°2.4.603.09F) and the Communauté française de Belgique-Actions de Recherche Concertées (10/15-026).

7. Abolition of peroxiredoxin 5 mitochondrial targeting in canids

RESEARCH ARTICLE

To be submitted to MOLECULAR BIOLOGY AND EVOLUTION

Valérie Van der Eecken[a], André Clippe[a], Sophie Dekoninck[a], Paul P. Van Veldhoven[b] and Bernard Knoops[a]

[a] Université catholique de Louvain, Institut des Sciences de la Vie (ISV), 4-5 place Croix du Sud, B-1348 Louvain-la-Neuve, Belgium.
[b] Katholieke Universiteit Leuven, Department of Molecular Cell Biology, LIPIT, Campus Gasthuisberg, Herestraat, 3000 Leuven, Belgium.

Abstract

Peroxiredoxin 5 (PRDX5) is a thioredoxin peroxidase able to reduce hydrogen peroxide, alkyl hydroperoxides and peroxynitrite. In human, this antioxidant enzyme is found in the cytosol, the mitochondria, the peroxisomes and the nucleus. Mitochondrial distribution results from the presence of an N-terminal mitochondrial targeting sequence (MTS). In human, PRDX5 subcellular targeting is dependent on the use of multiple alternative transcription start sites and two alternative in-frame translation initiation sites, which determine whether or not the region encoding the MTS is translated. In the present study, the abolition of PRDX5 mitochondrial targeting in dog is highlighted and the molecular mechanism underlying the loss of mitochondrial PRDX5 during evolution is examined. Here, we show that the absence of mitochondrial PRDX5 is generalized among the extant canids and that the first events leading to PRDX5 MTS

abolition in canids involve a mutation in the more 5′ translation initiation codon as well as the appearance of a STOP codon. Furthermore, we found that PRDX5 MTS functionality is maintained in giant panda and northern elephant seal, which are phylogenetically closely related to canids. Also, the functional consequences of the restoration of mitochondrial PRDX5 in dog Madin-Darby canine kidney (MDCK) cells were investigated. We show that the restoration of PRDX5 mitochondrial targeting in MDCK cells provokes deleterious effects following peroxide exposure, indicating that mitochondrial PRDX5 gains cytotoxic properties under acute oxidative stress in MDCK cells. This led us to suggest that, although PRDX5 cytoprotective function against oxidative stress has been clearly demonstrated in several studies in human and rodents, the conservation of mitochondrial PRDX5 would not confer necessarily an advantage in all mammalian species.

***Keywords*:** Peroxiredoxin 5, Dog, Canid, Subcellular targeting, Mitochondrion, Evolution

Running head: PRDX5 mitochondrial targeting is abolished in canids

Abbreviations used: CHO: Chinese hamster ovary; GFP: Green Fluorescent Protein; GPX: glutathione peroxidase; LDH: lactate dehydrogenase; L-PRDX5: long form of peroxiredoxin 5; MDCK: Madin-Darby canine kidney; MTS: mitochondrial targeting sequence; mya: million years ago; PRDX: peroxiredoxin; RNS: reactive nitrogen species; ROS: reactive oxygen species; S-PRDX5: short form of peroxiredoxin 5; *t*-BHP: *tert*-butyl hydroperoxide.

7.1. Introduction

Due to the presence of the electron transport chain, mitochondria are particularly exposed to oxidative attacks caused by reactive oxygen species (ROS) and reactive nitrogen species (RNS). To scavenge ROS/RNS, the mitochondrial matrix is equipped with antioxidant enzymes. Among them, manganese superoxide dismutase (MnSOD) is responsible for the dismutation of the superoxide radical ($O_2^{\bullet -}$) to hydrogen peroxide (H_2O_2). H_2O_2 is subsequently reduced to water by mitochondrial peroxidases, i.e. glutathione peroxidase 1 (GPX1), glutathione peroxidase 4 (GPX4), peroxiredoxin 3 (PRDX3) and peroxiredoxin 5 (PRDX5) (Halliwell and Gutteridge 2007).

PRDX5 is a thiol-specific peroxidase able to reduce H_2O_2, alkyl hydroperoxides and peroxynitrite (Knoops et al. 1999; Seo et al. 2000; Dubuisson et al. 2004; Trujillo et al. 2007). The importance of PRDX5 in antioxidant defence was demonstrated in several studies, recently reviewed in Knoops et al. (2011). The subcellular distribution of human PRDX5 is not restricted to mitochondria, as it is also localized in the cytosol, the peroxisomes and, in some situations, in the nucleus (Yamashita et al. 1999; Kropotov et al. 1999; Knoops et al. 1999; Seo et al. 2000; Lu et al. 2006). PRDX5 uses cytosolic and mitochondrial thioredoxins (TXNs or Trxs) as physiological electron donors. In turn, TXNs are reduced by mitochondrial or cytosolic thioredoxin reductases (TXNRDs or TrxRs), finally relying on NADPH as electron donor (Seo et al. 2000; Zhou et al. 2000; Dubuisson et al. 2004; Trujillo et al. 2007).

In human, the complex subcellular distribution of PRDX5 is a consequence of the existence of two protein isoforms. The latter are encoded

by a single gene containing alternative transcription start sites and two alternative in-frame translation initiation sites (Fig. 7.1). Translation at the more 3' start codon produces a short PRDX5 form (S-PRDX5) which is found in the cytosol, the peroxisomes and the nucleus (Nguyen-Nhu et al. 2007). Peroxisomal targeting is linked to the presence of a weak C-terminal peroxisomal targeting signal (PTS1) (Knoops et al. 1999; Yamashita et al. 1999). Translation at the more 5' start codon produces a long PRDX5 form (L-PRDX5) containing an additional N-terminal mitochondrial targeting sequence (MTS) or presequence (Knoops et al. 1999; Nguyen-Nhu et al. 2007). This MTS is cleaved after mitochondrial import, releasing the mature mitochondrial PRDX5 which is identical to S-PRDX5. Moreover, mitochondrial targeting of PRDX5 seems to be a conserved feature in animal kingdom. Up to now, the mitochondrial localization of the protein was experimentally verified in human, rat, mouse, hamster, bovine and fruitfly (Knoops et al. 1999; Oberley et al. 2001; Banmeyer et al. 2004; Leyens et al. 2004; Pagliarini et al. 2008; Radyuk et al. 2009). Furthermore, presequences were identified in orthologous PRDX5 of invertebrate species (Zhang et al. 2003; Radyuk et al. 2009; Li et al. 2011; Van der Eecken et al. 2011) (see also Fig 7.2 and annex 1). Some of these invertebrate species belong to basal metazoan phyla, i.e. porifera and placozoa. However, we reported recently that mitochondrial PRDX5 is absent in some mammalian species, such as in pig (Van der Eecken et al. 2011). Moreover, according to sequence analysis, we also predicted that mitochondrial PRDX5 would be absent in dog (Fig. 7.2) (Nguyen-Nhu et al. 2007). While the present work was in progress, the absence of dog L-PRDX5 was also evidenced by another team (Usmanova et al. 2011).

In this work, we confirm that dog PRDX5 is not addressed to mitochondria and we examined the molecular basis responsible for the abolition of mitochondrial targeting. Furthermore, we show that the loss of mitochondrial PRDX5 is generalized throughout the Canidae family. Finally, the functional consequences of the restoration of mitochondrial PRDX5 in dog MDCK cells were also studied.

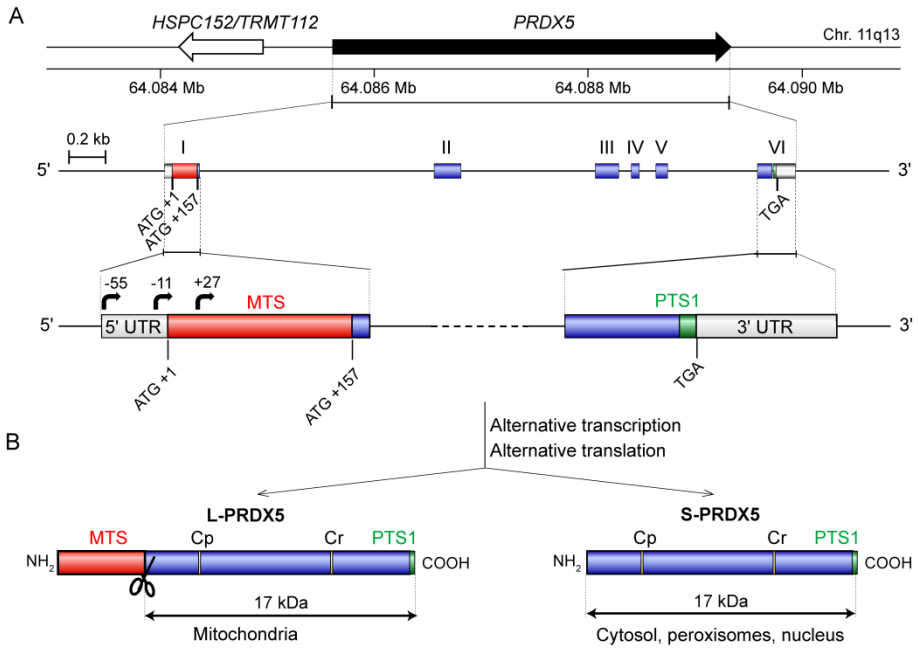

Fig. 7.1. Human *PRDX5* gene organisation and protein forms. (A) Human PRDX5 gene is located on chromosome 11q13 and is flanked by the *HSPC152/TRMT112* gene, positioned in opposite direction. Human *PRDX5* contains six exons (boxes) and five introns. 5′ and 3′ UTRs are indicated by open boxes. In human liver, three alternative transcription initiation sites were identified (black arrows) (Nguyen-Nhu et al. 2007). Also, Exon I contains two in-frame ATG initiation codons. The regions encoding the mitochondrial targeting sequence (MTS) and peroxisomal targeting signal (PTS1) are in red and green, respectively. (B) The presence of alternative transcription and translation start sites in human *PRDX5* gene results in the production of a long PRDX5 form (L-PRDX5) and a short PRDX5 form (S-PRDX5). L-PRDX5 contains a cleavable (scissors) N-terminal MTS (red) and is therefore imported into mitochondria. S-PRDX5 contains a weak C-terminal PTS1 (green) and is targeted to the cytosol and the peroxisomes. Peroxidatic (Cp) and resolving (Cr) Cys implicated in catalysis are indicated. [Adapted from Nguyen-Nhu et al. (2007) and Knoops et al. (2011)].

Fig. 7.2 (next two pages). ClustalX 2.0.7 amino acid sequence alignment of human PRDX5 and animal orthologs. Asterisks (*) indicate identities, dots (.) and double dots (:) indicate conservative and highly conservative substitutions, respectively. Methionines encoded by the two alternative translation initiation sites are indicated in bold type. Peroxidatic (Cp) and resolving (Cr) Cys implicated in catalysis are highlighted in yellow. The peroxisomal targeting signal (PTS1) is highlighted in green. Mitochondrial targeting sequence (MTS) predictions were performed with TargetP (Nielsen et al. 1997; Emanuelsson et al. 2000) and Mitoprot (Claros and Vincens 1996). MTS predicted by TargetP are highlighted in red. MitoProt and TargetP subcellular localization predictions for PRDX5 were similar, excepting for *X. laevis* PRDX5, which was predicted to be imported into mitochondria with high probabilities when using Mitoprot, while the protein was predicted to be secreted with TargetP. Taxonomic groups are indicated between brackets. GenBank accession numbers are NP_036226.1 (human, *Homo sapiens*); XP_533241.1 (domestic dog, *Canis lupus familiaris*); XP_003230134.1 (green anole, *Anolis carolinensis*); NP_001085580.1 (African clawed frog, *Xenopus laevis*); ADI78068.1 (gilthead seabream, *Sparus aurata*); AAM18076.1 (Japanese lancelet, *Branchiostoma belcheri tsingtaunese*); NP_650679.3 (fruitfly, *Drosophila melanogaster*); ADQ57291.1 (bay scallop, *Argopecten irradians*); AAY96293.1 (lugworm, *Arenicola marina*); XP_001629337.1 (Starlet sea anemone, *Nematostella vectensis*); XP_002108078.1 (*Trichoplax adhaerens*); XP_003384607.1 (*Amphimedon queenslandica*).

Figure 7.2.

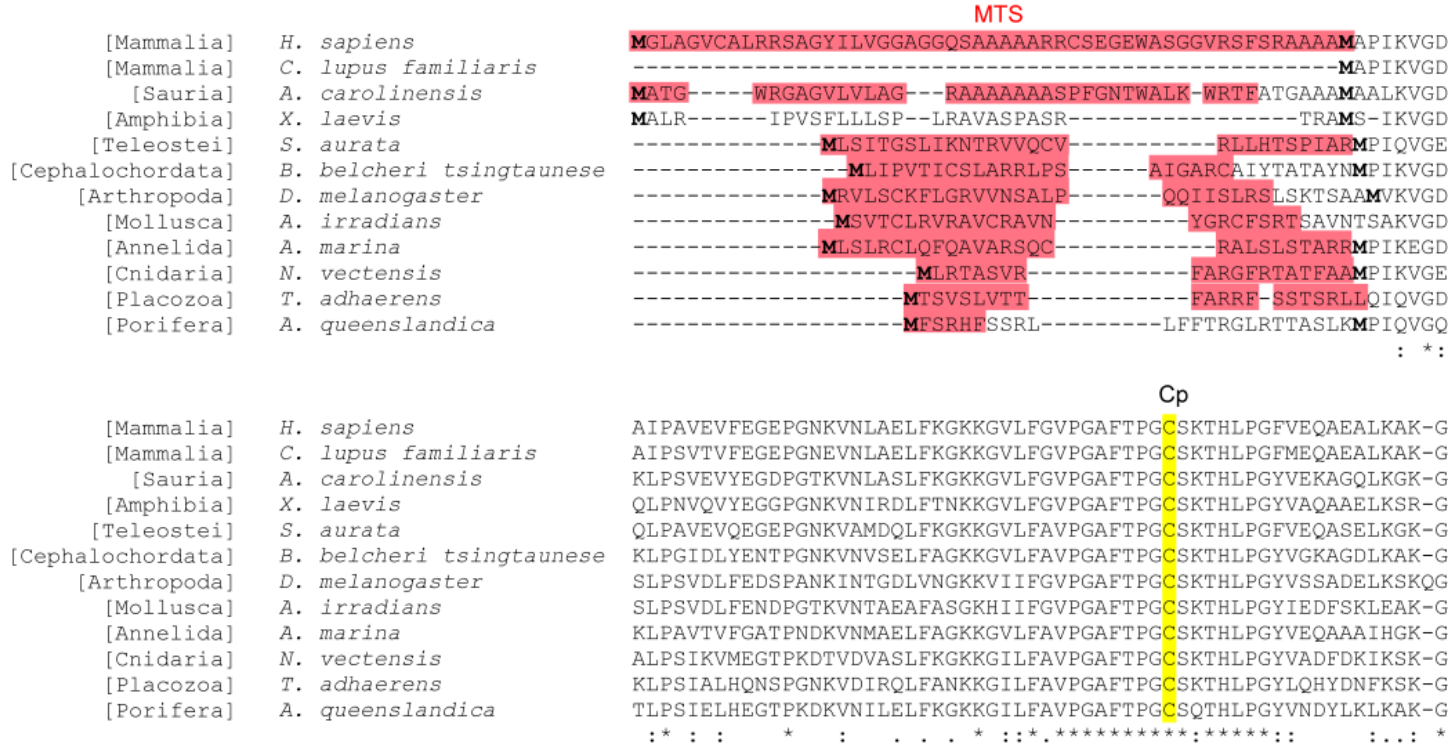
MTS
Cp
[Mammalia] H. sapiens
[Mammalia] C. lupus familiaris
[Sauria] A. carolinensis
[Amphibia] X. laevis
[Teleostei] S. aurata
[Cephalochordata] B. belcheri tsingtaunese
[Arthropoda] D. melanogaster
[Mollusca] A. irradians
[Annelida] A. marina
[Cnidaria] N. vectensis
[Placozoa] T. adhaerens
[Porifera] A. queenslandica


[Mammalia] H. sapiens VQVVACLSVNDAFVTGEWGRAHKAEGKVRLLADPTGAFGKETDLLLD-DSLVSIFGNRRL
[Mammalia] C. lupus familiaris VQVIACLSVNDVFVTEAWGRAHNSGGKVRLLADPTGAFGKETDLLLD-DSLVSLFGNHRL
[Sauria] A. carolinensis VEIIACLSVNDVFVMKEWGNAHHAEGKVRMLADPTGAFGKATNLLLDKEPLRDLFGTNRS
[Amphibia] X. laevis AAVVACISVNDVFVVSEWGKVHEAEGKVCMLADPCGEFAKACGLLLDKKELSELFGNQRC
[Teleostei] S. aurata IQEVACISVNDAFVMAAWGKEHGTDGKVRMLADPTGAFTKAVDLLLDSDQIVQVLGNKRS
[Cephalochordata] B. belcheri tsingtaunese VQVIACVSVNDPFVMEAWGKDQKAEGKVRMLADTGAEFTKAIGLDLD---ATGLLGNIRS
[Arthropoda] D. melanogaster VDEIVCVSVNDPFVMSAWGKEHGAAGKVRLLADPAGGFTKALDVTID----LPPLGGVRS
[Mollusca] A. irradians VKSVNCVSVNDPFVMQAWGENQGAAGKVRMLADTCGAFTSQLGLDLP--AVKDVLGNVRC
[Annelida] A. marina VDIIACMAVNDSFVMDAWGKAHGADDKVQMLADPGGAFTKAVDMELD---LSAVLGNVRS
[Cnidaria] N. vectensis VDVVACIAVNDPFVMSAWGEANGCQGKIQMLADVHGEFTKAVDLELD---ATPFLGNIRS
[Placozoa] T. adhaerens IDVIACVSVNDAFVVDAWSKSNNVDDRLEMLADTSAQFTKSVGLDFD---ATPVLGNIRS
[Porifera] A. queenslandica FEVIACVSVNDAFVMSAWGIERKATGKIRMLADPAGEFTKAVDLGFD---ATPALGNIRS
Cr
PTS
[Mammalia] H. sapiens KRFSMVVQDGIVKALNVEPDGTGLTCSLAPNIISQL-
[Mammalia] C. lupus familiaris KRFSMVIENGIVKSLNVEPDGTGLTCSLAPNILSQL-
[Sauria] A. carolinensis KRFSMVVDDGIVKSLNVEEDGTGLTCSLATNIVSQL-
[Amphibia] X. laevis KRFSMVVEDGKIKAINVEEDGTGLTCSLAGNIISQL-
[Teleostei] S. aurata KRYSMLVEDGVVKKINVEPDGTGLTCSLASSILSDL-
[Cephalochordata] B. belcheri tsingtaunese KRYSMLVEDGEVKQLNVEPDGTGLTCSLAEGLKL---
[Arthropoda] D. melanogaster KRYSLVVENGKVTELNVEPDGTGLSCSLANNIGKK--
[Mollusca] A. irradians KRFAMVVNDGKIEKLNVEPDGTGLTCSLSTSLCDEL-
[Annelida] A. marina KRYSLVIEDGVVTKVNVEPDGKGLTCSLAPNILSQL-
[Cnidaria] N. vectensis KRYAMLVEDGVVKQLHVEPDGTGLTCSLSNSILSQL-
[Placozoa] T. adhaerens KRYAMIIEDTVVKQINVEPDGTGLSCSLAQNILEQLS
[Porifera] A. queenslandica KRYAMTIEDGVVKSVAIEPDATGLTVSLSCSILNE--

7.2. Materials and methods

7.2.1. Computer analysis

Multiple sequence alignment was performed with ClustalX 2.0.7 (Larkin et al. 2007). TargetP 1.1 and MitoProt II v.1.101 were used for MTS prediction (Claros and Vincens 1996; Emanuelsson et al. 2000).

7.2.2. Dog liver fractionation

Fresh beagle dog liver was homogenized and centrifuged to obtain nuclear fractions (N) and postnuclear supernatants (E). E-fraction was further fractionated by differential centrifugation into heavy mitochondrial (M), light mitochondrial (L), microsomal (P) and cytosolic (S) fractions. Sub-fractions of the L-fraction were obtained by centrifugation through a Percoll gradient. Marker enzymes and protein content were measured in each fraction (see annexes 3 and 4). Based on glutamate dehydrogenase (GDH, mitochondrial marker) and catalase (peroxisomal marker) activities (see annex 4), Percoll fractions 2 and 10 were chosen to represent mitochondrial (Mito) and peroxisomal (Perox) fractions respectively. Experimental procedures were described before (Declercq et al. 1984; Van Veldhoven et al. 1996).

7.2.3. Western Blotting

Western blotting was performed as described before (Van der Eecken et al. 2011). Blots were probed overnight with 1:4000 polyclonal rabbit anti-human PRDX5 (Wang et al. 2001), 1 μg/ml monoclonal mouse anti-heat shock protein 90 (Hsp90; Millipore), 1:2000 monoclonal mouse anti-cytochrome c oxidase subunit 4 (COX4; Molecular Probes), 1:3000 polyclonal rabbit anti-catalase (Rockland) or 1:1500 polyclonal rabbit anti-actin (Sigma).

Subsequently, blots were incubated for one hour with peroxidase-congugated goat anti-rabbit IgG or goat anti-mouse IgG (Dako). Blots were developed with the Western Lightning Chemiluminescence kit according to manufacturer's instructions.

7.2.4. Cell culture

MDCK (dog kidney) cell line was cultured in Dulbecco's Modified Eagle medium (DMEM) containing 4,5 g/l D-glucose with GlutaMAX (Gibco), supplemented with 10% foetal calf serum (FCS; Gibco), 1% non-essential amino acids, 100 U/ml streptomycin and 100 U/ml penicillin (Gibco). Cells were maintained at 37°C in 5% CO_2.

7.2.5. Immunofluorescence

Mitotracker (Molecular Probes) staining and immunofluorescence were performed as described previously (Van der Eecken et al. 2011), using 1:200 rabbit anti-human PRDX5 and 1:50 FITC-conjugated donkey anti-rabbit IgG (Jackson ImmunoResearch Laboratories Inc.). Co-localization experiment with catalase was performed using 1:200 rabbit anti-human PRDX5, 1:100 sheep anti-human catalase (San Bio), 1:50 TRITC-conjugated donkey anti-rabbit IgG (Jackson ImmunoResearch Laboratories Inc.) and 1:50 FITC-conjugated donkey anti-sheep IgG (Jackson ImmunoResearch Laboratories Inc.). The coverslips were mounted in Vectashield (Vector Laboratories, Inc.) containing 50μg/ml 4', 6-diamidino-2-phenylindole dihydrochloride (DAPI) and analyzed by fluorescence microscopy.

7.2.6. Sequencing the 5' region of PRDX5 from caniformia species

The species examined in this experiment are the following: arctic wolf (*Canis lupus arctos*), American black bear (*Ursus americanus*), domestic dog (*Canis lupus familiaris*), giant panda (*Ailuropoda melanoleuca*), gray fox (*Urocyon cinereoargenteus*), maned wolf (*Chrysocyon brachyurus*), northern elephant seal (*Mirounga angustirostris*), raccoon dog (*Nyctereutes procyonoides*) and red fox (*Vulpes vulpes*). Arctic wolf blood sample was kindly provided by Dr. JC Bertho, zoological park "Le Monde Sauvage", Aywaille, Belgium. American black bear heart sample is described in (Van Der Heyden et al. 2007) and was generously given by Pr. MAG Van Der Heyden, University Medical Center Utrecht, The Netherlands. Gray fox and maned wolf DNA samples, described in (Lindblad-Toh et al. 2005), were kindly provided by Pr. RK Wayne, University of California, USA. Northern elephant seal blood sample was provided by C Louis and Pr. C Debier, Université catholique de Louvain, Belgium. Tissue samples of raccoon dog and red fox were taken at necropsy of animals that have been found dead accidentally respectively in Finland and in Belgium.

Genomic DNA was extracted from blood or muscle using the DNeasy Blood and tissue Kit (Qiagen) following manufacturer's instructions. Primers 5'-CCAGCGGTCACCTTGATTGGGGC-3' (forward) and 5'-ATGCGAGCTCAGCAGGTTGTGG-3' (reverse) were used to amplify the genomic region comprised between the first exon of *PRDX5* and the first exon of *HSPC152/TRMT112*, which is in close proximity of *PRDX5* and positioned in opposite direction (Fig. 7.1 and Nguyen-Nhu et al. (2007)). The primers were designated to map on regions sharing 100% identity between giant panda and dog sequences. The PCR reaction was performed using the Taq DNA polymerase (Eurogentec) in the presence of 5% (v/v) dimethyl

sulfoxide (DMSO). The PCR products were cloned into pCR2.1 vector and sequenced. At least eight clones, deriving from three independent PCR reactions, were sequenced for each species.

7.2.7. Expression of giant panda and northern elephant seal PRDX5 MTS in fusion with Green Fluorescent protein (GFP) in MDCK cells

Based on Genbank database sequence XM_002916664, the sequence encoding giant panda PRDX5 MTS was synthetized and cloned into pEX-A vector by Eurofins MWG Operon. The sequence coding for giant panda PRDX5 MTS was subsequently PCR-amplified using forward primer 5′-GGGATCGGCATGAAGCTTTTTCCGCACCG-3′ and reverse primer 5′-CCATGGCTGAGGCGGCGCTTCTGAAACC-3′. The sequence encoding the MTS of northern elephant seal PRDX5 was PCR-amplified from a pCR2.1 vector containing northern elephant seal *PRDX5* 5′ flanking region (see point 7.2.7.) using forward primer 5′-GGTTTGGGCATGCCGTTCGTTCAGCTACG-3′ and reverse primer 5′-CCATGGCTGAGGCGGCGCTTCTGAAACC-3′. PCR products were cloned in the pcDNA3.1/CT-GFP-TOPO vector (Invitrogen) and the resulting plasmids were sequenced. MDCK cells were transiently transfected using Amaxa Nucleofection system (Lonza AG) according to manufacturer's instructions. 72 h after transfection, cells were incubated with Mitotracker Red prior to fixation. The coverslips were mounted in Vectashield containing 50 μg/ml DAPI and analyzed by fluorescence microscopy.

7.2.8. Generation of stable MDCK clones expressing mitochondrial or cytosolic/peroxisomal human PRDX5

Plasmid pEF-BOS containing an EF-1-α promoter, a puromycin resistance gene and G-CSF-poly(A) adenylation signal was used as mammalian expression vector. pEF-BOS-Mito-PRDX5 (*PRDX5* cDNA sequence encoding human L-PRDX5) and pEF-BOS-Cyto-PRDX5 (*PRDX5* cDNA sequence encoding human S-PRDX5) were described previously (Banmeyer et al. 2004).

For the construction of pEF-BOS-Mito-PRDX5-C47A (*PRDX5* cDNA sequence encoding human L-PRDX5 with the residue Cys47 mutated into Ala) vector, human *PRDX5* cDNA was PCR-amplified from pEF-BOS-Mito-PRDX5 using forward primer 5′-ACAGGGATTTCTTGTCTCCCACG-3′ and reverse primer 5′-TCTCAAGCCTCAGACAGTGG-3′. The C47A mutation was generated by PCR-mediated site-directed mutagenesis using the complementary primers containing a base mismatch 5′-ACCCCTGGAGCTAGCAAGACACACCTG-3′ (forward) and 5′-TGTGTCTTGCTAGCTCCAGGGGTGAAGG-3′ (reverse). The resulting amplicon was ligated in the pCR2.1 vector and subcloned into the *Spe*I and *Not*I sites of pEF-BOS vector.

For the construction of pEF-BOS-Cyto-PRDX5-C47S (*PRDX5* cDNA sequence encoding human S-PRDX5 with the residue Cys47 mutated into Ser) vector, human *PRDX5* cDNA containing the mutation C47S (Plaisant et al. 2003) was PCR-amplified using forward primer 5′-AGCGACTAGTCCGCCATGGCCCCAATCAAGGTGGGAGATGC-3′ (*Spe*I site underlined) and reverse primer 5′-TATCTGGCGGCCGCCACTCAGAGCTGTGAGATGATATTGGG- 3′ (*Not*I

site underlined). The resulting amplicon was ligated in the pCR2.1 vector and subcloned into the *Spe*I and *Not*I sites of pEF-BOS vector.

MDCK cells were transfected with the plasmids using Amaxa Nucleofection system according to manufacturer's instructions. Two days after transfection, cells were selected 16 days with 2 μg/ml puromycin (Sigma-Aldrich). Subsequently, stably transfected cell lines were obtained by isolation of individual clones by a dilution technique. At least three clones per cell line were obtained and characterized.

Overexpression of PRDX5 was confirmed by immunofluorescence and immunoblotting (see points 7.2.4 and 7.2.6). Incorporation of puromycin resistance gene in the genome of MDCK control cells was verified by PCR on genomic DNA. The latter was extracted from $5x10^6$ cells using the DNeasy Blood and Tissue kit (Qiagen) following the manufacturer's instructions. The puromycin N-acetyltransferase gene was amplified by using forward primer 5'-GACCGAGTACAAGCCCACGGTGCG-3' and reverse primer 5'-CGAGACGCC GACGGTGGCCAGGAACCACG-3'.

7.2.9. Cell treatment with hydrogen peroxide and tert-butyl hydroperoxide (t-BHP) and lactate dehydrogenase (LDH) assay

MDCK cells were seeded at a density of $3x10^4$ cells/cm^2 into 24-well plates. After 15-18 h culture, stress was induced during one hour in DMEM without phenol red containing 4.5 g/l D-glucose and supplemented with 1% FBS, 100 U/ml penicillin, 100 U/ml streptomycin, 1% non-essential amino acids and 200 nM GlutaMAX. Cytotoxicity was evaluated by the lactate dehydrogenase (LDH) release assay (Cytotoxicity detection Kit, Roche). Fifty μl of supernatants were used for LDH assay. The total LDH release (100%

cell death) was determined for each well after lysis of cells with 2% Triton X-100 detergent. Cell mortality was calculated according to this scale.

7.2.10. Statistical analysis

Cell death values were calculated from triplicates within an experiment. Each experiment was repeated three times for one clone, allowing the calculation of means and SEM. Statistical analysis was performed using two-way ANOVA with the Bonferroni post hoc test. Significance is designated as *$p<0.05$, **$p<0.01$, ***$p<0.001$. At least three clones were tested for each cell line.

7.3. Results

7.3.1. Mitochondrial PRDX5 is absent in domestic dog

The absence of mitochondrial PRDX5 in domestic dog was demonstrated by subcellular fractionation of a liver homogenate. Marker analysis on post-nuclear (E), cytosolic (S), mitochondrial (Mito) and peroxisomal (Perox) fractions was performed by Western blotting (Fig. 7.3A). The results indicated that the cytosolic, mitochondrial and peroxisomal fractions are enriched in Hsp90 (cytosolic marker), COX4 (mitochondrial marker) and catalase (peroxisomal marker) respectively. Evaluation of PRDX5 content by Western blotting revealed the presence of PRDX5 in cytosolic and peroxisomal fractions but its absence from the mitochondrial fraction.

To confirm the absence of mitochondrial PRDX5 in domestic dog, PRDX5 expression was examined using immunofluorescence in the MDCK (dog) cell line. PRDX5 was detected in the cytosol but no colocalization with the mitochondrial marker was observed (Fig. 7.3B-D). PRDX5 detection by

immunofluorescence also evidenced the peroxisomal localization of the protein, as illustrated by colocalization with peroxisomal catalase (Fig. 7.3E-G).

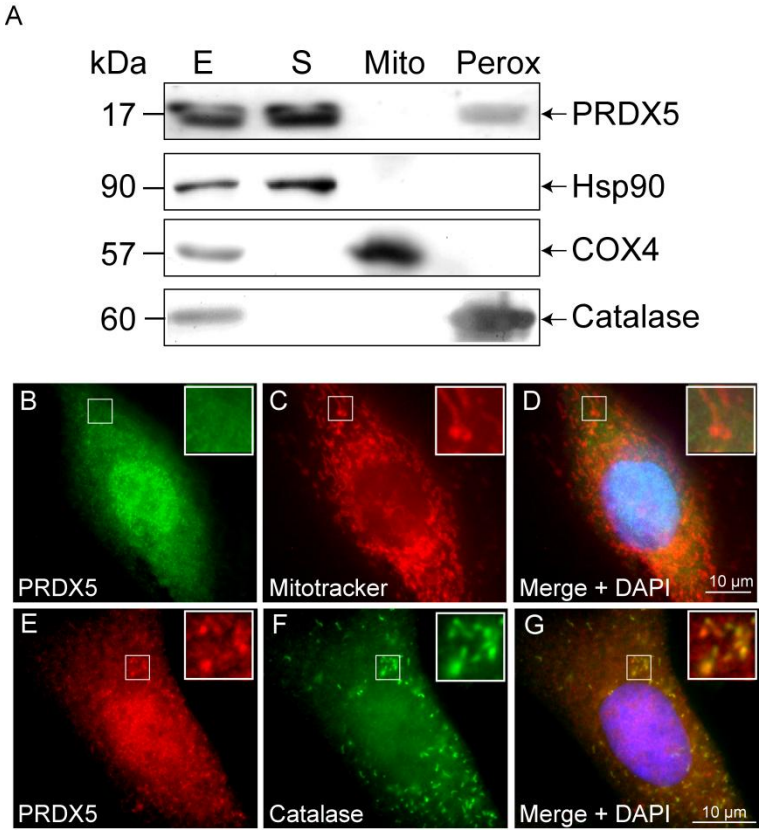

Fig. 7.3. Dog PRDX5 subcellular distribution. (A) Intracellular localization of dog PRDX5 was assessed by liver subcellular fractionation. Post-nuclear (E), cytosolic (S), mitochondrial (Mito) and peroxisomal (Perox) fractions were analyzed for marker enzyme and PRDX5 content by western blotting, using anti-Hsp90 (cytosolic), anti-COX4 (mitochondrial), anti-catalase (peroxisomal) and anti-PRDX5 antibodies. Fifteen µg of soluble proteins from each fraction were loaded. PRDX5 subcellular localization was also assessed by immunofluorescence detection of endogenous PRDX5 in MDCK cells (B, E) with co-localization with MitoTracker Red (C) or with peroxisomal catalase (F). Nuclei were counterstained with DAPI. *Hsp90*, heat shock protein 90; *COX4*, cytochrome c oxidase subunit 4.

Analysis of domestic dog *PRDX5* sequences from GenBank databases (GeneID: 476032) revealed the presence of a single translation initiation codon. This ATG codon corresponds to the second translation initiation site of human PRDX5 that produces the short form of the protein (S-PRDX5). The first translation initiation codon that enables the synthesis of the long form of PRDX5 (L-PRDX5) is not present in domestic dog.

7.3.2. L-PRDX5 is absent in other canids

To date, giant panda (Ursidae) is the phylogenetically closest related species to domestic dog (Canidae) for which *PRDX5* mRNA sequence is available in Genbank databases. These two species belong both to the Caniformia phylum (Fig. 7.4A). Analysis of the 5′ region of giant panda *PRDX5* mRNA (GenBank ID: XM_002916664) revealed the existence of two in-frame translation initiation codons (AUG+1 and AUG+172). These two codons are presumed to lead to the translation of both L-PRDX5 and S-PRDX5. Moreover, subcellular prediction programs predicted a mitochondrial distribution for giant panda L-PRDX5 protein (TargetP: 0.804 and MitoProt II: 0.859 compared with human PRDX5 TargetP: 0.830 and MitoProtII: 0.832; Claros and Vincens 1996; Emanuelsson et al. 2000). Since the translation initiation codon of L-PRDX5 appears to be maintained in giant panda but not in domestic dog, the loss of this translation initiation site was likely to have occurred in additional species which are phylogenetically positioned between domestic dog and giant panda, like the other canids (Fig. 7.4A). Family Canidae contains three major phylogenetic groups: the fox-like canids, the South American canids and the wolf-like canids (Fig. 7.4B). Additionally, several canids do not belong to any of the three main clades, such as the gray fox, which was shown to be more primitive (Lindblad-Toh et al. 2005). To assess the presence of a sequence encoding an MTS in *PRDX5*

of other canids, the *PRDX5* 5′ region of gray fox, raccoon dog (fox-like canid), red fox (fox-like canid), maned wolf (South American canid) and arctic wolf (dog-like canid) was sequenced. Moreover, *PRDX5* 5′ region was also sequenced in northern elephant seal (Phocidae) and American black bear (Ursidae). To obtain the sequence of *PRDX5* 5′ region in these species, the sequence was first PCR-amplified using genomic DNA as template (Fig. 7.4C). The primers were designated to map on regions sharing 100% identity between giant panda and domestic dog sequences. PCR products were cloned in pCR2.1 vector and were subsequently sequenced. Genbank accession numbers are presented in Table 1. The alignment of the 5′ *PRDX5* sequences revealed that the ATG+1 of giant panda, northern elephant seal and American black bear *PRDX5* corresponds to a GTG codon in all the studied canids (Fig. 7.4D). Moreover, in gray fox and fox-like canids, a STOP codon (position -90) is present in the same reading frame as the ATG+1. Furthermore, in the South American and dog-like canids *PRDX5*, the GTG-171 codon is not in the same reading frame as the ATG+1 codon. In the nucleotidic alignment, this shift in the reading frame corresponds to a gap between nucleotides -64 and -63. It is also worth noting that two slightly different sequences, corresponding to two different alleles, were found in gray fox and American black bear *PRDX5* 5′ region (Table 1).

Table 1. Sequences of *PRDX5* 5' flanking region: Genbank accession numbers

Species	Accession number
Northern elephant seal	JQ411224
American black bear (Allele 1)	JQ411225
American black bear (Allele 2)	JQ411226
Gray fox (Allele 1)	JQ411227
Gray fox (Allele 2)	JQ411228
Raccoon dog	JQ411229
Red fox	JQ411230
Maned wolf	JQ411231
Arctic wolf	JQ411232

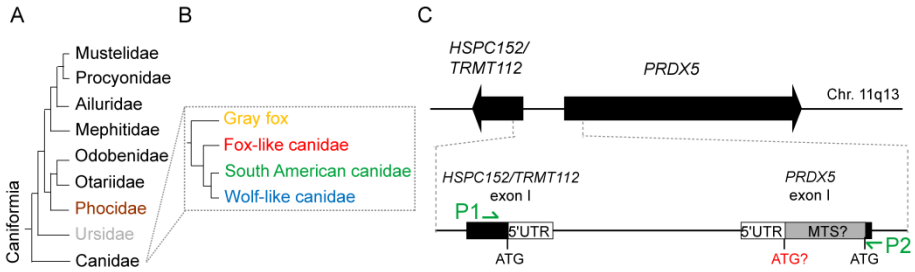

D

```
Northern elephant seal   -31  GGGCGGAGCGGCAGTGCGCTCCGGTTTGGGCATGCCGTTCGTTCAGCTAC  +19
Giant panda              -31  GGGCGGGGCGATCGTGCGTTCTGGGATCGGCATGAAGCTTTTTCCGCACC  +19
American black bear      -31  GGGCGGGGCGATCGTGCGCTCTGGGATCTGCATGAAGCTTTTTCCGCACG  +19
Gray fox                 -202 GGGCCGGGCCGTCGTGCGCGCCGGGATCGGCGTGCAGCTGCTTTCGTTGA  -153
Raccoon dog              -202 GGGCCGGGCGGTCGTGCGCGCTGGGATCGGCGTGCAGCTGCTTTCGTTGG  -153
Red fox                  -202 GGGCCGGGCCGTCGTGCGCGCTGGGCTCGGCGTGGAGCTGCTTTCGTCGA  -153
Maned wolf               -201 GGGCCGGGCCGTGGTGCGCGCCGGGGTCTGCGTGCAGCCGCTTTCGTTGA  -152
Arctic wolf              -201 GGGCCGGGCCGTGGTGCGCAGCGGGGTCGGCGTGCGGCCGCTTGCGTTGG  -152
Domestic dog             -201 GGGCCGGGCCGTGGTGCGCGGCGGGGTCGGCGTGCGGCCGCTTGCGTTGG  -152
                              **** * **    *****    **  *  ** **  *    **  *

Northern elephant seal   +20  GCGTCCTGAGTGGTGGGGCAGGCTCGGTTCTCGTCCGGGCAGCTGCCGTC  +69
Giant panda              +20  GTGTTCTGAGTCGTCTGCCAGGCTCGCTTTTCGTCCGTGCTACTGTCGTC  +69
American black bear      +20  GTGTTCTGAGTCGTCTGCTAGGCTCGCTTTTCGTCCGTGCAACTGTCGTC  +69
Gray fox                 -152 ACGTCCTGATCGGCCGGGTGGGCTCGGGTTTCGTCCCCGCGGCTGCCTTC  -103
Raccoon dog              -152 ACGTCCTGACCGGCCGGGTGGGCTCGGGTTTCGTCCCCGCGGCTGCCTTC  -103
Red fox                  -152 ACGTCCTGAACCGCCGGGTGGGCTCGGCTTTCGTCCCCGCGGCTGCCTTC  -103
Maned wolf               -151 ACGCCCTGACCGGCCGGGTGGGCTCCGGGTTCGTCCCCGCGGCTGCCTTC  -102
Arctic wolf              -151 ACGCCCTGACCGGCCCGGTGGGCTCCGGGTTCGTCCCCGCGGCTGCCTTC  -102
Domestic dog             -151 ACGCCCTGACCGGCCCGGTGGGCTCCGGGTTCGTCCCCGCGGCTGCCTTC  -102
                                *  ****   *   *   *****     ******  **  *** * **

Northern elephant seal   +70  GAGTCTGCAGCATCGGCGCCGTCGAGAGCAGGCGGGCGCCGGCGACCAGG  +119
Giant panda              +70  GAGTCTGCAGTTTCGGCGGCGTCGAGAGCAGGCGGGTGCCGGCAACGAGG  +119
American black bear      +70  GAGTCTGCAGCTTCGGCGGCGTCGAGAGCAGGCGGGTGCCGGCAACGAGG  +119
Gray fox                 -102 GGGTCTGCAGCATAGGCAGCGTCGACAGCCGGAGGGTGCCAGCAACGAGG  -53
Raccoon dog              -102 GGGTCTGCAGCATAGGCAGTGTCGACAGCCGGAGGGTGCCAGCAACGAGG  -53
Red fox                  -102 GGGTCTGCAGCATAGGCCGTGTCGACAGCCGGAGGGTGCCAGCAACGAGG  -53
Maned wolf               -101 GGGTCTGCAGCACAGGCAGTGTCGACAGCCGGAGGGTGC-GGCAACGAGG  -53
Arctic wolf              -101 GGGTCTGCAGCACAGGCAGTGTCGGCAGCCGGAGGGTGC-GGCAGCGAGG  -53
Domestic dog             -101 GGGTCTGCAGCACAGGCAGTGTCGACAGCCGGAGGGTGC-GGCAGCGAGG  -53
                              * ********    ***   ****  *** ** *** **  **  * ***

Northern elephant seal   +120 CAGGGAGTGGACGCTTGGCGGGGCCTACGGTTTCAGAAGCGCCGCCTCAG  +169
Giant panda              +120 CCAGGAGTGGACGCTTGGCGGGGCCCACGGTTTCAGAAGCGCCGCCTCAG  +169
American black bear      +120 CAAGGAGTGGACGCTTGGCGGGGCCCACGGTTTCAGAAGCGCCGCCTCAG  +169
Gray fox                  -52 CAGGGACTGGACGCTTGGCGGGGCCCACGGTTTCAGAAGCGCCGCCTCCG  -3
Raccoon dog               -52 CAGGGACTGGACGCTTGGCGGGGCCCACGGTTTCAGAAGCGCCGCCTCCG  -3
Red fox                   -52 CAGGGACTGGACGCTTGGCGGGGCCCACGGTTTCAGAAGCGCCGCCTCCG  -3
Maned wolf                -52 CAGGGACTGGACGCTTGGCGGGGCCCACGGTTTCAGAAGCGCCGCCTCCG  -3
Arctic wolf               -52 CAGGGACTGGACGCTTGGCGGGGCCCACGGTTTCAGAAGCGCCGCCTCCG  -3
Domestic dog              -52 CAGGGACTGGACGCTTGGCGGGGCCCACGGTTTCAGAAGCGCCGCCTCCG  -3
                              *  *** ****************** ********************** *

Northern elephant seal   +170 CCATG  +174
Giant panda              +170 CGATG  +174
American black bear      +170 CGATG  +174
Gray fox                   -2 CTATG  +3
Raccoon dog                -2 CTATG  +3
Red fox                    -2 CTATG  +3
Maned wolf                 -2 CGATG  +3
Arctic wolf                -2 CGATG  +3
Domestic dog               -2 CGATG  +3
                              * ***
```

Fig. 7.4. Sequencing of the *PRDX5* 5′-region in some Canidae, Ursidae and Phocidae (facing page). (A) Phylogenetic relationships between the nine families composing the suborder Caniformia. The phylogeny of Caniformia is currently not completely stabilized, e.g. concerning the position of Ailuridae. The presented phylogenetic tree is based on multiple nuclear gene sequences and is adapted from Van Valkenburgh and Wayne (2010). (B) Phylogeny of Canidae, based on ~15kb from 12 exons and 4 introns, resolved by Lindblad-Toh et al. (2005). Canidae family contains three major phylogenetic groups, which are indicated in red for the fox-like canids, green for the South American canids and blue for the wolf-like canids. Additionally, several canids do not belong to any of the three main clades, such as the gray fox (yellow), which was shown to be more primitive. [Adapted from Lindblad-Toh et al. (2005)] (C) Schematic diagram of *HSPC152/TRMT112* and *PRDX5* genes and cloning strategy. Exons I from both genes are detailed. 5′ UTRs are indicated by open boxes. Gray box represents the sequence encoding the potential PRDX5 MTS. Conserved translation start sites are indicated in black. The potential translation start site enabling the translation of L-PRDX5 is indicated in red. P1 and P2 indicate the positions to which the PCR primers (green arrows) map. The primers were designated to map on regions sharing 100% identity between giant panda and domestic dog sequences. (D) ClustalX 2.0.7. nucleotidic sequence alignment of *PRDX5* 5′ region from nine Caniformia. Asterisks (*) indicate identities. Sequences encoding a potential MTS are highlighted in gray. Translation initiation codons are highlighted in black. STOP codons being in-frame with the ATG+1 codon are underlined. Gaps are boxed. Species names are written in brown for Phocidae, gray for Ursidae, yellow for gray fox, red for the fox-like canids, green for the South American canids and blue for the wolf-like canids. Only one of the two alleles (Allele 1) found for gray fox and American black bear *PRDX5* are represented. GenBank accession numbers are detailed in Table 1. The sequences of domestic dog and giant panda *PRDX5* 5′ region were downloaded from the Genbank references GeneID:476032 (domestic dog) and GeneID:100473172 (giant panda). Arctic wolf, *Canis lupus arctos;* American black bear, *Ursus americanus*; domestic dog, *Canis lupus familiaris*; giant panda, *Ailuropoda melanoleuca;* gray fox, *Urocyon cinereoargenteus*; maned wolf, *Chrysocyon brachyurus*; northern elephant seal, *Mirounga angustirostris*; raccoon dog, *Nyctereutes procyonoides* ; red fox, *Vulpes vulpes*.

7.3.3. A functional MTS is present in giant panda and northern elephant seal PRDX5

Given that giant panda and northern elephant seal *PRDX5* present two in-frame ATG codons, it was interesting to assess if the region comprised between these codons encodes a functional MTS. To this end, two pcDNA3.1 plasmids containing the sequence encoding the 58 N-terminal residues of giant panda or northern elephant seal PRDX5 fused with the green fluorescent protein (GFP) were generated (Fig. 7.5A and E). After transient transfection of MDCK cells with these vectors, the reporter protein was detected in mitochondria, as demonstrated by colocalization with Mitotracker Red (Fig. 7.5 B-D and F-H).

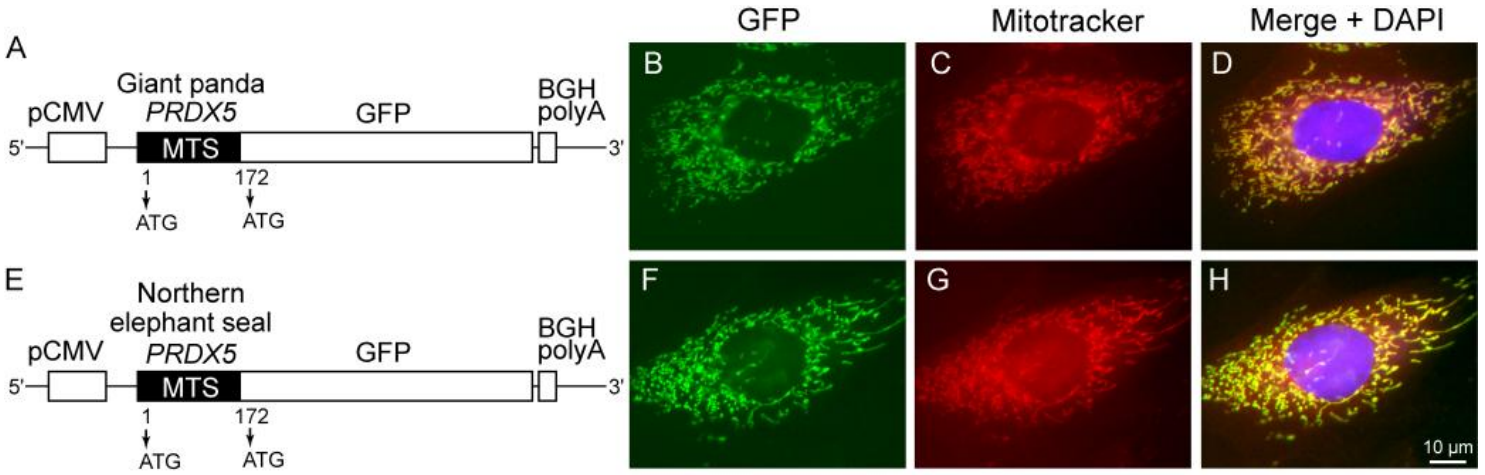

Fig. 7.5. Subcellular localization of giant panda (A-D) and northern elephant seal (E-H) PRDX5 MTS expressed in fusion with GFP in MDCK cells. Structure of the constructs cloned into mammalian expression vector pcDNA3.1 and used for MDCK transfection (A and E). Both alternative ATG initiation codons are indicated (arrows). Transfected cells were examined for GFP fusion expression (B and F). Mitochondria were stained with Mitotracker Red (C and G) and nuclei were counterstained with DAPI. *BGH polyA*, bovine growth hormone polyadenylation signal; *GFP*, green fluorescent protein; *MTS*, mitochondrial targeting sequence; *pCMV*, promoter of cytomegalovirus.

7.3.4. Human L-PRDX5 makes MDCK cells more vulnerable to acute oxidative stress

Since PRDX5 is absent in dog mitochondria, it was interesting to assess the functional consequences of the restoration of mitochondrial localization of the protein in MDCK (dog) cells. pEF-BOS was used as mammalian expression vector (Fig. 7.6A). Fig. 7.6B presents the proteins encoded by the constructs used for MDCK transfection. pEF-BOS-mito-PRDX5 and pEF-BOS-cyto-PRDX5 vectors encode human L-PRDX5 (Mito-hum) and S-PRDX5 (Cyto-hum) respectively and were described previously (Banmeyer et al. 2004). pEF-BOS-mito-PRDX5-C47A and pEF-BOS-cyto-PRDX5-C47S vectors encode the enzymatically inactive human L-PRDX5 (Mito-hum-C47A) and S-PRDX5 (Cyto-hum-C47S) respectively. The two latter were used in experiments which are described in the following section (see point 7.3.5.)

After transfection of MDCK cells with the empty expression vector (control cells), with pEF-BOS-mito-PRDX5 or with pEF-BOS-cyto-PRDX5 vectors, stable clones were selected. The clones were named MDCK control, MDCK mito-hum or MDCK cyto-hum, according to the name of the proteins encoded by the expression vectors. Overexpression of PRDX5 was quantified by immunoblotting (Fig. 7.6C). Immunoblots of total cell lysates revealed a 15- to 30-fold overexpression compared to the MDCK control cells, and a 1.5- to 3-fold higher PRDX5 content compared to human SH-SY5Y cells (Fig. 7.6D). These cells contain endogenous mitochondrial PRDX5 (De Simoni et al. 2008). The intracellular localization of PRDX5 was verified by immunofluorescence (Fig. 7.7). In the MDCK mito-hum cells, PRDX5 was largely located in the mitochondria, while MDCK cyto-hum cells strongly expressed PRDX5 in the cytosol. Incorporation of puromycin resistance gene

in the genome of MDCK control cells was verified by PCR on genomic DNA (data not shown).

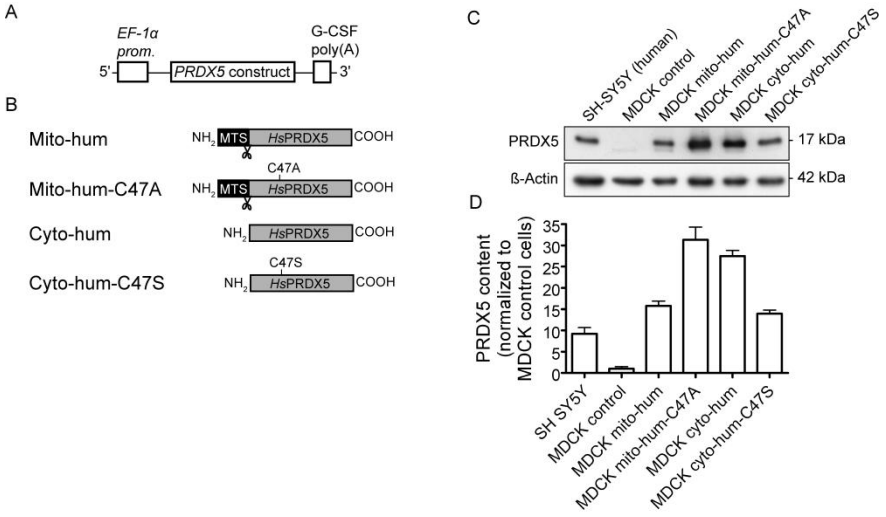

Fig. 7.6. Overexpression of human PRDX5 in MDCK cells. (A) Organization of the construct cloned into mammalian expression vector pEF-BOS. EF-1α prom, promoter region of human EF-1α chromosomal gene; G-CSF poly(A), polyadenylation signal from human granulocyte colony-stimulating factor. (B) Representation of the proteins encoded by the different constructs used for transfection. Mito-hum and Mito-hum-C47A correspond to the enzymatically active and inactive mitochondrial human PRDX5 with the cleavable (scissors) presequence (MTS), respectively. Cyto-hum and Cyto-hum-C47S correspond to enzymatically active and inactive cytosolic human PRDX5, respectively. PRDX5 content of each MDCK clone was verified by Western Blotting (C) and a quantification of the total expression level was performed (D). PRDX5 protein levels were normalized with β-actin and were expressed in relative units of PRDX5 content in MDCK control cells. Values are means ± SEM of triplicates. The subcellular localization of PRDX5 in the MDCK clones was verified by immunofluorescence (E). Mitochondria were stained with MitoTracker Red prior to cell fixation. Cell nuclei were counterstained with DAPI. *Hs*PRDX5: human PRDX5.

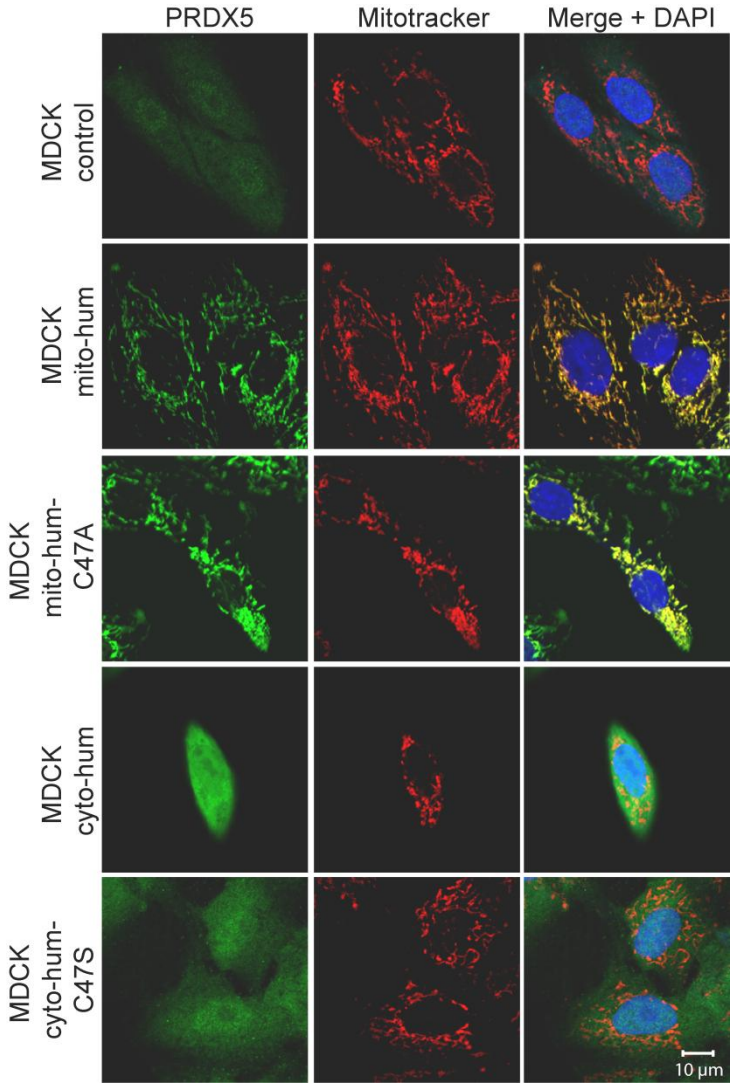

Fig. 7.7. Overexpression of human PRDX5 in MDCK cells. The subcellular localization of PRDX5 in the MDCK clones was verified by immunofluorescence. Mitochondria were stained with MitoTracker Red prior to cell fixation. Cell nuclei were counterstained with DAPI. *Hs*PRDX5: human PRDX5.

The MDCK clones were exposed to acute oxidative stress with growing concentrations of H_2O_2 or *t*-BHP (Fig. 7.8). In basal conditions, the MDCK cells expressing human PRDX5 exhibited no significantly different LDH release compared to control cells. Cell death increased with H_2O_2 and *t*-BHP exposure. Surprisingly, cell death was significantly more important in MDCK mito-hum cells compared to control cells at 15 mM H_2O_2 and 70-80 mM *t*-BHP. On the contrary, cell death was significantly decreased in MDCK cyto-hum cells compared to control cells at high concentrations of H_2O_2 and *t*-BHP.

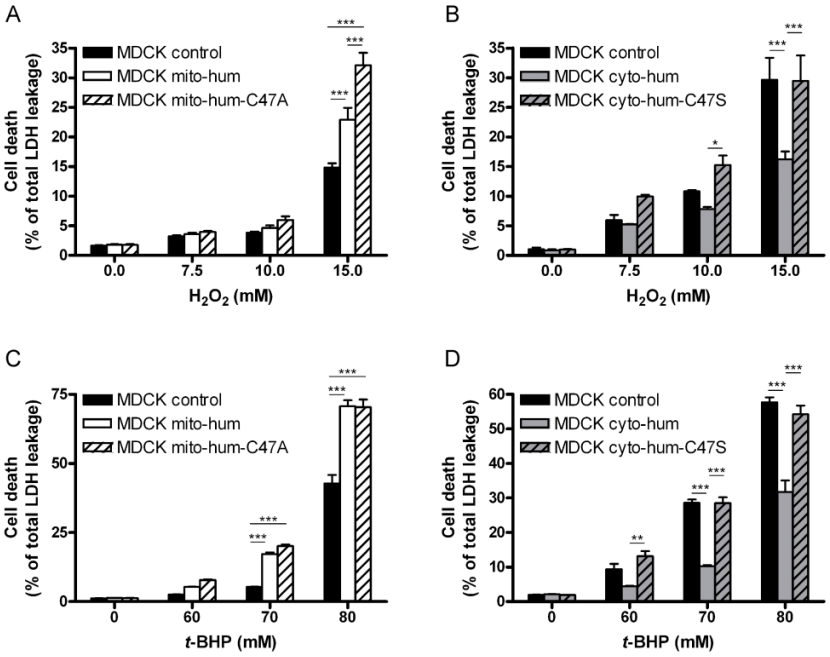

Fig. 7.8. Cytotoxicity induced by hydrogen peroxide (A-B) and *t*-BHP (C-D) in MDCK cells overexpressing human PRDX5. After one hour exposure to high levels of peroxide, cell death was evaluated by LDH release. The total LDH release (100% cell death) was determined after lysis of the cells with 2% Triton X-100. Assays were performed three times for each clone and values are means ± SEM. Significance is designated as *p<0.05, **p<0.01, ***p<0.001. *t-BHP*, *tert*-butyl hydroperoxide.

7.3.5. Increased cell death of MDCK mito-hum cells during acute oxidative stress is not linked to PRDX5 peroxidatic activity

Since human L-PRDX5 provoked increased cell mortality during acute peroxide-induced oxidative stress in MDCK cells, it was interesting to assess whether this deleterious effect was linked to PRDX5 peroxidatic activity. This latter depends on the presence of a peroxidatic cysteine (Cp). Therefore, MDCK mito-hum-C47A cells were generated, which expressed human L-PRDX5 with the Cp replaced by an alanine (C47A mutation; Fig. 7.6B). This mutation inactivates peroxidatic activity. Also, MDCK cyto-hum-C47S cells were generated, expressing the enzymatically inactive human S-PRDX5 containing the C47S mutation. After transfection and puromycin resistance selection, stable clones were selected and overexpression was quantified by immunoblotting (Fig. 7.6C). Immunoblots of total cell lysates revealed a 10- to 30-fold overexpression compared to MDCK control cells, and a 1.5- to 3-fold higher PRDX5 content compared to human SH-SY5Y cells (Fig. 7.6D). The intracellular localization of PRDX5 was verified in MDCK clones by immunofluorescence (Fig. 7.6E). In the MDCK mito-hum-C47A cells, PRDX5 was largely located in the mitochondria, while MDCK cyto-hum-C47S cells strongly expressed PRDX5 in the cytosol.

MDCK cell lines were exposed to acute oxidative stress induced by H_2O_2 or *t*-BHP exposure (Fig. 7.8). Cell death was significantly more important in MDCK mito-hum-C47A cells compared to control cells at 15 mM H_2O_2 and 70-80 mM *t*-BHP. On the other hand, expression of Cyto-hum-C47S protein had no effect on MDCK cell viability following H_2O_2 or *t*-BHP exposure.

7.4. Discussion

In this work, we show that mitochondrial PRDX5 (L-PRDX5) is absent in domestic dog although cytosolic/peroxisomal PRDX5 (S-PRDX5) is conserved. A sequence analysis of the *PRDX5* 5′ region revealed that the abolition of L-PRDX5 in domestic dog results from the loss of one nucleotide as well as the mutation of the first ATG initiation codon. To determine whether the abolition of mitochondrial PRDX5 occurred only in dog, we analyzed the *PRDX5* 5′ region of some species which are phylogenetically closely related to dog and Canidae: giant panda (Ursidae), American black bear (Ursidae) and northern elephant seal (Phocidae). We found that, unlike in domestic dog, the translation initiation codon allowing the synthesis of L-PRDX5 is maintained in these three species. Moreover, we experimentally confirmed that the 58 N-terminal residues of giant panda and northern elephant seal L-PRDX5 are able to target the GFP reporter protein into mitochondria. This indicates that the N-terminal region of giant panda and northern elephant seal L-PRDX5 corresponds to a functional MTS. Since PRDX5 MTS is abolished in domestic dog but neither in giant panda nor in northern elephant seal, it was interesting to assess the existence of an MTS in PRDX5 in other canids. We found that the first ATG codon is mutated in a GTG codon in PRDX5 in all canids that were examined. From these results, we conclude that the loss of mitochondrial PRDX5 is generalized among the extant canids. Moreover, in gray fox, raccoon dog and red fox *PRDX5*, a STOP codon at position -90 is present in the same reading frame as the translation initiation codon of S-PRDX5 (TCG/TAG mutation). Thus, in these more basal canids, two factors impede L-PRDX5 synthesis: the absence of L-PRDX5 translation initiation codon and the presence of a STOP codon. Taken together, our results suggest that the 5′ region of *PRDX5* in canids

corresponds to a sequence that was able to encode a presequence ancestrally. The first events leading to PRDX5 MTS abolition in canids would involve the mutation of the first translation initiation codon (ATG/GTG mutation) as well as the apparition of a STOP codon (TCG/TAG mutation). However, from our results, we cannot conclude which of these two events occurred first during evolution. Furthermore, in South-American canids (maned wolf) and wolf-like canids (domestic dog and arctic wolf), the ATG/GTG mutation would have been maintained but the STOP codon would further have evolved to a CAG codon. Also, in the ancestral PRDX5 MTS from these species, a single nucleotide would have been lost. Finally, our results indicate that the abolition of PRDX5 MTS would have occurred after the divergence of Canidae from the other Caniformia members. The family Canidae diverged from other Caniformia about 50 million years ago (mya), but extant canids have diverged from a common ancestor within the last 10 million years (Ostrander and Wayne 2005). Therefore, the loss of mitochondrial PRDX5 in canids would have occurred between 50 and 10 mya.

It is interesting to note that two different alleles were found in gray fox *PRDX5* 5′ region. The presence of these two alleles would not result in the generation of two different PRDX5 proteins since the heterozygous site is not localized in the coding region. On the opposite, we found also two alleles in American black bear *PRDX5* 5′ region which would result in the generation of two different PRDX5 protein sequences. Indeed, sequence analysis of allele 2 revealed the presence of an additional ATG codon at position -6 which refers to the ATG+1 codon from allele 1 (Table 1). Noteworthy, the existence of these two alleles is confirmed by numerous expressed sequence tags (for example, Genbank accession numbers

GW308481.1 and GW308562.1). Therefore, it would be interesting to investigate the consequences of the expression of these two alleles on PRDX5 subcellular distribution in American black bear.

The abolition of PRDX5 MTS in canids suggests that mitochondrial PRDX5 is not essential in canid species. Some of them have encountered high evolutionary success, like the raccoon dog or the red fox. It appears thus that the absence of mitochondrial PRDX5 does not impair species' ability to meet a huge evolutionary success. The abolition of mitochondrial PRDX5 in canids is nevertheless surprising. Indeed, it appears that mitochondrial localization is conserved in various other vertebrate and invertebrate species (Knoops et al. 1999; Oberley et al. 2001; Zhang et al. 2003; Banmeyer et al. 2004; Leyens et al. 2004; Pagliarini et al. 2008; Radyuk et al. 2009; Li et al. 2011; Van der Eecken et al. 2011), even belonging to basal metazoan phyla, like placozoa and porifera. Furthermore, the abolition of L-PRDX5 is unexpected since mitochondria are particularly exposed to oxidative attacks caused by ROS and RNS (Halliwell and Gutteridge 2007). Moreover, the cytoprotective function of mitochondrial PRDX5 was described in several studies. For example, it has been shown that overexpression of L-PRDX5 confers resistance to peroxide or drug-induced cell death and DNA damage (Nguyen-Nhu and Knoops 2003; Banmeyer et al. 2004; Peng et al. 2004a; Peng et al. 2004b; Banmeyer et al. 2005).

In a recent paper, we have shown that domestic pig has also lost mitochondrial PRDX5 according to a similar molecular mechanism, namely by the loss of the translation initiation codon of L-PRDX5 (Van der Eecken et al. 2011). Since mitochondrial PRDX5 is maintained in bovine, we concluded that PRDX5 MTS was lost during Cetartiodactyla evolution. Therefore, the loss of L-PRDX5 in canids and domestic pig results from two distinct events

during mammalian evolution, i.e. one having occurred during Caniformia diversification, the other taking place during Cetartiodactyla evolution. However, given that PRDX5 distribution was analyzed in a limited number of species so far, we cannot exclude that its subcellular distribution would have changed at more occasions during the evolution of mammals. Accordingly, it would be interesting to study PRDX5 subcellular distribution in additional phylogenetic groups. To our knowledge, few enzymes have been reported to have changed their subcellular distribution during mammalian evolution. One example concerns the intermediary metabolic enzyme alanine:glyoxylate aminotransferase (AGT), whose subcellular localization was reported to change during mammalian evolution (Holbrook et al. 2000; Birdsey et al. 2004). Interestingly, the molecular mechanism responsible for the loss of mitochondrial targeting in AGT and PRDX5 is very similar.

Since mitochondrial PRDX5 is absent in dog, it was interesting to study the functional consequences of the restoration of L-PRDX5 in a dog cellular model. In order to evaluate the ability of mitochondrial PRDX5 to afford antioxidant protection in dog during oxidative stress, we generated MDCK (dog) cell lines expressing human mitochondrial PRDX5. Moreover, to compare PRDX5 ability to exert a cytoprotective effect according to its subcellular localization, we also generated MDCK expressing human cytosolic/peroxisomal PRDX5. Surprisingly, PRDX5 expression in MDCK mitochondria resulted in an increased cell mortality at high peroxide concentrations, while PRDX5 expression in MDCK cytosol/peroxisomes afforded a greater resistance to acute oxidative stress. As mentioned in the introduction, L-PRDX5 differs from S-PRDX5 by the presence of an additional N-terminal MTS. However, this MTS is cleaved after

mitochondrial import, releasing a functionally active 17 kDa mature mitochondrial PRDX5 which is identical to S-PRDX5 (Knoops et al. 2011). In MDCK mito-hum cells, no PRDX5 signal at higher molecular weight was detected by western blotting, indicating that the MTS was removed efficiently. Therefore, it appears that mitochondrial and cytosolic/peroxisomal human PRDX5, although being identical, do not equally protect MDCK cells, depending on their subcellular localization. Moreover, PRDX5 does not only appear to be an ineffective antioxidant protective enzyme in MDCK mitochondria – which would have resulted in an unchanged cell viability during oxidative stress – but this protein seems also to gain cytotoxic properties under acute oxidative stress, resulting in an increased cell mortality. Furthermore, given that MDCK mito-hum cells exhibit an increased cell death during oxidative stress but not under basal conditions, one could hypothesize that the sensitization is linked to PRDX5 peroxidatic activity. However, MDCK cells expressing enzymatically inactive mitochondrial PRDX5 exhibited also a higher cell mortality following oxidative stress, indicating that human PRDX5 provokes deleterious effects in MDCK mitochondria independently of its enzymatic activity. It seems thus that the presence of the protein, rather than its peroxidatic activity, is inappropriate in the MDCK mitochondrial matrix during acute oxidative stress. At this stage, it is difficult to establish which molecular mechanism is responsible for the peroxide-induced sensitization of the MDCK mito-hum cells. A possible explanation is that PRDX5 cytotoxic property is linked to a redox-dependent interaction with another MDCK mitochondrial protein, impairing the function of the binding partner. Interactions of PRDXs with various proteins have been described, such interactions having been shown to modulate the functions of the binding partners (Rhee and Woo 2011). However, so far, little is known about PRDX5

interactions with mitochondrial proteins. Therefore, it would be interesting to study and compare the interactions of PRDX5 with other MDCK mitochondrial proteins in basal *versus* oxidative conditions. Finally, it is important to note that, in a previous study, we used the same expression vectors to assess the cytoprotective function of human L-PRDX5 and S-PRDX5 in Chinese hamster ovary (CHO) cells (Banmeyer et al. 2004). In these cells, which contain endogenous mitochondrial PRDX5, both L-PRDX5 and S-PRDX5 afforded antioxidant protection during acute oxidative stress. It appears thus that human L-PRDX5 triggers deleterious effects during acute oxidative stress in cells lacking endogenous mitochondrial PRDX5, while the same protein confers antioxidant resistance in cells possessing endogenous mitochondrial PRDX5. This led us to suggest that, despite the fact that PRDX5 cytoprotective function has been clearly demonstrated by several studies in human and rodents, the conservation of mitochondrial PRDX5 would not confer necessarily an advantage in all mammalian species. Also, although the loss of L-PRDX5 in canids could have occurred without link with this phenomenon, it is tempting to speculate that the cytotoxic property of L-PRDX5 in mitochondria is at the origin of the abolition of mitochondrial PRDX5 in canids.

Interestingly, analysis of PRDX5 sequences from different animal species reveals that the non-conservation of PRDX5 mitochondrial targeting represents only a fraction of PRDX5 subcellular variability that is found through animal kingdom (see Fig. 7.2.). Indeed, in addition to the lack of PRDX5 MTS in some mammals, the PTS1, responsible for peroxisomal localization, appears also to be abolished in some animal species. Moreover, the presence of the second translation initiation codon, permitting the translation of S-PRDX5, appears to be absent in some species, like in bay

scallop. In these species, only L-PRDX5 (mitochondrial) is likely to be translated. Taken together, it seems that PRDX5 relocalizations occurred at many occasions during mammalian evolution. Whether this variability permits an adaptation to specific needs, metabolic pathways or life environments remains a matter of speculation.

To conclude, the present study shows that mitochondrial PRDX5 is not essential in canids. Our results suggest that the abolition of mitochondrial PRDX5 in the family Canidae would have occurred between 50 and 10 mya and involves the mutation of the first translation initiation codon of PRDX5 as well as the appearance of a STOP codon in the ancestral MTS. Finally, our work shows that the restoration of mitochondrial PRDX5 in MDCK cells triggers deleterious effects during acute oxidative stress conditions. Further studies will be necessary to investigate the mechanism by which MDCK mitochondrial matrix is inappropriate to PRDX5 antioxidant protective function.

7.5. Acknowledgements

We thank D Cantinieaux for her preliminary work on the ancestral presequence of dog PRDX5. We thank Pr. YJ Schneider (Université Catholique de Louvain, Belgium) for providing MDCK cell line. We thank Dr. JC Bertho (zoological park "Le Monde Sauvage", Aywaille, Belgium), Pr. MAG Van Der Heyden (University Medical Center Utrecht, The Netherlands), Pr. RK Wayne (University of California, USA), C Louis and Pr. C Debier (Université catholique de Louvain, Belgium) and Pr. E Le Boulengé (Université Catholique de Louvain, Belgium) for providing tissue or DNA samples. We thank M Pirson and Dr. J Goemaere for critical reading. This work was supported by grants from the National Fund for Scientific

Research (FRFC N°2.4.603.09F) and the Communauté française de Belgique-Actions de Recherche Concertées (10/15-026).

8. Overexpression of dog PRDX5 in Madin-Darby canine kidney (MDCK) cells does not confer antioxidant protection during acute oxidative stress

Abstract

The antioxidant enzyme PRDX5 is unusual as its subcellular distribution appeared to be variable among mammals. Indeed, in some species, like human, this enzyme is localized in the cytosol, the mitochondria, the peroxisomes and in the nucleus. In other species, like pig and dog, PRDX5 mitochondrial targeting has been lost. Previously, in order to study the functional consequences of the restoration of PRDX5 mitochondrial targeting in dog, we expressed human mitochondrial PRDX5 in Madin-Darby canine kidney (MDCK) cells. Unexpectedly, we showed that the expression of this human protein in MDCK mitochondria increased cell mortality under acute peroxide-induced oxidative stress, while expression of this protein in MDCK cytosol/peroxisomes had a protective effect under the same experimental conditions. Here, we examine the consequences of the restoration of mitochondrial targeting of dog PRDX5 in MDCK cells. Like with human mitochondrial PRDX5, expression of dog PRDX5 in MDCK mitochondria resulted in increased cell death during acute oxidative stress. However, unlike human cytosolic/peroxisomal PRDX5, dog PRDX5 overexpression in MDCK cytosol/peroxisomes resulted also in a sensitization during acute oxidative stress. Thus, overexpression of dog PRDX5 in MDCK cells provokes deleterious effects under oxidative stress independently of the subcellular localization. Therefore, for a yet unknown reason, it appears that dog PRDX5 is unable to exert its antioxidant protective function in the MDCK cellular model.

***Keywords*:** Peroxiredoxin 5, Subcellular targeting, Mitochondrion, *Canis lupus familiaris*, MDCK cells, oxidative stress

Abbreviations used: LDH: lactate dehydrogenase; L-PRDX5: long form of peroxiredoxin 5; MDCK: Madin-Darby canine kidney; MTS: mitochondrial targeting sequence; PRDX: peroxiredoxin; S-PRDX5: short form of peroxiredoxin 5; *t*-BHP: *tert*-butyl hydroperoxide

8.1. Introduction

PRDX5 is the last member of the mammalian PRDX family that has been identified. This antioxidant enzyme exhibits a wide subcellular distribution. Indeed, in human, PRDX5 can be targeted to the cytosol, the mitochondria, the peroxisomes and, in several situations, to the nucleus (Knoops et al. 1999; Kropotov et al. 1999; Yamashita et al. 1999; Seo et al. 2000; Kinnula et al. 2002; Lu et al. 2006). This complex subcellular distribution results from the existence of two PRDX5 forms encoded by a single gene. The short PRDX5 form (S-PRDX5) corresponds to the cytosolic/peroxisomal form while the long PRDX5 form (L-PRDX5) is targeted to mitochondria thanks to a cleavable mitochondrial targeting sequence (MTS) (Knoops et al. 2011). Interestingly, in mammals, PRDX5 subcellular localization has changed at least at two different occasions during mammalian evolution. Indeed, although the cytosolic/peroxisomal distribution seems to be conserved in mammals, mitochondrial localization of PRDX5 is lacking in some species, like pig and dog (see chapters 6 and 7).

In chapter 7, we investigated the functional consequences of the restoration of mitochondrial PRDX5 in dog by overexpressing human L-PRDX5 in MDCK cells. Surprisingly, peroxide-induced cell death was increased in MDCK cells expressing human PRDX5 in mitochondria. On the other hand, expression of human S-PRDX5 protected MDCK cells against

peroxide-induced oxidative stress. We concluded that, for an unknown reason, human PRDX5 gains cytotoxic properties in MDCK mitochondria under acute oxidative conditions. These cytotoxic properties were not related to PRDX5 enzymatic activity. However, we cannot exclude that PRDX5 heterologous expression (human PRDX5 was expressed in dog mitochondria) is at the origin of the deleterious effects in MDCK cells. Therefore, we assessed whether dog PRDX5 targeted to mitochondria would also provoke deleterious effects in MDCK cells during acute oxidative stress. In this work, we study the consequences of the (over-)expression of dog PRDX5 in MDCK mitochondria or cytosol/peroxisomes.

8.2. Materials and methods

8.2.1. Computer analysis

Multiple sequence alignment was performed with ClustalX 2.0.7 software (Larkin et al. 2007).

8.2.2. Cloning of MDCK PRDX5 cDNA

Total RNA from MDCK cells was isolated using NucleoSpin RNAII kit (Macherey-Nagel) following manufacturer's instructions. The cDNA strand was synthesized from total RNA using oligo(dT) and ReverAid™ H Minus First Strand cDNA Synthesis Kit (Fermentas). cDNA was amplified by RT-PCR using forward primer 5'-GGTCTGCAGCACAGGCAGTGTCG-3' and reverse primer 5'-CCTTTGTCCAGGGCTGGGCAGGTGC-3'. The amplified sequence was ligated into the pCR2.1-TOPO vector (Invitrogen) and subsequently sequenced.

8.2.3. Plasmid construction

Plasmid pEF-BOS containing an EF-1-α promoter, a puromycin resistance gene and G-CSF-poly(A) polyadenylation signal was used as mammalian expression vector (Banmeyer et al. 2004).

To target dog PRDX5 to the mitochondria, the MTS of human PRDX5 was fused to the N-terminus of dog S-PRDX5. The plasmid pEF-BOS-mito-can-PRDX5 (encoding human PRDX5 MTS in fusion with dog S-PRDX5) was constructed as follows. The sequence encoding human PRDX5 MTS was PCR-amplified (PCR1) from human *PRDX5* cDNA (Knoops et al. 1999) using forward primer 5′-GGCCGTACTAGTGGTATGGGACTAGCTGGCGTGTGCGCC-3′ (*Spe*I restriction site underlined) and reverse primer 5′-GGCATCTCCCACCTTGATTGGGGCCATGGCTGC-5′. The sequence encoding dog S-PRDX5 was amplified (PCR2) from dog *PRDX5* cDNA (see point 8.2.2) using forward primer 5′-GCCATGGCCCCAATCAAGGTGGGAGATGCC-3′ and reverse primer 5′-TATCTGGCGGCCGCCACTCAGAGCTGCGAGAGGATGTTGGG-3′ (*Not*I restriction site underlined). The two fragments were joined by overlapping PCR using forward primer from PCR1 and reverse primer from PCR2. The resulting amplicon was ligated in the pCR2.1 vector and subcloned into the *Spe*I and *Not*I sites of the pEF-BOS vector.

The plasmid pEF-BOS-cyto-can-PRDX5 (encoding dog S-PRDX5), was generated by PCR amplification of dog *PRDX5* cDNA (see point 8.2.2) using forward primer 5′-AGCGACTAGTCCGCCATGGCCCCAATCAAGGTGGGAGATGC-3′ (*Spe*I restriction site underlined) and reverse primer 5′-TATCTGGCGGCCGCCACTCAGAGCTGCGAGAGGATGTTGGG-3′ (*Not*I restriction site underlined). The resulting amplicon was ligated in the

pCR2.1 vector and subcloned into the *Spe*I and *Not*I sites of the pEF-BOS vector.

8.2.4. Stable transfection of MDCK cells

Transfection was performed using Amaxa™ Nucleofector™ Technology (Lonza AG). Cells were selected for puromycin resistance and individual clones were isolated. At least three clones were obtained and characterized for each cell line. PRDX5 overexpression was verified by immunostaining and Western blotting. Experimental procedures were described in Chapter 7.

8.2.5. Cell treatment with H_2O_2 and t-BHP and lactate dehydrogenase (LDH) assay

Cells were exposed for one hour to increasing concentrations of H_2O_2 or *t*-BHP (Sigma). Cytotoxicity was evaluated by the lactate dehydrogenase (LDH) release assay. Experimental procedures were described in Chapter 7. Cell death values were calculated from triplicates within an experiment. The experiment was repeated three times, allowing the calculation of means and SEM. Statistical analysis was performed using two-way ANOVA with the Bonferroni post-hoc test. Significance versus control is designated as *$p<0.05$, ** $p<0.01$, *** $p<0.001$.

8.3. Results

8.3.1 Generation of MDCK clones (over-)expressing dog PRDX5 in mitochondria or cytosol/peroxisomes

To study the effect of the (over-)expression of dog PRDX5 in mitochondria or cytosol/peroxisomes during acute oxidative stress, stable MDCK transfectants were generated. pEF-BOS was used as mammalian expression vector (Fig. 8.1.A). Figure 8.1.B. presents schemes of the proteins encoded by the different constructs used for transfection. pEF-BOS-mito-can-PRDX5 encodes human PRDX5 MTS in fusion with the N-terminal part of dog S-PRDX5 (Mito-can). pEF-BOS-cyto-can-PRDX5 vector encodes dog S-PRDX5 (Cyto-can). After transfection of MDCK cells with the empty expression vector (control cells) or with one of the two PRDX5 expression vectors, stable clones were selected. The cell lines were named MDCK control, MDCK mito-can and MDCK cyto-can according to the name of the proteins encoded by the expression vectors. Overexpression of PRDX5 was quantified by immunoblotting (Fig. 8.1.D). PRDX5 expression in MDCK mito-can cells was ~4-fold higher than in control cells while in MDCK cyto-can cells, this expression was ~22-fold higher (Fig. 8.1.E). Subcellular localization of PRDX5 was verified by immunofluorescence. In MDCK control and MDCK cyto-can cells, a cytosolic and nuclear signal, as well as a typical peroxisomal granular pattern, were detected (Fig. 8.1.C). In MDCK mito-can cells, PRDX5 was mainly detected in the mitochondria.

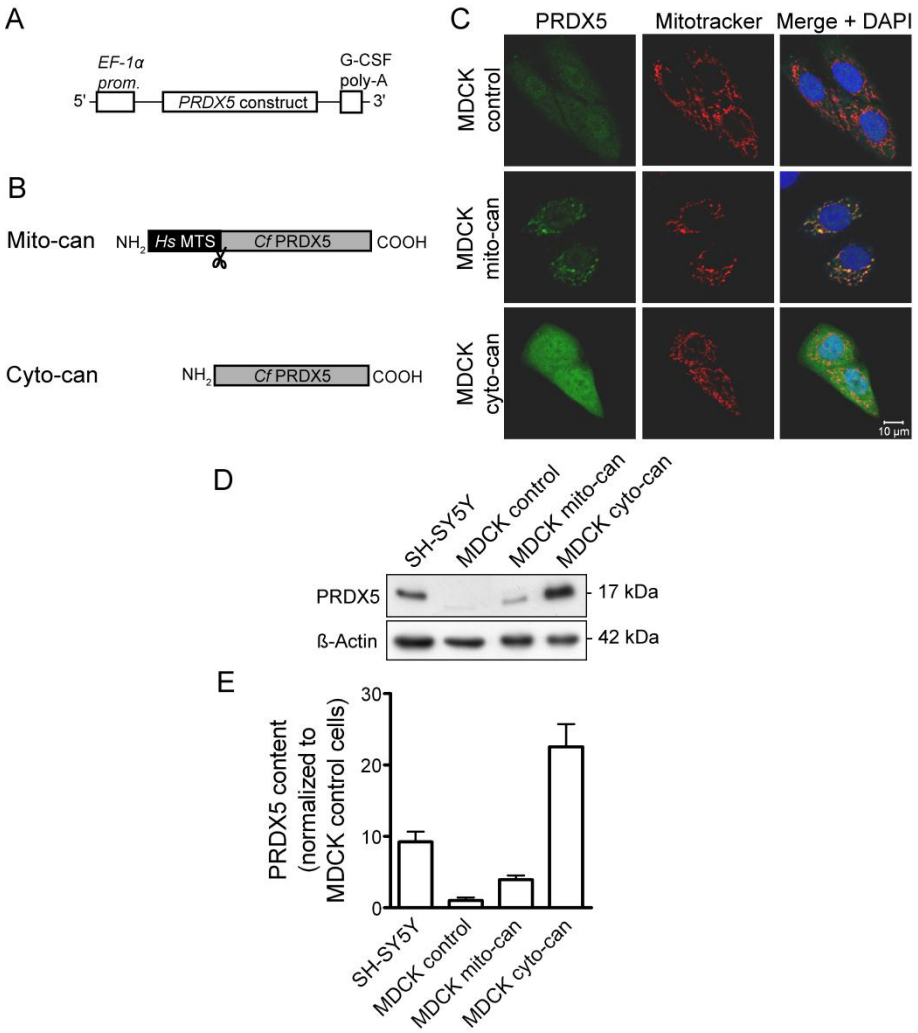

Fig. 8.1. Overexpression of dog PRDX5 in MDCK cells. (A) Organization of the construct cloned into mammalian expression vector pEF-BOS. EF-1α prom, promoter region of human EF-1α chromosomal gene; G-CSF-poly-A, poly(A) adenylation signal from human granulocyte colony-stimulating factor. (B) Representation of the proteins encoded by the different constructs used for transfection. Mito-can corresponds to the cleavable (scissors) human PRDX5 mitochondrial targeting sequence (*Hs* MTS) expressed in fusion with the N-terminal part of dog PRDX5 (*Cf* PRDX5). Cyto-can corresponds to dog PRDX5. (C) The subcellular localization of PRDX5 was verified by immunofluorescence in each clone. (D) PRDX5 overexpression was verified by Western blotting. (E) PRDX5 protein levels were quantitated, normalized with β-actin levels and expressed in relative units of PRDX5 content in MDCK control cells. Values are means ± SEM of triplicates.

8.3.2. Cytotoxicity induced by high concentrations of H_2O_2 and t-BHP

To determine whether dog PRDX5 targeted to mitochondria could protect against oxidative stress induced by peroxides, MDCK control and MDCK mito-can cells were exposed for one hour to various H_2O_2 (Fig. 8.2.A) and *t*-BHP concentrations (Fig. 8.2.C). Under basal conditions, the MDCK mito-can and control cells exhibited equivalent LDH release. At high levels of H_2O_2 and *t*-BHP, cell death was significantly higher in MDCK mito-can cells compared to MDCK control cells. On the other hand, MDCK cyto-can cells were also subjected to acute oxidative stress (Fig 8.2.B and 8.2.D). Cell death was significantly increased in cyto-can cells compared to control cells at high concentrations of H_2O_2 and *t*-BHP.

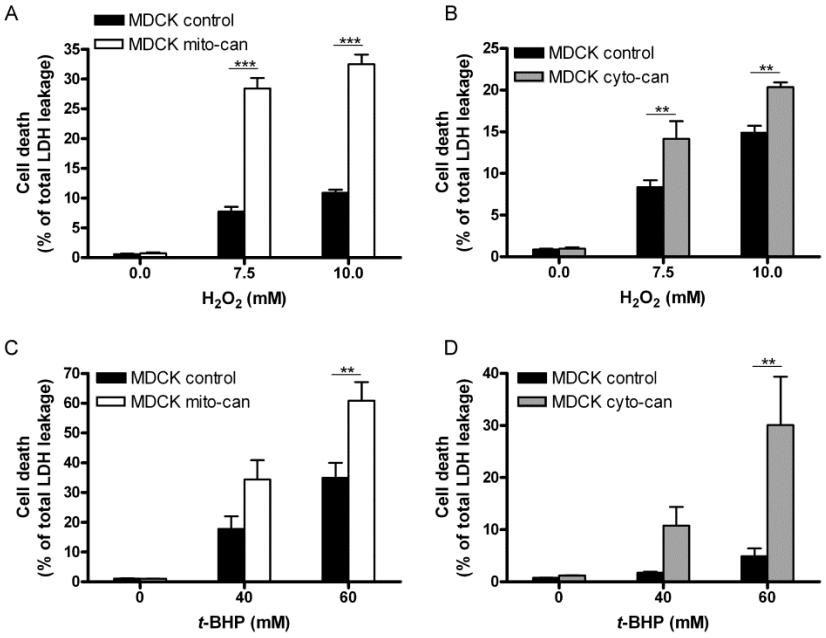

Fig. 8.2. Cytotoxicity induced by hydrogen peroxide (A-B) and *t*-BHP (C-D) in MDCK cells overexpressing dog PRDX5. After one hour exposure to high peroxide levels, cell death was evaluated by the lactate dehydrogenase (LDH) release. The total LDH release (100% cell death) was determined after lysis of the cells with 2% Triton X-100. Values are means ± SEM of three independent assays. Significance is designated as *p<0.05, **p<0.01, ***p<0.001.

8.4. Discussion

8.4.1. Human PRDX5 versus dog PRDX5

In Chapter 7, we showed that human PRDX5 expression in MDCK mitochondria increased cell death during acute peroxide-induced oxidative stress, while expression of the enzyme in the cytosol/peroxisomes had the opposite effect (see Fig. 8.3). This result was unexpected, and suggests that PRDX5 gains cytotoxic properties in MDCK mitochondria under acute oxidative stress conditions. However, we cannot exclude that the cytotoxicity was linked to the heterologous expression of the protein. To test this hypothesis, we targeted dog PRDX5 to MDCK mitochondria and reiterated the experiment. As a control, dog PRDX5 was overexpressed in MDCK cytosolic/peroxisomal compartment. We expected that mitochondria-targeted dog PRDX5 would provoke deleterious effects in MDCK cells while overexpression of dog cytosolic/peroxisomal PRDX5 (S-PRDX5) would confer resistance to oxidative stress. In this case, we would have concluded that the cytotoxic properties of human PRDX5 in MDCK mitochondria were not linked to heterologous expression. Unexpectedly, increased cell death was observed in both MDCK mito-can and MDCK cyto-can cells during acute oxidative stress (see Fig. 8.3). Given the increased cell death in MDCK cyto-can cells, the present work does not answer our primary question.

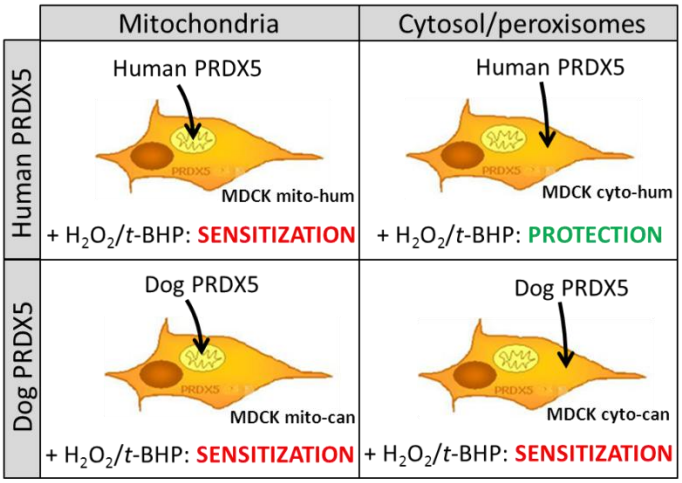

Fig. 8.3. Peroxide-induced cytotoxicity in MDCK cells (over-)expressing human/dog PRDX5 in mitochondria or cytosol/peroxisomes: summary of the results. Overexpression of human mitochondrial PRDX5, dog cytosolic/peroxisomal PRDX5, as well as dog mitochondria-targeted PRDX5 triggered increased MDCK cell mortality during acute oxidative stress. On the other hand, expression of human cytosol/peroxisomal PRDX5 in MDCK cells conferred antioxidant protection.

8.4.2. Dog and human S-PRDX5 exhibit different properties

Our results do not respond to our main question, but rather they raise another important issue: why does the overexpression of canine S-PRDX5 provoke deleterious effects during acute oxidative stress, while expression of human S-PRDX5 prevents cell death under the same experimental conditions? It is worth noting that PRDX5 expression level in MDCK cyto-hum (MDCK expressing human S-PRDX5) and MDCK cyto-can cells (MDCK overexpressing dog S-PRDX5) are similar (see Figs. 7.6 and 8.1). Human and dog S-PRDX5 opposite effects in MDCK cells are thus not due to different expression levels, but suggest that human and dog S-PRDX5 possess different intrinsic properties. This is unexpected because human and dog S-PRDX5 peptidic sequences are not divergent, presenting 89% identity and 96% similarity (see Fig. 8.4). Also, the catalytic sites of dog S-PRDX5 are conserved. Furthermore, based on tertiary structure predictions, no specific

constraints would hinder dog PRDX5 to adopt a similar tertiary structure as human PRDX5 (Declecq JP, personal communication). Taken together, these data suggest that dog S-PRDX5 should act as an efficient antioxidant enzyme. However, we cannot totally exclude that the slightly different sequences could confer new properties to dog PRDX5. For example, some amino acid substitutions could create new interaction sites for another dog cytosolic or peroxisomal protein. Furthermore, dog and human PRDX5 different properties could possibly be linked to post-translational modifications, which would differ on dog and human PRDX5. Interestingly, the generation of MDCK cells expressing human PRDX5 revealed that dog PRDX5 possesses a lower apparent molecular weight compared to human PRDX5 (see Fig. 7.6). Amino acid comparison of dog and human PRDX5 suggests that this apparent molecular weight difference (~1.5 kDa), could not be caused by a variation in the primary structure of the protein. It is thus possible that some post-translational modifications that occur in human PRDX5 are absent in dog PRDX5. The absence of these post-translational modifications could possibly alter dog PRDX5 antioxidant function, or confer new properties to the protein. Interestingly, *in silico* analysis of human and dog PRDX5 protein sequences revealed that Ser74 and Ser118 residues are predicted to be phosphorylated in human but not in dog PRDX5 (see Fig. 8.4.). In this context, although it was shown that the typical 2-Cys PRDXs may undergo different posttranslational modifications (Rhee and Woo 2011), little is known about such modifications of PRDX5. Unlike typical 2-Cys PRDXs, PRDX5 is not known to be a good candidate to undergo hyperoxidation (Woo and Rhee 2010). By contrast, it was shown that PRDX5 can be glutathionylated in rat hepatocytes exposed to oxidative stress (Fratelli et al. 2003). To further investigate the origin of the different properties of dog and human PRDX5, a two-dimensional gel electrophoresis purification of the proteins with subsequent analysis would be necessary.

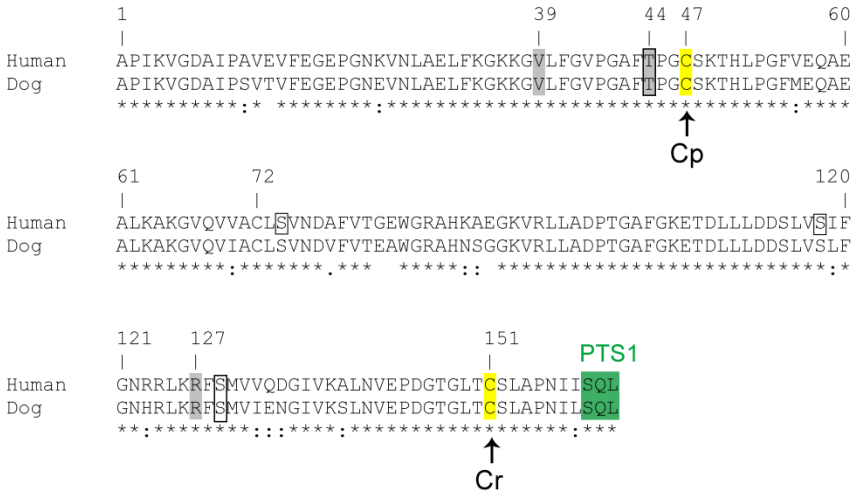

Fig. 8.4. ClustalX 2.0.7 amino acid sequence alignment (Larkin et al. 2007) of human and dog PRDX5. Asterisks indicate identities, dots and double dots indicate conservative and highly conservative substitutions, respectively. Amino acid numbering refers to mature human PRDX5 (Declercq et al. 2001). Peroxidatic (Cp) and resolving (Cr) cysteines are indicated in yellow. Residues involved in the stabilization of the catalytic pocket are highlighted in grey. Phosphorylated residues predicted with the NetPhos server (Blom et al. 1999) are boxed. The peroxisomal targeting sequence (PTS1) is indicated in green.

8.4.3. Mechanism underlying dog PRDX5 cytotoxicity in MDCK cells

It is difficult to establish which mechanism is responsible for the sensitization observed in the MDCK cyto-canis cells during acute oxidative stress. In the previous section, we propose that the absence of some post-translational modifications could impair PRDX5 peroxidatic activity. However, the absence of peroxidatic activity would have no effect on cell viability and does not explain the increased cell death of MDCK cyto-can cells. It is thus possible that dog PRDX5 is able to function as an efficient antioxidant enzyme in MDCK cells, but that the protein concomitantly provokes deleterious effects which surpass the antioxidant protection conferred by PRDX5. These deleterious effects, which would be linked to dog-specific PRDX5 properties, could be driven by different mechanisms, such as a redox-dependent interaction with another protein, leading to the dysfunction of this protein. Also, an altered interaction with the reducing

protein thioredoxin 1 (TXN1) could account for the deleterious effects observed in MDCK cyto-can cells. For example, dog PRDX5/TXN1 complex could be more stable as human PRDX5/TXN1 complex, increasing the complex half-life and rendering thereby TXN1 less available for the reduction of other oxidized proteins. Interestingly, it has been suggested recently that, in yeast, under oxidative stress conditions, it would be critical to allow TXN to act on substrates other than PRDXs to ensure repair of oxidized proteins and cell survival (Day et al. 2012). Finally, dog PRDX5 could also trigger deleterious effects by inducing a decreased expression of other antioxidant enzymes. Therefore, it would be interesting to evaluate the expression levels of catalase, GPXs and the other members of the PRDX family in MDCK cyto-can cells.

8.4.4. Dog cytosolic/peroxisomal PRDX5 is conserved

Although mitochondrial PRDX5 is abolished in dog, we show that the cytosolic/peroxisomal form of the protein is maintained (see Chapter 7). From this observation, one could logically hypothesize that cytosolic PRDX5 is essential in dog, or, at least, confers an advantage to the species. This is not consistent with the fact that overexpression of dog S-PRDX5 in MDCK cells provokes deleterious effects during acute oxidative stress. However, we cannot conclude from our results that the presence of endogenous S-PRDX5 in dog makes no sense. First, the high peroxide resistance of MDCK cells led us to use very high H_2O_2 concentrations (10-15 mM) to induce peroxide cytotoxicity. These concentrations are not physiologically relevant, as it was estimated that cells may experience up to 0.01-1 mM H_2O_2 during their life history (Schroder and Eaton 2008). Testing lower peroxide concentrations during longer periods would permit to mimic more physiological relevant situations, and could possibly lead to different results. Secondly, it is interesting to note that endogenous PRDX5 content in MDCK cells is low compared to human SH-SY5Y cells (see Fig 8.1). Transfection of MDCK cells

led to a 22-fold PRDX5 overexpression, which is considerable. Therefore, the presence of S-PRDX5 in low concentrations could be beneficial in MDCK cells, but, beyond a critical threshold, could provoke deleterious effects under oxidative conditions. It would be interesting to compare cytosolic/peroxisomal PRDX5 content in more dog and rat tissues to evaluate whether PRDX5 expression level is globally lower in dog compared to other species. Also, it would be useful to test the consequences of PRDX5 overexpression in another dog cell line, like in Cf2Th (dog thymus) cell line. Finally, to study the function of dog PRDX5, it would be of interest to evaluate the consequences of PRDX5 silencing in MDCK cells.

8.4.5. Conclusion

This work, although not responding to our primary objective, raises new questions. Here, we show that dog PRDX5 presents specific features not only because the absence of the mitochondrial form, but also through an atypical behavior of its cytosolic/peroxisomal form following acute oxidative stress. This makes dog cytosolic/peroxisomal PRDX5 an interesting tool to study the consequences of PRDX5 interspecific variability.

IV. General discussion, perspectives and conclusions

9. General discussion

This work focuses on interspecific variability of PRDX5 mitochondrial targeting sequence. In this chapter, a general view of the major outcomes of this work will be given. However, before discussing our experimental results, this section will situate our key issue in a more general context. Indeed, it seems critical to us to emphasize that interspecific variability of PRDX5 mitochondrial targeting represents only a fraction of PRDX5 subcellular distribution variability that is found through the animal kingdom (Fig. 9.1). Despite the fact that we can find some disparate elements representing this variability in the literature, this point was never underlined nor deeply investigated until now.

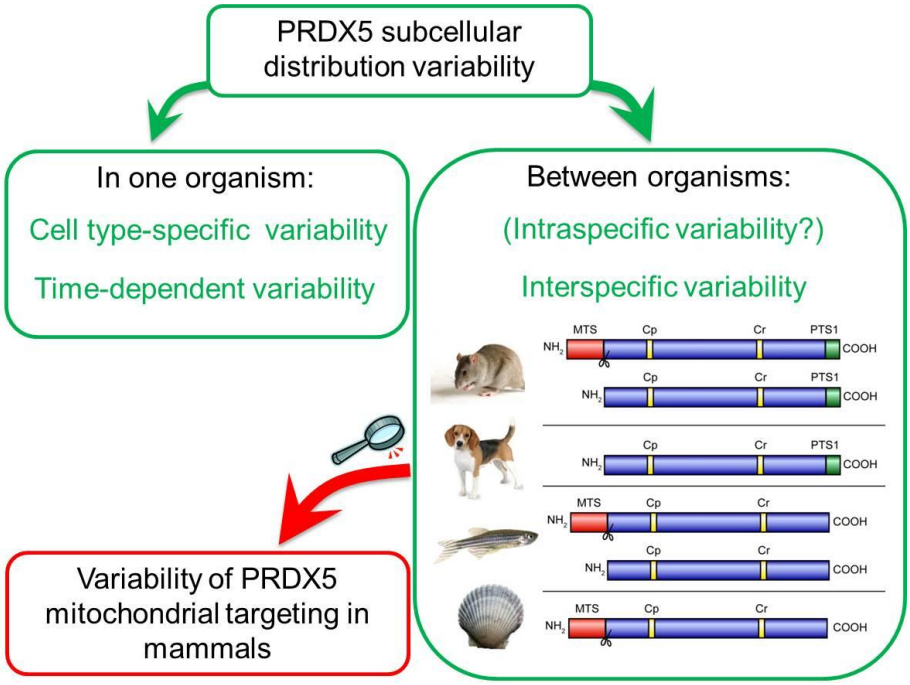

Fig. 9.1. General context (green) in which our key issue (red) lies. PRDX5 subcellular distribution may vary within an organism (according to cell type and during time) and during animal evolution (according to species). In the latter case, PRDX5 subcellular distribution variation concerns not only mitochondrial targeting. Intraspecific variability (variability between organisms in the same species) could also occur, but no evidence of such variability is reported in the literature.

9.1. PRDX5: from a complex gene organization to variable subcellular distribution

9.1.1. Multiple targeting of human PRDX5

In eukaryotes, a protein can be located in several subcellular compartments; a phenomenon termed multiple targeting, multiple distribution or multiple localization. Differentially localized proteins are termed isoproteins (Karniely and Pines 2005; Yogev and Pines 2011). Human PRDX5, being distributed in mitochondria, cytosol, peroxisomes and in several situations, in the nucleus, is an example of multiply targeted protein. In eukaryotes, multiple targeting can be achieved by several mechanisms (for review see Karniely and Pines (2005); Yogev and Pines (2011)). These are principally divided up into two groups, based on the presence of one or two translation products. If two translation products are present, one of the two translation products possesses a targeting signal while the other lacks it. The production of two translation products can result from (i) the presence of two genes, (ii) the presence of multiple RNAs, involving alternative transcription initiation or alternative splicing or (iii) alternative translation initiation, based on the ability of the ribosome to skip the first AUG. More complicated mechanisms are those allowing multiple targeting of single translation products. These mechanisms involve (i) the presence of an ambiguous targeting signal, being recognized by more than one organelle, (ii) inefficient or incomplete targeting, allowing a subpopulation of molecules to be targeted to one organelle while other molecules remain in the cytosol, (iii) multiple targeting sequences, (iv) changes in targeting sequence accessibility in a subpopulation of molecules, (v) reverse translocation during mitochondrial import, or (vi) release of proteins from organelles by membrane leakage or export (Knott et al. 2000; Karniely and Pines 2005; Yogev and Pines 2011). It is interesting to note that not less than three features allowing multiple

targeting in eukaryotes are present in human PRDX5. Indeed, three alternative transcription initiation sites were identified in liver *PRDX5* (Nguyen-Nhu et al. 2007) and two in-frame translation initiation codons are present. This allows the synthesis of two translation products: L-PRDX5 and S-PRDX5 (see Fig. 3.2). It is generally accepted that L-PRDX5, exhibiting a strong N-terminal MTS, is exclusively targeted to the mitochondria, while S-PRDX5 is again multiply targeted to the cytosol and the peroxisomes. S-PRDX5 multiple targeting is thought to rely on low efficiency of peroxisomal targeting (Banmeyer et al. 2004; Nguyen-Nhu et al. 2007; Knoops et al. 2011). Indeed, the non-canonical PRDX5 PTS1 sequence (SQL) has a two-out-of-three match with the consensus sequence (S/A/C)-(K/R/H)-(L/M). This would allow a subpopulation of PRDX5 to remain in the cytosol while other PRDX5 molecules are targeted to peroxisomes. Interestingly, in mammals, other examples of dual peroxisomal/cytosolic distribution have been attributed to the presence of a non-consensus PTS1, like for alanine:glyoxylate aminotransferase (AGT) (Knott et al. 2000) or epoxide hydrolase (Arand et al. 1991).

In addition to be localized in mitochondria, cytosol and peroxisomes, human PRDX5 was also reported to be present in the nucleus, although not being found at high levels in all cell types (Kropotov et al. 1999; Kinnula et al. 2002; Kropotov et al. 2004; Lu et al. 2006; Poncin et al. 2008). It was proposed that nuclear PRDX5 corresponds to one isoprotein of S-PRDX5 (Banmeyer et al. 2004; Nguyen-Nhu et al. 2007; Knoops et al. 2011). However, the mechanism of PRDX5 nuclear import is still unclear. Until now, no nuclear localisation signal (NLS) was described for PRDX5. Therefore, PRDX5 nucleocytosolic transport could occur by passive diffusion through the nuclear pore complex, which allows crossing of macromolecules up to ~40 kDa (Stewart 2007). Also, PRDX5 could cross the nuclear membrane actively by interacting with a carrier protein containing an NLS.

Since the importance of nuclear localization varies according to cell-type, the hypothesis of a carrier-dependent translocation seems the most likely.

Taken together, the remarkably wide PRDX5 distribution in human cells results from a complex gene organization and involves the use of various multiple targeting mechanisms. While the multiple targeting to mitochondria, cytosol and peroxisomes is quite well understood (Knoops et al. 2011), the targeting mechanism of S-PRDX5 to the nucleus needs to be clarified.

9.1.2. Variability of PRDX5 multiple targeting in a single organism: time-dependent and tissue-specific regulations

PRDX5 isoproteins derive from a single gene. The presence of multiple PRDX5 genes would have the advantage of a completely independent expression control of the different isoproteins. Nevertheless, in eukaryotes, it becomes clear that sophisticated regulation mechanisms allow a modulation of the ratio between different isoproteins, even though they derive from a single gene (Yogev and Pines 2011). This allows subcellular distribution to be tissue-specific and/or time-dependent in response to cellular signalling or changing extracellular conditions. Evidence suggests that such regulations exist for PRDX5. For example, we noticed that the peroxisomal distribution of PRDX5 was not evenly important in all human cell lines. Indeed, peroxisomal distribution was relatively important in human SAOS-2 cells (see Fig. 6.5), while we did not, or scarcely, detect the protein by immunofluorescence in peroxisomes of human SH-SY5Y and HepG2 cells (see annex 5). Thus, the ratio between the different PRDX5 isoproteins seems to be cell type-specific. Moreover, it was suggested that, albeit PRDX5 peroxisomal localization in HepG2 cells is not detectable by immunofluorescence in normal growing conditions, the exposure of these cells during 16h with 150µM *t*-BHP induces a massive PRDX5 translocation in peroxisomes (Bogard and Knoops (1999), unpublished data). Despite the

fact that these data need to be confirmed, it seems that the ratio between the different PRDX5 isoproteins could also vary during time, depending on stress or metabolic conditions. This time-dependent and cell type-specific variability is also illustrated by variations of PRDX5 nuclear distribution. Indeed, as mentioned before, the importance of PRDX5 nuclear localization varies according to cell type. Also, PRDX5 nuclear translocation was observed under pathophysiological situations in thyrocytes (Gerard et al. 2005; Poncin et al. 2008). All these evidence suggests that PRDX5 multiple targeting is a finely regulated process, although the regulation mechanisms are not understood yet. These mechanisms represent an unexplored and fascinating field of investigation.

The ratio between the different PRDX5 isoproteins could possibly be regulated through modulation of the production of L-PRDX5 and S-PRDX5. This regulation should occur at the transcription level, by favoring one transcription initiation site. A second route to control the ratio between isoproteins could be the regulation of S-PRDX5 multiple localization. For example, the importance of PRDX5 peroxisomal distribution could be regulated through a modulation of its interaction with peroxin 5 (PEX5), the cytosolic receptor for peroxisomal import (Rucktaschel et al. 2011). PEX5 interaction with a peroxisome-targeted protein relies on the presence of the PTS1 signal. The identity of the residues in the C-terminal tripeptide (with respect to the consensus sequence), but also the accessibility of the PTS1, modulate the complex stability between the receptor and the peroxisome-targeted protein (Brocard and Hartig 2006). Therefore, PRDX5 peroxisomal import could be regulated by the modulation of its PTS1 accessibility, which in turn depends on PRDX5 protein folding. It is thus possible that, under specific conditions or in specific cell types, PRDX5 PTS1 presentation is facilitated by factors that alter PRDX5 folding, like chaperones (e.g. Hsp70) or post-translational modifications. Another way to regulate S-PRDX5 multiple targeting is the regulation of nuclear localization, which most

probably relies on the interaction with carrier proteins (see point 9.1.1). Consequently, nucleocytosolic transport regulation could depend on either the carrier protein or S-PRDX5. Mechanism such as protein folding, post-translational modifications or binding to another protein could be involved in such regulations. Finally, it is important to note that, while nuclear import is reversible (Stewart 2007), peroxisomal/mitochondrial export machineries were never described. However, time-dependent relocalization of mitochondrial/peroxisomal isoproteins would be possible, involving for example membrane leakage. Also, transport of PRDX5 from mitochondria to peroxisomes could occur through the recently identified vesicular transport pathway that shuttles selected cargo between mitochondria and peroxisomes (Neuspiel et al, 2008; Braschi et al, 2010). Finally, time-dependent regulation of mitochondrial/peroxisomal PRDX5 isoprotein levels could possibly involve PRDX5 degradation.

9.1.3. Variability of PRDX5 multiple targeting during animal evolution: species-specific subcellular distribution

Analysis of PRDX5 sequences from different species (see figs. 6.1 and 7.2) reveals that PRDX5 subcellular targeting varied during animal evolution. This variation relies on variability in *PRDX5* gene sequence, resulting in the production of variable translation products, possessing or lacking the MTS/PTS1. We found that, besides the "classical" human PRDX5 gene organisation described in point 9.1.1, three major "variants" exist (Fig. 9.2). In the first variant, found in domestic pig and domestic dog *PRDX5*, the first translation initiation codon is absent. This leads to the abolition of mitochondrial PRDX5 (see Chapters 6 and 7). In the second variant, the two in-frame translation start codons are maintained but the PTS1 is absent. In this variant, both L-PRDX5 (mitochondrial) and S-PRDX5 are translated, but S-PRDX5 would not be targeted to peroxisomes. This second variant concerns for example zebrafish and fruitfly *PRDX5*. In the last variant, found

in bay scallop and *Trichoplax adhaerens PRDX5*, the second translation initiation codon is abolished, leading to L-PRDX5 (mitochondrial) translation only. Taken together, among the four variants, "classical" human *PRDX5* gene organization would permit the largest subcellular distribution, while the other variants would lead to a more restrictive subcellular distribution. Interestingly, species presenting the same *PRDX5* variant are not necessarily closely phylogenetically related. For example, lugworm (annelid) and human present the same *PRDX5* variant. Moreover, it is worth to note that this interspecific variability of PRDX5 subcellular distribution results from mutations in five codons only, namely the two translation initiation codons and the three codons encoding the PTS1. This allows, through an on-off mechanism, the abolition/appearance of mitochondrial, peroxisomal or cytosolic PRDX5 targeting. Taken together, PRDX5 subcellular relocalization has occurred at many occasions during animal evolution. Whether this variability permits an adaptation to specific needs, metabolic pathways or life environments, remain matters of speculations. It is interesting to note that none of the PRDX5 isoproteins is totally conserved throughout the animal kingdom, indicating that each PRDX5 isoprotein is dispensable in at least a few animal species. Furthermore, it is not impossible that more than four *PRDX5* variants exist in the animal kingdom. Sequencing of more *PRDX5* orthologs would possibly permit to reveal the existence of other *PRDX5* variants.

PRDX5 forms		Predicted subcellular localization	Examples of species
	L-PRDX5	M	*H. sapiens* (Mammalia) *M. musculus* (Mammalia) *B. taurus* (Mammalia) *A. carolinensis* (Sauria) *A. marina* (Annelida) *N. vectensis* (Cnidaria)
	S-PRDX5	C, P, (N)	
	S-PRDX5	C, P, (N)	*C. lupus familiaris* (Mammalia) *S. scrofa domesticus* (Mammalia)
	L-PRDX5	M	*S. aurata* (Teleostei) *D. rerio* (Teleostei) *B. belcheri tsingtaunese* (Cephalochordata) *D. melanogaster* (Arthropoda) *A. queenslandica* (Porifera)
	S-PRDX5	C, (N)	
	L-PRDX5	M	*A. irradians* (Mollusca) *T. adhaerens* (Placozoa)

Figure 9.2. Interspecific variability of PRDX5 subcellular targeting. According to the amino acid alignments presented in Figs 6.1 and 7.2, four cases exist: (i) expression of both L-PRDX5 (long form of PRDX5) and S-PRDX5 (short form of PRDX5), each containing a peroxisomal targeting signal (PTS1); (ii) expression of S-PRDX5 only, containing a PTS1; (iii) expression of both L-PRDX5 and S-PRDX5, each lacking the PTS1; (iv) expression of L-PRDX5 only. Predicted subcellular localizations are indicated. M: mitochondria; C: cytosol; P: peroxisome; N: nucleus. Taxonomic groups are indicated between brackets. Human, *Homo sapiens*; house mouse, *Mus musculus*; cattle, *Bos taurus*; green anole, *Anolis carolinensis*; lugworm, *Arenicola marina*; starlet sea anemone, *Nematostella vectensis*; domestic dog, *Canis lupus familiaris*; domestic pig, *Sus scrofa domesticus*; gilthead seabream, *Sparus aurata*; zebrafish, *Danio rerio*; Japanese lancelet, *Branchiostoma belcheri tsingtaunese*; fruitfly, *Drosophila melanogaster*; *Amphimedon queenslandica*; bay scallop, *Argopecten irradians*; *Trichoplax adhaerens*.

PRDX5 is not the only protein that exhibits subcellular relocalization during animal evolution. However, so far, most of the examples of protein subcellular relocalizations that are described in the literature occurred quickly following gene duplication (Schmidt et al. 2003; Rosso et al. 2008a; Rosso et al. 2008b; Wang et al. 2009; Szklarczyk and Huynen 2009), which is not the case for PRDX5. One example concerns CDC14B*retro*, which originated from CDC14B cell cycle gene through a duplication event in the great ape ancestor (18-25 mya). In the first million years following gene duplication, subcellular localization of CDC14B*retro* did not evolve. Accordingly, orangutan CDC14B*retro* is associated to microtubules (stabilizing them), like CDC14B. However, it was shown that CDC14B*retro* subcellular localization changed in the African ape ancestor (~7-12 mya) due to missense mutations in the N- and C-terminal parts of the protein. Consequently, CDC14B*retro* from human, chimpanzee and gorilla is located on the cytosolic face of the endoplasmic reticulum instead of being associated with microtubules. The functional significance of this new subcellular localization remains unknown (Rosso et al. 2008b). Examples of animal protein subcellular relocalizations which do not occur quickly after gene duplication, like for PRDX5, are rare. It remains uncertain whether this small number of examples reflects the lack of such relocalizations or the lack of studies investigating this phenomenon. However, it was recently suggested that protein subcellular relocalization occurred also frequently in single-copy genes during yeast evolution, leading to subcellular localization variability between yeast orthologous proteins (Qian and Zhang 2009). In animals, one example of protein subcellular relocalization which did not occur after gene duplication concerns the intermediary metabolic enzyme alanine:glyoxylate aminotransferase (AGT), whose subcellular targeting has been shown to have changed at many occasions during mammalian evolution as a consequence of dietary selection pressures (Holbrook et al. 2000; Birdsey et al. 2004).

Furthermore, as this work focusses on PRDX5 subcellular relocalizations during animal evolution, one could wonder whether this variability is also found in plants and yeasts. Interestingly, the ortholog protein of mammalian PRDX5 in yeast *Saccharomyces cerevisiae* (Ahp1p) is cytosolic while its ortholog in yeast *Candida boidinii* (Pmp20) is exclusively peroxisomal (Horiguchi et al, 2001). Thus, PRDX5 subcellular relocalizations appear to occur also in yeasts. On the opposite, to our knowledge, such species-specific variability was never studied in plant PRDXs. PrxIIE, the mammalian PRDX5 ortholog in *Arabidopsis thaliana*, is chloroplastic (Dietz et al, 2003). It would not be surprising to find some subcellular relocalizations of PRDX5 othologs during plant evolution. Indeed, amino acid composition of mitochondrial and chloroplast targeting sequences are similar (Byun-McKay and Geeta, 2007). Therefore, little variability in the PrxIIE N-terminal sequence could be sufficient to provoke PRDX5 relocalization from chloroplast to mitochondria.

In addition to the on/off mechanisms responsible for PRDX5 subcellular relocalization described above, PRDX5 multiple targeting could also vary more finely between species through some mutations that alter the isoprotein ratios. Indeed, L-PRDX5/S-PRDX5 ratio could vary from one species to another even though they exhibit the same *PRDX5* gene organization (same *PRDX5* variant). For example, the positions of the transcription initiation start sites as well as the sequence context surrounding the AUG (Kozak consensus) could have an impact on the translation ratio of L-PRDX5 and S-PRDX5. It is interesting to note that in house mouse *PRDX5*, the sequence around the first translation initiation codon appears to be a weak Kozak sequence compared to the sequence surrounding the second translation initiation codon (see annex 6). This could favor the translation of S-PRDX5 instead of L-PRDX5. On the opposite, in Norway rat PRDX5, the sequence surrounding the first and the second ATG appears to match well the Kozak consensus. Therefore, PRDX5 isoprotein

ratio could differ in rat and mouse. Furthermore, the importance of peroxisomal targeting could vary according to the identity of the residues upstream of the PTS1. Indeed, it was reported that, in some cases, the residues adjacent to the PTS1 are required for peroxisomal import. Accordingly, the PTS1 has been redefined as a C-terminal dodecamer (Brocard and Hartig 2006). Therefore, although little is currently known about the residues implicated in PRDX5/PEX5 interaction, the identity of the residues upstream the PTS1 could possibly determine the importance of PRDX5 peroxisomal targeting in a species. Moreover, it was shown for proteins containing non-consensus PTS1s that the efficiency by which PEX5 mediates peroxisomal import is variable according to species. For example, it was shown that guinea pig PEX5 was much less efficient than human PEX5 in mediating catalase and AGT peroxisomal import (Knott et al. 2000). By this way, the importance of PRDX5 peroxisomal distribution could also vary between species.

9.2. Interspecific variability of PRDX5 mitochondrial targeting

A central observation in this thesis is that mitochondrial PRDX5 is absent in domestic pig and domestic dog (see Figs 6.3, 6.4 and 7.3). From this statement arose four main questions. To answer these questions, several experimental schemes have been formulated. The major conclusions as well as some further considerations are drawn in the following paragraphs.

9.2.1. When did the abolition of mitochondrial PRDX5 occur during mammalian evolution?

Mitochondrial PRDX5 is maintained in bovine (Leyens et al. 2004) but not in pig (Van der Eecken et al. 2011). From this observation, we concluded that PRDX5 MTS was lost during Cetartiodactyla evolution. It was evaluated that Cetartiodactyla diverged from other placental mammals approximately 84.6

mya (Murphy and Eizirik 2009), but neither phylogenetic relationships nor divergence times between the Cetartiodactyla suborders are resolved yet. Therefore, we cannot precisely determine when PRDX5 MTS abolition occurred. The abolition should nevertheless have occurred within the last 84.6 million years. In a second part of this work, we showed that PRDX5 MTS was lost during Caniformia evolution. Indeed, we highlighted that, while a functional MTS was present in giant panda (ursid) and northern elephant seal (phocid) PRDX5 (see Fig. 7.5), PRDX5 MTS was abolished in some species belonging to the three main canid clades as well as in the most basal canid (gray fox) (see Fig. 7.4). Therefore, we postulated that PRDX5 MTS was lost during Caniformia evolution after divergence of the Canidae from the other Caniformia members. Since canids diverged from other Caniformia ~50 mya and extant canids diverged from a common ancestor within the 10 last million years (Ostrander and Wayne 2005), the loss of PRDX5 in canids would have occurred between 50 and 10 mya. Taken together, abolition of mitochondrial PRDX5 in canids and pig results from two distinct events during mammalian evolution and occurred within the last 84.6 million years.

PRDX5 sequences are available in a limited number of mammalian species so far. The release of more mammalian *PRDX5* sequences would probably permit to identify additional mammals lacking mitochondrial PRDX5. This would allow establishing whether the absence of mitochondrial PRDX5 in mammals is an exception or not.

9.2.2. Which molecular mechanism underlies the abolition of PRDX5 mitochondrial targeting?

In both pig and dog, L-PRDX5 is abolished while S-PRDX5 is present (see Figs 6.3, 6.4 and 7.3). We found that L-PRDX5 translation initiation codon is absent in these species. This impedes the synthesis of mitochondrial PRDX5 (see annex 7 and Fig. 7.4). The molecular mechanism responsible for the

abolition of mitochondrial PRDX5 was studied more deeply in the context of Caniformia evolution. We found that, in the most basal canids (gray fox, red fox and raccoon dog), two factors impede L-PRDX5 synthesis: the absence of the more 5′ ATG codon and the presence of a STOP codon (Fig. 9.3). In the other canids (maned wolf, arctic wolf and domestic dog), the more 5′ ATG codon is absent but the STOP codon is not present. Therefore, we hypothesized that the PRDX5 5′ region in canids corresponds to a sequence that was able to encode a presequence ancestrally. This ancestral MTS would have been lost by the mutation of the ATG translation initiation codon to a GTG codon as well as by the mutation of a TCG codon to a TAG (STOP) codon. From our results, we are not able to conclude whether the STOP codon appeared before or after the ATG/GTG mutation. The STOP codon would further have evolved to a CAG codon in South-American canids and wolf-like canids. Also, a single nucleotide should have been lost in the ancestral PRDX5 presequence from South-American canids and wolf-like canids.

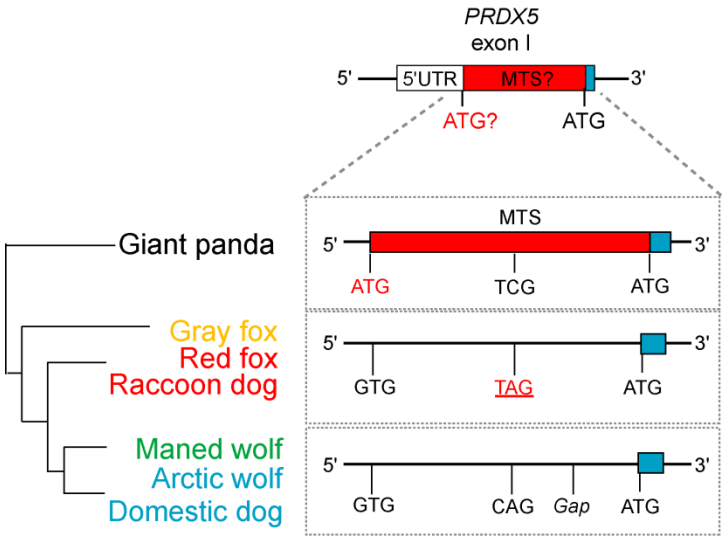

Fig. 9.3. Schematic view of the evolution of *PRDX5* 5′ region in canids. Species names are indicated in red for the fox-like canids, in green for the South-American canids and in blue for the wolf-like canids.

Regarding our results, we conclude that the abolition of the ATG codon in dog and pig *PRDX5* leads to the loss of L-PRDX5 translation. This was verified by the fact that only S-PRDX5 (cytosolic, peroxisomal and nuclear) was detected in these two species (see Figs 6.3, 6.4 and 7.3). However, in a small number of mammalian mRNAs, translation can initiate from a non-AUG codon in addition to initiate at a downstream in-frame AUG codon. Most of the known examples encode regulatory proteins, like transcription factors or growth factors (Touriol et al. 2003). Therefore, although unlikely, we cannot exclude that alternative translation at a non-AUG codon does not occur in the gray fox, red fox, raccoon dog and/or maned wolf PRDX5. For the maned wolf, this alternative translation initiation site could potentially lead to the translation of mitochondrial PRDX5. By contrast, in gray fox, red fox and raccoon dog *PRDX5*, the presence of the STOP codon in the ancestral presequence involves that alternative translation initiation at a non-AUG codon would occur downstream of this STOP codon. This would lead to the synthesis of a PRDX5 form with an N-terminal extension that does not possess MTS characteristics, and that consequently would not be targeted to mitochondria.

9.2.3. Is the loss of mitochondrial PRDX5 compensated by an increased expression of other mitochondrial peroxidases?

In domestic pig and domestic dog, the lack of mitochondrial PRDX5 could have been counterbalanced by higher expression of other mitochondrial peroxidases, i.e. PRDX3 (Watabe et al. 1994; Araki et al. 1999; Oberley et al. 2001; Mowbray et al. 2008), GPX1 (Panfili et al. 1991; Utsunomiya et al. 1991; Asayama et al. 1994; Esworthy et al. 1997; Legault et al. 2000) and GPX4 (Arai et al. 1996; Ursini et al. 1999; Schneider et al. 2009). The expression of PRDX3, GPX1 and GPX4 was studied in pig but not in dog. Our results suggest the existence of compensatory mechanisms counterbalancing the

absence of mitochondrial PRDX5 in pig liver. Indeed, we showed that PRDX3 and GPX4 are significantly more abundant in pig liver mitochondria compared to rat liver mitochondria (see Figs 6.6 and 6.7). On the other hand, GPX1 expression was similar in pig and rat liver mitochondria. Since the experiment was carried out on one rat liver and one pig liver, it would be useful to confirm these results with mitochondrial extracts from more organisms as well from other species, like dog and other mammals. Also, it would be interesting to compare PRDX3, GPX1 and GPX4 expression in mitochondrial extracts from more tissues to support this hypothesis at the level of the whole organism. Actually, it was shown that GPX activity displays marked tissue-specific variations in pig, with a particularly high GPX activity in pig liver. In rat tissues, the tissue-dependent variability of GPX activity was shown to be less important than in pig (Daun and Akesson 2004). Furthermore, we showed that, despite higher PRDX3 and GPX4 contents in pig mitochondria, the lack of mitochondrial PRDX5 in pig liver would not be without consequences. Indeed, *t*-BHP reduction rates by liver mitochondrial extracts are dramatically lower in pig compared to rat (see Fig. 6.8), suggesting that compensatory mechanisms are not sufficient to maintain high alkyl hydroperoxide reduction rates. This phenomenon illustrates that the multiple mitochondrial peroxidases are not necessarily redundant. Each peroxidase has its own substrate specificity and the increased expression of one peroxidase to compensate the absence of another would not necessarily permit the efficient reduction of every substrate. Interestingly, it was suggested recently that PRDX5 possesses a more specific function in mitochondria through its high reactivity towards alkyl hydroperoxides and peroxynitrite (Trujillo et al. 2007; Cox et al. 2010). On the other hand, PRDX3 is known to be a very efficient H_2O_2 scavenger while GPX4 would reduce more efficiently phospholipid hydroperoxides (Cox et al. 2010). In this context, it is interesting to note that PRDX5 is the only mitochondrial peroxidase for which a peroxynitrite reductase activity

was demonstrated so far. Since mitochondrial PRDX5 is absent in pig, it would be interesting to measure peroxidase activity of pig mitochondrial extracts in presence of peroxynitrite. Finally, it is important to note that, *in vivo*, mitochondrial peroxidases rely on recycling by physiological reductants. The availability of these reductants is likely to modulate the contribution of PRDX3, PRDX5, GPX1 and GPX4 to mitochondrial peroxide removal.

9.2.4. Would the restoration of mitochondrial PRDX5 confer an advantage in dog and pig?

Given the abolition of PRDX5 mitochondrial targeting in dog and pig, we hypothesized that mitochondrial PRDX5 is not essential in these species. However, reproductive occurrences in these two domesticated species were finely regulated by human intervention, biasing the natural selection process. Therefore, we could not conclude from these results that the abolition of mitochondrial PRDX5 can occur without hindering natural evolutionary success. To clarify this point, we sequenced the PRDX5 5′ region in other canids and found that mitochondrial PRDX5 is absent also in some wild species. Some of them, like the raccoon dog and the red fox, encountered a huge evolutionary success. This permits to confirm that mitochondrial PRDX5 abolition does not impair the ability of some mammals to meet a huge evolutionary success. Also, it appears that PRDX5 abolition can occur in some species without any major functional consequence that would be visible at the level of the whole organism.

The abolition of mitochondrial PRDX5 in pig and canids is nevertheless surprising. Indeed, due to the presence of the electron transport chain, mitochondria are particularly exposed to oxidative attacks caused by ROS (Halliwell and Gutteridge 2007). Furthermore, the cytoprotective function of mitochondrial PRDX5 was described in several studies. For example, overexpression of mitochondrial PRDX5 was shown to confer resistance to

cell lines exposed to peroxide or drug-induced oxidative damage (Banmeyer et al. 2004; Peng et al. 2004a; Peng et al. 2004b; Banmeyer et al. 2005). Therefore, although it appears that mitochondrial PRDX5 is dispensable in some mammalian species, one could wonder whether the conservation of mitochondrial PRDX5 would nevertheless have constituted an advantage to these species. To answer this question, we studied the functional consequences of the restoration of L-PRDX5 in dog MDCK cells. We showed that the expression of human L-PRDX5 in MDCK cells does not afford any antioxidant protection against peroxide-induced acute oxidative stress, but rather provokes an increased cell death. However, we did not find the mechanism by which mitochondrial PRDX5 induces such deleterious effects in MDCK cells. On the other hand, it was previously shown that the expression of human L-PRDX5 in Chinese hamster ovary (CHO) cells, possessing mitochondrial PRDX5 endogenously, conferred resistance to peroxide-induced acute oxidative stress. Therefore, we suggest that, albeit the cytoprotective function of mitochondrial PRDX5 is clearly established by several studies in human and rodents, the conservation of mitochondrial PRDX5 would not necessarily constitute an advantage in all mammalian species. To support this hypothesis, we studied the functional consequences of the expression of mitochondria-targeted dog PRDX5 in MDCK cells. As a control, we also overexpressed dog S-PRDX5 in these cells. Unexpectedly, peroxide-induced cell death was increased in both MDCK cells expressing mitochondria-targeted dog PRDX5 and in MDCK cells overexpressing dog S-PRDX5 (see Fig 8.2). These results, largely discussed in Chapter 8, do not permit to support our hypothesis and rises other questions which go beyond the general context of this thesis. Therefore, to support our hypothesis according to which mitochondrial PRDX5 conservation would not necessarily constitute an advantage in all mammalian species, it would be interesting to confirm our results by using another dog cell line, like Cf2Th (canine thymus) cells, or a pig cell line (LLC-PK10 cells). Finally, we are

tempted to speculate that the deleterious effects provoked by mitochondrial PRDX5 in MDCK cells reflect the reason of the abolition of mitochondrial PRDX5 in canids. In this case, unravelling the mechanism by which mitochondrial PRDX5 causes deleterious effects in MDCK cells would permit to highlight the functional reasons of mitochondrial PRDX5 abolition in dog. On the other hand, the loss of mitochondrial PRDX5 in canids could also have occurred without link with these deleterious effects. Another possible scenario would be the abolition of PRDX5 mitochondrial targeting as an adaptation to a need of increased levels of cytosolic/peroxisomal/nuclear PRDX5. Also, the presence of mitochondrial PRDX5 could be superfluous in some species due to a particular low mitochondrial ROS/RNS production, and would therefore not be selected during their evolution. Indeed, it has been shown that mitochondrial ROS generation occurs at species-specific rates, depending on the ability of the electron transport chain to avoid electron leaks (see Pamplona, 2011 for review). For example, the pigeon has lower rates of mitochondrial ROS generation than rats, even though their metabolic rates and body sizes are of a similar magnitude (Lambert et al, 2010). Therefore, comparing mitochondrial ROS generation rates in species having maintained *versus* species lacking mitochondrial PRDX5 would be of particular interest. Taken together, by tempting to answer our fourth main question, our work ends on a major and unresolved fifth question.

10. Perspectives

Our general discussion highlights some questions that are still to be answered. We propose some perspectives to complete this study and to test our hypotheses.

First, it would be of great interest to assess the sub-mitochondrial localization of PRDX5 in mammals having maintained mitochondrial PRDX5. Indeed, although it is generally accepted that human PRDX5 is located in the mitochondrial matrix, the precise localization of PRDX5 inside the mitochondria was never determined experimentally. Moreover, it is interesting to note that, in MDCK clones overexpressing S-PRDX5, the merged signals obtained with PRDX5 immunofluorescence detection and Mitotracker Red staining resulted in a yellow pattern (see Figs 7.7 and 8.1). Since the cells were observed with a confocal microscope, these results suggest that S-PRDX5 could be associated or localized to the periphery of mitochondria in MDCK cells. Further investigations are needed to clarify this point.

To complete this study, it would be interesting to sequence the PRDX5 5′ region of more Cetartiodactyla species, like peccaries, camels and llamas. This would give more accuracy about the timing and the molecular mechanism of L-PRDX5 abolition during Cetartiodactyla evolution. Also, PRDX5 5′ sequence could be useful in studies assessing Cetartiodactyla phylogeny, which remains still unresolved. Indeed, PRDX5 (ancestral) MTS is a rapidly evolving nuclear sequence and represents therefore a potential phylogenetically informative sequence that could be used, together with other rapidly evolving sequences, to resolve phylogenetic relationships between closely related species. Furthermore, it would be interesting to sequence the 5′ region from more mammals to establish if the absence of mitochondrial PRDX5 is an exception or not. These data could potentially

provide some indications about the functional reasons of the abolition of mitochondrial PRDX5 in these mammals.

In this work, compensatory mechanisms counterbalancing the absence of mitochondrial PRDX5 were studied only sparsely by comparing PRDX3, GPX1 and GXP4 expression as well as H_2O_2 and *t*-BHP peroxide reduction rates in rat and pig liver mitochondrial extracts. As mentioned in the general discussion, it would be useful to perform a large-scale study involving more organisms, more species and more tissues. Tissues like thyroid gland, lung and kidney, in which PRDX5 is especially highly expressed (Knoops et al. 1999), would be of particular interest. Also, given the high reactivity of PRDX5 towards peroxynitrite, it would be interesting to compare peroxynitrite reduction rates in mitochondrial extracts from species possessing L-PRDX5 *versus* species lacking L-PRDX5.

Furthermore, in this thesis, we tested the functional consequences of the restoration of mitochondrial PRDX5 in MDCK cells. We showed that mitochondrial PRDX5 provokes deleterious effects during acute oxidative stress, suggesting that the conservation of mitochondrial PRDX5 should not have necessarily conferred an advantage in dog. These results need to be substantiated using another dog cellular model, like Cf2Th (canine thymus) cells. Also, in our experiments, transfection of MDCK cells led to considerable PRDX5 expression (see Figs. 7.6. and 8.1.). Therefore, in order to obtain more physiological PRDX5 expression levels in MDCK mitochondria, it would be useful to use an expression vector containing PRDX5 endogenous or inducible promoter. Moreover, the use of MDCK cells overexpressing mitochondrial protein which is not relevant for oxidative stress would constitute an additional control for the cytotoxicity experiments. Furthermore, it would be interesting to assess whether mitochondrial PRDX5 would provoke also peroxide-dependent deleterious effects in pig LLC-PK10 cells. If mitochondrial PRDX5 provokes deleterious

effects in MDCK, Cf2Th and LLC-PK10 cells, it is likely that the deleterious effects provoked by mitochondrial PRDX5 are related to the reason of L-PRDX5 abolition. In this case, it would be crucial to study the mechanism by which L-PRDX5 provoked peroxide-dependent deleterious effects in dog and pig cells, for example by comparing the interactions of PRDX5 with other mitochondrial proteins in basal *versus* oxidative conditions. Also, it would be interesting to assess if PRDX5 undergoes subcellular relocalizations in MDCK clones following acute oxidative stress. Indeed, such PRDX5 relocalizations were observed earlier in preliminary experiments on HepG2 cells, in which *t*-BHP exposure induced massive PRDX5 translocation in peroxisomes (Bogard and Knoops (1999), unpublished data).

In our GFP fusion (see Figs. 6.2. and 7.5.) and PRDX5 overexpression (see Figs. 7.6. and 8.1.) experiments, mitochondrial localization was verified using immunofluorescence detection. To corroborate our results, it would be useful to confirm mitochondrial localization using subcellular fractionation and *in vitro* mitochondrial import assays.

It would be of great interest to study the selection pressures in *PRDX5* (ancestral) MTS region. Indeed, if the abolition of L-PRDX5 in pig and dog is linked to peroxide-dependent protein toxicity in the mitochondrial compartment, signatures of Darwinian selection should be present in PRDX5 5′ region. We are currently collaborating with the Institut de Génétique et Dévoloppement de Rennes to examine the possibility to evaluate the presence of such selection pressures. Methods evaluating selection pressures are usually based on the calculation of the nonsynonymous/synonymous substitution rate ratio ($\omega = d_N/d_S$). In such models, values of the ω ratio for amino-acid sites are evaluated. If a site is under positive (diversifying) selection pressure, nonsynonymous changes will be fixed at higher rate than synonymous substitutions. Therefore, a $\omega >$

1 ratio ($d_N > d_S$) is an evidence of adaptive molecular evolution. If nonsynonimous substitutions are deleterious, negative selection (i.e. pressure for conservation) will reduce their fixation rate, and $\omega < 1$. Neutral nonsynonymous substitutions result in $\omega = 1$ (Anisimova et al. 2001). However, in the case of the evolution of PRDX5 MTS, it is difficult to apply this classical method. Indeed, PRDX5 (ancestral) MTS switches from "coding" to "non-coding" during evolution. Therefore, evaluating d_N/d_S ratios on this sequence seems to be inadequate. To our knowledge, no specific tools exist to test whether the accumulation of mutations leading to the loss of coding function is driven by positive selection pressures.

This work focuses more specifically on the interspecific variability of PRDX5 mitochondrial targeting. Intraspecific variability of PRDX5 mitochondrial targeting was never studied but would merit a particular attention. Indeed, in human *PRDX5*, six missense single nucleotide polymorphisms (SNPs) were identified within the region encoding the MTS (Genbank IDs: rs144769220, rs148589018, rs143054032, rs7938623, rs140015234, rs11551856 and rs143723178). Based on TargetP predictions, none of them are predicted to alter L-PRDX5 mitochondrial targeting, but two of them are predicted to change the position of the MTS cleavage site (rs140015234 and rs11551856). This could potentially have an impact on PRDX5 function in mitochondria. Furthermore, as mentioned in our general discussion, variability of PRDX5 mitochondrial targeting represents only a fraction of the variability that PRDX5 exhibits at the level of subcellular distribution. Time-dependent as well as tissue-specific subcellular variations represent a very interesting and unexplored field of investigations.

Finally, nuclear PRDX5 remains an enigmatic isoprotein which merits particular attention. Until now, no NLS has been described for human PRDX5. Moreover, when using PSORTII and NLStradamus prediction softwares (Nakai and Horton, 1999; Nguyen et al., 2009), no supplementary

NLS was detected in PRDX5 sequences from all the species studied in this work (see Figs 6.1 and 7.2. for species names and Genbank accession numbers). Therefore, PRDX5 nuclear import mechanism as well as its regulation should be investigated. Also, the function of nuclear PRDX5 was only sparsely studied until now. It was suggested that nuclear PRDX5 could protect genomic DNA against oxidation (Banmeyer et al. 2004; Kropotov et al. 2006b) and may possibly control the transcription of noncoding DNA (Kropotov et al. 1999; Kropotov et al. 2006b). Interestingly, the importance of nuclear PRDX5 is variable within HEPG2 cells, with a particular strong nuclear localization in cells undergoing mitosis (Nguyen, personal communication). Therefore, it would be interesting to assess the role of nuclear PRDX5 in cell cycle regulation.

11. Conclusions

PRDX5 differs from the five other PRDX members by its wide subcellular localization. Moreover, although it was never clearly emphasized in the literature, it seems that PRDX5 subcellular distribution exhibits a remarkable variability. This variability is found at different levels, since PRDX5 subcellular distribution appears to be time-dependent, cell type-specific and species-specific.

This work focuses on the interspecific variability of PRDX5 mitochondrial targeting in mammals. We show that mitochondrial targeting has been lost in pig and canids as a consequence of two distinct events having occurred within the last 84.6 million years. Thus, it appears that mitochondrial PRDX5 abolition can occur in some mammalian species without any apparent and major functional consequence and without impairing survival or evolutionary success. Moreover, since the restoration of mitochondrial PRDX5 in dog MDCK cells provoked deleterious effects during acute oxidative conditions, we propose that, although PRDX5 cytoprotective function is clearly established in human and rodents, the conservation of mitochondrial PRDX5 would not confer necessarily an evolutionary advantage in all mammalian species. On the other hand, our results suggest that, despite high PRDX3 and GPX4 expression levels, the loss of mitochondrial PRDX5 correlates with particularly low alkyl hydroperoxide reduction rates in pig liver mitochondrial extracts. Therefore, even if major functional consequences are not observed at the level of the whole organism, we cannot exclude that the abolition of mitochondrial PRDX5 leads to a certain weakness at the cellular level in specific oxidative stress conditions. Finally, one major question remains unresolved at the end of this work, as our results do not permit to establish the functional reason of the abolition of mitochondrial PRDX5 in pig and canids. Whether this abolition permits an adaptation to specific needs or constraints remain

matters for speculation. Further investigations are needed to solve this enigma.

V. Bibliography

Abe Y, Shodai T, Muto T, Mihara K, Torii H, Nishikawa S, Endo T, Kohda D. 2000. Structural basis of presequence recognition by the mitochondrial protein import receptor Tom20. Cell 100: 551-560.

Agnarsson I, May-Collado LJ. 2008. The phylogeny of Cetartiodactyla: the importance of dense taxon sampling, missing data, and the remarkable promise of cytochrome b to provide reliable species-level phylogenies. Mol. Phylogenet. Evol. 48: 964-985.

Angermuller S, Islinger M, Volkl A. 2009. Peroxisomes and reactive oxygen species, a lasting challenge. Histochem. Cell Biol. 131: 459-463.

Anisimova M, Bielawski JP, Yang Z. 2001. Accuracy and power of the likelihood ratio test in detecting adaptive molecular evolution. Mol. Biol. Evol. 18: 1585-1592.

Arai M, Imai H, Sumi D, Imanaka T, Takano T, Chiba N, Nakagawa Y. 1996. Import into mitochondria of phospholipid hydroperoxide glutathione peroxidase requires a leader sequence. Biochem. Biophys. Res. Commun. 227: 433-439.

Araki M, Nanri H, Ejima K, Murasato Y, Fujiwara T, Nakashima Y, Ikeda M. 1999. Antioxidant function of the mitochondrial protein SP-22 in the cardiovascular system. J. Biol. Chem. 274: 2271-2278.

Arand M, Knehr M, Thomas H, Zeller HD, Oesch F. 1991. An impaired peroxisomal targeting sequence leading to an unusual bicompartmental distribution of cytosolic epoxide hydrolase. FEBS Lett. 294: 19-22.

Asayama K, Yokota S, Dobashi K, Hayashibe H, Kawaoi A, Nakazawa S. 1994. Purification and immunoelectron microscopic localization of cellular glutathione peroxidase in rat hepatocytes: quantitative analysis by postembedding method. Histochemistry 102: 213-219.

Avila PC, Kropotov AV, Krutilina R, Krasnodembskay A, Tomilin NV, Serikov VB. 2008. Peroxiredoxin V contributes to antioxidant defense of lung epithelial cells. Lung 186: 103-114.

Banmeyer I, Marchand C, Verhaeghe C, Vucic B, Rees JF, Knoops B. 2004. Overexpression of human peroxiredoxin 5 in subcellular compartments of Chinese hamster ovary cells: effects on cytotoxicity and DNA damage caused by peroxides. Free Radic. Biol. Med. 36: 65-77.

Banmeyer I, Marchand C, Clippe A, Knoops B. 2005. Human mitochondrial peroxiredoxin 5 protects from mitochondrial DNA damages induced by hydrogen peroxide. FEBS Lett. 579: 2327-2333.

Basu A, Banerjee H, Rojas H, Martinez SR, Roy S, Jia Z, Lilly MB, De LM, Casiano CA. 2011. Differential expression of peroxiredoxins in prostate cancer: consistent upregulation of PRDX3 and PRDX4. Prostate 71: 755-765.

Becker T, Bottinger L, Pfanner N. 2012. Mitochondrial protein import: from transport pathways to an integrated network. Trends Biochem. Sci. 37: 85-91.

Birdsey GM, Lewin J, Cunningham AA, Bruford MW, Danpure CJ. 2004. Differential enzyme targeting as an evolutionary adaptation to herbivory in carnivora. Mol. Biol. Evol. 21: 632-646.

Biswas TK, Getz GS. 2002. Import of yeast mitochondrial transcription factor (Mtf1p) via a nonconventional pathway. J. Biol. Chem. 277: 45704-45714.

Biswas TK, Getz GS. 2004. Requirement of different mitochondrial targeting sequences of the yeast mitochondrial transcription factor Mtf1p when synthesized in alternative translation systems. Biochem. J. 383: 383-391.

Blom N, Gammeltoft S, Brunak S. 1999. Sequence and structure-based prediction of eukaryotic protein phosphorylation sites. J. Mol. Biol. 294: 1351-1362.

Bogard, C., Knoops, B., 1999. Localisation subcellulaire de la protéine AOEB166 chez la lignée HepG2. In: Mémoire de licence en sciences biologiques, Université catholique de Louvain.

Boisserie JR, Fisher RE, Lihoreau F, Weston EM. 2011. Evolving between land and water: key questions on the emergence and history of the Hippopotamidae (Hippopotamoidea, Cetancodonta, Cetartiodactyla). Biol. Rev. Camb. Philos. Soc. 86: 601-625.

Boyko AR, Boyko RH, Boyko CM et al. 2009. Complex population structure in African village dogs and its implications for inferring dog domestication history. Proceedings of the National Academy of Sciences of the United States of America 106: 13903-13908.

Braschi E, Goyon V, Zunino R, Mohanty A, Xu L, McBride HM. 2010. Vps35 mediates vesicle transport between the mitochondria and peroxisomes. Curr. Biol. 20: 1310-1315.

Brigelius-Flohe R. 1999. Tissue-specific functions of individual glutathione peroxidases. Free Radic. Biol. Med. 27: 951-965.

Brocard C, Hartig A. 2006. Peroxisome targeting signal 1: is it really a simple tripeptide? Biochim. Biophys. Acta 1763: 1565-1573.

Byun-McKay SA, Geeta R. 2007. Protein subcellular relocalization: a new perspective on the origin of novel genes. Trends Ecol. Evol. 22: 338-344.

Cha MK, Yun CH, Kim IH. 2000. Interaction of human thiol-specific antioxidant protein 1 with erythrocyte plasma membrane. Biochemistry 39: 6944-6950.

Chacinska A, Koehler CM, Milenkovic D, Lithgow T, Pfanner N. 2009. Importing mitochondrial proteins: machineries and mechanisms. Cell 138: 628-644.

Chae HZ, Kim HJ, Kang SW, Rhee SG. 1999. Characterization of three isoforms of mammalian peroxiredoxin that reduce peroxides in the presence of thioredoxin. Diabetes Res. Clin. Pract. 45: 101-112.

Chang TS, Jeong W, Choi SY, Yu S, Kang SW, Rhee SG. 2002. Regulation of peroxiredoxin I activity by Cdc2-mediated phosphorylation. J. Biol. Chem. 277: 25370-25376.

Chang TS, Cho CS, Park S, Yu S, Kang SW, Rhee SG. 2004. Peroxiredoxin III, a mitochondrion-specific peroxidase, regulates apoptotic signaling by mitochondria. J. Biol. Chem. 279: 41975-41984.

Chen L, Na R, Gu M et al. 2008. Reduction of mitochondrial H2O2 by overexpressing peroxiredoxin 3 improves glucose tolerance in mice. Aging Cell 7: 866-878.

Chen L, Yoo SE, Na R, Liu Y, Ran Q. 2012. Cognitive impairment and increased Abeta levels induced by paraquat exposure are attenuated by enhanced removal of mitochondrial H(2)O(2). Neurobiol. Aging 33: 432.e15-432.e26.

Chen W, Ji J, Ru B. 2005. Proteomic analysis of corticobasal degeneration: a case study of corticobasal degeneration at the proteome level. J. Neuropsychiatry Clin. Neurosci. 17: 364-371.

Cheng WH, Ho YS, Valentine BA, Ross DA, Combs GF, Jr., Lei XG. 1998. Cellular glutathione peroxidase is the mediator of body selenium to protect against paraquat lethality in transgenic mice. J. Nutr. 128: 1070-1076.

Chevallet M, Wagner E, Luche S, van Dorsselaer A, Leize-Wagner E, Rabilloud T. 2003. Regeneration of peroxiredoxins during recovery after oxidative stress - Only some overoxidized peroxiredoxins can be reduced during recovery after oxidative stress. J. Biol. Chem. 278: 37146-37153.

Cho CS, Lee S, Lee GT, Woo HA, Choi EJ, Rhee SG. 2010. Irreversible inactivation of glutathione peroxidase 1 and reversible inactivation of peroxiredoxin II by H2O2 in red blood cells. Antioxid. Redox. Signal. 12: 1235-1246.

Choi JH, Kim TN, Kim SY, Baek SH, Kim JH, Lee SR, Kim JR. 2002. Overexpression of mitochondrial thioredoxin reductase and peroxiredoxin III in hepatocellular carcinomas. Anticancer Res. 22: 3331-3335.

Claros MG, Vincens P. 1996. Computational method to predict mitochondrially imported proteins and their targeting sequences. Eur. J. Biochem. 241: 779-786.

Conrad M, Moreno SG, Sinowatz F et al. 2005. The nuclear form of phospholipid hydroperoxide glutathione peroxidase is a protein thiol peroxidase contributing to sperm chromatin stability. Mol. Cell Biol. 25: 7637-7644.

Cox AG, Peskin AV, Paton LN, Winterbourn CC, Hampton MB. 2009. Redox Potential and Peroxide Reactivity of Human Peroxiredoxin 3. Biochemistry 48: 6495-6501.

Cox AG, Pearson AG, Pullar JM, Jonsson TJ, Lowther WT, Winterbourn CC, Hampton MB. 2009. Mitochondrial peroxiredoxin 3 is more resilient to hyperoxidation than cytoplasmic peroxiredoxins. Biochem. J. 421: 51-58.

Cox AG, Winterbourn CC, Hampton MB. 2010. Mitochondrial peroxiredoxin involvement in antioxidant defence and redox signalling. Biochem. J. 425: 313-325.

Daun C, Akesson B. 2004. Glutathione peroxidase activity, and content of total and soluble selenium in five bovine and porcine organs used in meat production. Meat. Sci. 66: 801-807.

Day AM, Brown JD, Taylor SR, Rand JD, Morgan BA, Veal EA. 2012. Inactivation of a Peroxiredoxin by Hydrogen Peroxide Is Critical for Thioredoxin-Mediated Repair of Oxidized Proteins and Cell Survival. Mol. Cell. 45:398-408.

de Haan JB, Bladier C, Griffiths P et al. 1998. Mice with a homozygous null mutation for the most abundant glutathione peroxidase, Gpx1, show increased susceptibility to the oxidative stress-inducing agents paraquat and hydrogen peroxide. J. Biol. Chem. 273: 22528-22536.

De Simoni S, Goemaere J, Knoops B. 2008. Silencing of peroxiredoxin 3 and peroxiredoxin 5 reveals the role of mitochondrial peroxiredoxins in the protection of human neuroblastoma SH-SY5Y cells toward MPP+. Neurosci. Lett. 433: 219-224.

Declercq JP, Evrard C, Clippe A, Vander Stricht D, Bernard A, Knoops B. 2001. Crystal structure of human peroxiredoxin 5, a novel type of mammalian peroxiredoxin at 1.5 A resolution. J. Mol. Biol. 311: 751-759.

Declercq PE, Haagsman HP, Van Veldhoven P, Debeer LJ, Van Golde LM, Mannaerts GP. 1984. Rat liver dihydroxyacetone-phosphate acyltransferases and their contribution to glycerolipid synthesis. J. Biol. Chem. 259: 9064-9075.

Dubuisson M, Vander Stricht D, Clippe A, Etienne F, Nauser T, Kissner R, Koppenol WH, Rees JF, Knoops B. 2004. Human peroxiredoxin 5 is a peroxynitrite reductase. FEBS Lett. 571: 161-165.

Eizirik, E., Murphy, W.J., 2009. Carnivores (Carnivora). In: Hedges, S.B., Kumar, M. (Eds.), The Timetree of Life, Oxford University Press, pp. 504-507.

Eizirik E, Murphy WJ, Koepfli KP, Johnson WE, Dragoo JW, Wayne RK, O'Brien SJ. 2010. Pattern and timing of diversification of the mammalian order Carnivora inferred from multiple nuclear gene sequences. Mol. Phylogenet. Evol. 56: 49-63.

Emanuelsson O, Nielsen H, Brunak S, von Heijne G. 2000. Predicting subcellular localization of proteins based on their N-terminal amino acid sequence. J. Mol. Biol. 300: 1005-1016.

Endo T, Yamano K, Kawano S. 2011. Structural insight into the mitochondrial protein import system. Biochim. Biophys. Acta 1808: 955-970.

Esposito LA, Kokoszka JE, Waymire KG, Cottrell B, MacGregor GR, Wallace DC. 2000. Mitochondrial oxidative stress in mice lacking the glutathione peroxidase-1 gene. Free Radic. Biol. Med. 28: 754-766.

Esworthy RS, Ho YS, Chu FF. 1997. The Gpx1 gene encodes mitochondrial glutathione peroxidase in the mouse liver. Arch. Biochem. Biophys. 340: 59-63.

Fan AC, Kozlov G, Hoegl A, Marcellus RC, Wong MJ, Gehring K, Young JC. 2011. Interaction between the human mitochondrial import receptors Tom20 and Tom70 in vitro suggests a chaperone displacement mechanism. J. Biol. Chem. 286: 32208-32219.

Fang J, Nakamura T, Cho DH, Gu Z, Lipton SA. 2007. S-nitrosylation of peroxiredoxin 2 promotes oxidative stress-induced neuronal cell death in Parkinson's disease. Proc. Natl. Acad. Sci. U. S. A 104: 18742-18747.

Faou P, Hoogenraad NJ. 2012. Tom34: A cytosolic cochaperone of the Hsp90/Hsp70 protein complex involved in mitochondrial protein import. Biochim. Biophys. Acta 1823: 348-357.

Fernandez-Ranvier GG, Weng J, Yeh RF et al. 2008. Candidate diagnostic markers and tumor suppressor genes for adrenocortical carcinoma by expression profile of genes on chromosome 11q13. World J. Surg. 32: 873-881.

Figaro S, Scrima N, Buckingham RH, Heurgue-Hamard V. 2008. HemK2 protein, encoded on human chromosome 21, methylates translation termination factor eRF1. FEBS Lett. 582: 2352-2356.

Fisher AB. 2011. Peroxiredoxin 6: A bifunctional enzyme with glutathione peroxidase and phospholipase A2 activities. Antioxid. Redox. Signal. 15: 831-844.

Flohe L, Toppo S, Cozza G, Ursini F. 2011. A Comparison of Thiol Peroxidase Mechanisms. Antioxid. Redox. Signal. 15: 763-780.

Flynn, J.J., Finarelli, J.A., Spaulding, M., 2010. Phylogeny of the carnivora and carnivoramorpha, and the use of fossil record to enhance understanding of evolutionary transformations. In: Goswami, A.V., Friscia, A. (Eds.), Carnivoran Evolution: New views on phylogeny, form, and function, Cambridge University Press, Cambridge, pp. 25-64.

Forman HJ, Maiorino M, Ursini F. 2010. Signaling functions of reactive oxygen species. Biochemistry 49: 835-842.

Frank S, Munz B, Werner S. 1997. The human homologue of a bovine non-selenium glutathione peroxidase is a novel keratinocyte growth factor-regulated gene. Oncogene 14: 915-921.

Fratelli M, Demol H, Puype M et al. 2002. Identification by redox proteomics of glutathionylated proteins in oxidatively stressed human T lymphocytes. Proc. Natl. Acad. Sci. U. S. A 99: 3505-3510.

Fratelli M, Demol H, Puype M, Casagrande S, Villa P, Eberini I, Vandekerckhove J, Gianazza E, Ghezzi P. 2003. Identification of proteins undergoing glutathionylation in oxidatively stressed hepatocytes and hepatoma cells. Proteomics. 3: 1154-1161.

Fu Y, Cheng WH, Porres JM, Ross DA, Lei XG. 1999. Knockout of cellular glutathione peroxidase gene renders mice susceptible to diquat-induced oxidative stress. Free Radic. Biol. Med. 27: 605-611.

Fu Y, Cheng WH, Ross DA, Lei X. 1999. Cellular glutathione peroxidase protects mice against lethal oxidative stress induced by various doses of diquat. Proc. Soc. Exp. Biol. Med. 222: 164-169.

Fu Y, Sies H, Lei XG. 2001. Opposite roles of selenium-dependent glutathione peroxidase-1 in superoxide generator diquat- and peroxynitrite-induced apoptosis and signaling. J. Biol. Chem. 276: 43004-43009.

Fujii T, Fujii J, Taniguchi N. 2001. Augmented expression of peroxiredoxin VI in rat lung and kidney after birth implies an antioxidative role. Eur. J. Biochem. 268: 218-225.

Gakh E, Cavadini P, Isaya G. 2002. Mitochondrial processing peptidases. Biochim. Biophys. Acta 1592: 63-77.

Gao MC, Jia XD, Wu QF, Cheng Y, Chen FR, Zhang J. 2011. Silencing Prx1 and/or Prx5 sensitizes human esophageal cancer cells to ionizing radiation and increases apoptosis via intracellular ROS accumulation. Acta Pharmacol. Sin. 32: 528-536.

Gatesy J, Matthee C, DeSalle R, Hayashi C. 2002. Resolution of a supertree/supermatrix paradox. Syst. Biol. 51: 652-664.

Gerard AC, Many MC, Daumerie C, Knoops B, Colin IM. 2005. Peroxiredoxin 5 expression in the human thyroid gland. Thyroid 15: 205-209.

Germonpre M, Sablin MV, Stevens RE, Hedges REM, Hofreiter M, Stiller M, Despres VR. 2009. Fossil dogs and wolves from Palaeolithic sites in Belgium, the Ukraine and Russia: osteometry, ancient DNA and stable isotopes. J. Archaeol. Sc. 36: 473-490.

Godoy JR, Oesteritz S, Hanschmann EM, Ockenga W, Ackermann W, Lillig CH. 2011. Segment-specific overexpression of redoxins after renal ischemia and reperfusion: protective roles of glutaredoxin 2, peroxiredoxin 3, and peroxiredoxin 6. Free Radic. Biol. Med. 51: 552-561.

Goswami AV, Chittoor B, D'Silva P. 2010. Understanding the functional interplay between mammalian mitochondrial Hsp70 chaperone machine components. J. Biol. Chem. 285: 19472-19482.

Hall A, Karplus PA, Poole LB. 2009. Typical 2-Cys peroxiredoxins--structures, mechanisms and functions. FEBS J. 276: 2469-2477.

Hall A, Nelson K, Poole L, Karplus PA. 2011. Structure-based insights into the catalytic power and conformational dexterity of peroxiredoxins. Antioxid. Redox. Signal. 15: 795-815

Hall A, Parsonage D, Poole LB, Karplus PA. 2010. Structural Evidence that Peroxiredoxin Catalytic Power Is Based on Transition-State Stabilization. J. Mol. Biol. 402: 194-209.

Halliwell, B., Gutteridge, M.C., 2007. Free Radicals in Biology and Medicine. New York.

Hallstrom BM, Janke A. 2010. Mammalian evolution may not be strictly bifurcating. Mol. Biol. Evol. 27: 2804-2816.

Hanschmann EM, Lonn ME, Schutte LD, Funke M, Godoy JR, Eitner S, Hudemann C, Lillig CH. 2010. Both thioredoxin 2 and glutaredoxin 2 contribute to the reduction of the mitochondrial 2-Cys peroxiredoxin Prx3. J. Biol. Chem. 285: 40699-40705.

Hassanin A, Delsuc F, Ropiquet A et al. 2012. Pattern and timing of diversification of Cetartiodactyla (Mammalia, Laurasiatheria), as revealed by a comprehensive analysis of mitochondrial genomes. C. R. Biol. 335: 32-50.

Hattori F, Murayama N, Noshita T, Oikawa S. 2003. Mitochondrial peroxiredoxin-3 protects hippocampal neurons from excitotoxic injury in vivo. J. Neurochem. 86: 860-868.

Herbette S, Roeckel-Drevet P, Drevet JR. 2007. Seleno-independent glutathione peroxidases - More than simple antioxidant scavengers. Febs J. 274: 2163-2180.

Ho YS, Magnenat JL, Bronson RT, Cao J, Gargano M, Sugawara M, Funk CD. 1997. Mice deficient in cellular glutathione peroxidase develop normally and show no increased sensitivity to hyperoxia. J. Biol. Chem. 272: 16644-16651.

Hofmann B, Hecht HJ, Flohe L. 2002. Peroxiredoxins. Biol. Chem. 383: 347-364.

Holbrook JD, Birdsey GM, Yang Z, Bruford MW, Danpure CJ. 2000. Molecular adaptation of alanine:glyoxylate aminotransferase targeting in primates. Mol. Biol. Evol. 17: 387-400.

Holley AK, Bakthavatchalu V, Velez-Roman JM, St Clair DK. 2011. Manganese superoxide dismutase: guardian of the powerhouse. Int. J. Mol. Sci. 12: 7114-7162.

Hoogenraad NJ, Ward LA, Ryan MT. 2002. Import and assembly of proteins into mitochondria of mammalian cells. Biochim. Biophys. Acta 1592: 97-105.

Horiguchi H, Yurimoto H, Kato N, Sakai Y. 2001. Antioxidant system within yeast peroxisome. Biochemical and physiological characterization of CbPmp20 in the methylotrophic yeast Candida boidinii. J. Biol. Chem. 276: 14279-14288.

Huang TT, Carlson EJ, Kozy HM, Mantha S, Goodman SI, Ursell PC, Epstein CJ. 2001. Genetic modification of prenatal lethality and dilated cardiomyopathy in Mn superoxide dismutase mutant mice. Free Radic. Biol. Med. 31: 1101-1110.

Iacono M, Mignone F, Pesole G. 2005. uAUG and uORFs in human and rodent 5'untranslated mRNAs. Gene 349: 97-105.

Imai H, Nakagawa Y. 2003. Biological significance of phospholipid hydroperoxide glutathione peroxidase (PHGPx, GPx4) in mammalian cells. Free Radic. Biol. Med. 34: 145-169.

Imai H, Hirao F, Sakamoto T et al. 2003. Early embryonic lethality caused by targeted disruption of the mouse PHGPx gene. Biochem. Biophys. Res. Commun. 305: 278-286.

Imai H, Hakkaku N, Iwamoto R et al. 2009. Depletion of selenoprotein GPx4 in spermatocytes causes male infertility in mice. J. Biol. Chem. 284: 32522-32532.

Ishii T, Kawane T, Taketani S, Bannai S. 1995. Inhibition of the thiol-specific antioxidant activity of rat liver MSP23 protein by hemin. Biochem. Biophys. Res. Commun. 216: 970-975.

Iwahara S, Satoh H, Song DX, Webb J, Burlingame AL, Nagae Y, Muller-Eberhard U. 1995. Purification, characterization, and cloning of a heme-binding protein (23 kDa) in rat liver cytosol. Biochemistry 34: 13398-13406.

Jang HH, Lee KO, Chi YH et al. 2004. Two enzymes in one; two yeast peroxiredoxins display oxidative stress-dependent switching from a peroxidase to a molecular chaperone function. Cell 117: 625-635.

Jang YC, Perez VI, Song W et al. 2009. Overexpression of Mn superoxide dismutase does not increase life span in mice. J. Gerontol. A Biol. Sci. Med. Sci. 64: 1114-1125.

Jara M, Vivancos AP, Hidalgo E. 2008. C-terminal truncation of the peroxiredoxin Tpx1 decreases its sensitivity for hydrogen peroxide without compromising its role in signal transduction. Genes Cells 13: 171-179.

Jezek P, Hlavata L. 2005. Mitochondria in homeostasis of reactive oxygen species in cell, tissues, and organism. Int. J. Biochem. Cell Biol. 37: 2478-2503.

Jiang D, Akopian G, Ho YS, Walsh JP, Andersen JK. 2000. Chronic brain oxidation in a glutathione peroxidase knockout mouse model results in increased resistance to induced epileptic seizures. Exp. Neurol. 164: 257-268.

Johnston AJ, Hoogenraad J, Dougan DA, Truscott KN, Yano M, Mori M, Hoogenraad NJ, Ryan MT. 2002. Insertion and assembly of human tom7 into the preprotein translocase complex of the outer mitochondrial membrane. J. Biol. Chem. 277: 42197-42204.

Kang SW, Chae HZ, Seo MS, Kim K, Baines IC, Rhee SG. 1998. Mammalian peroxiredoxin isoforms can reduce hydrogen peroxide generated in response to growth factors and tumor necrosis factor-alpha. J. Biol. Chem. 273: 6297-6302.

Karihtala P, Mantyniemi A, Kang SW, Kinnula VL, Soini Y. 2003. Peroxiredoxins in breast carcinoma. Clin. Cancer Res. 9: 3418-3424.

Karihtala P, Soini Y, Vaskivuo L, Bloigu R, Puistola U. 2009. DNA adduct 8-hydroxydeoxyguanosine, a novel putative marker of prognostic significance in ovarian carcinoma. Int. J. Gynecol. Cancer 19: 1047-1051.

Karniely S, Pines O. 2005. Single translation--dual destination: mechanisms of dual protein targeting in eukaryotes. EMBO Rep. 6: 420-425.

Kato H, Mihara K. 2008. Identification of Tom5 and Tom6 in the preprotein translocase complex of human mitochondrial outer membrane. Biochem. Biophys. Res. Commun. 369: 958-963.

Kim K, Kim IH, Lee KY, Rhee SG, Stadtman ER. 1988. The isolation and purification of a specific "protector" protein which inhibits enzyme inactivation by a thiol/Fe(III)/O2 mixed-function oxidation system. J. Biol. Chem. 263: 4704-4711.

Kim J, Lee J, Lee HN, Kim E, Ha B, Ahn S, Jang HH, Lee SY. 2012. RNA-binding properties and RNA chaperone activity of human peroxiredoxin 1. Biochem. Biophys. Res. Commun. 425: 730-734.

Kinnula VL, Lehtonen S, Sormunen R, Kaarteenaho-Wiik R, Kang SW, Rhee SG, Soini Y. 2002. Overexpression of peroxiredoxins I, II, III, V, and VI in malignant mesothelioma. J. Pathol. 196: 316-323.

Knoops B, Clippe A, Bogard C, Arsalane K, Wattiez R, Hermans C, Duconseille E, Falmagne P, Bernard A. 1999. Cloning and characterization of AOEB166, a novel mammalian antioxidant enzyme of the peroxiredoxin family. J. Biol. Chem. 274: 30451-30458.

Knoops B, Loumaye E, Van der Eecken V. 2007. Evolution of the peroxiredoxins. Subcell. Biochem. 44: 27-40.

Knoops B, Goemaere J, Van der Eecken V, Declercq JP. 2011. Peroxiredoxin 5: Structure, mechanism and function of the mammalian atypical 2-Cys peroxiredoxin. Antioxid. Redox. Signal. 15: 817-829.

Knott TG, Birdsey GM, Sinclair KE, Gallagher IM, Purdue PE, Danpure CJ. 2000. The peroxisomal targeting sequence type 1 receptor, Pex5p, and the peroxisomal import efficiency of alanine:glyoxylate aminotransferase. Biochem. J. 352 Pt 2: 409-418.

Kokoszka JE, Coskun P, Esposito LA, Wallace DC. 2001. Increased mitochondrial oxidative stress in the Sod2 (+/-) mouse results in the age-related decline of mitochondrial function culminating in increased apoptosis. Proc. Natl. Acad. Sci. U. S. A 98: 2278-2283.

Koo KH, Lee S, Jeong SY, Kim ET, Kim HJ, Kim K, Song K, Chae HZ. 2002. Regulation of thioredoxin peroxidase activity by C-terminal truncation. Arch. Biochem. Biophys. 397: 312-318.

Kozak M. 1978. How do eucaryotic ribosomes select initiation regions in messenger RNA? Cell 15: 1109-1123.

Krapfenbauer K, Engidawork E, Cairns N, Fountoulakis M, Lubec G. 2003. Aberrant expression of peroxiredoxin subtypes in neurodegenerative disorders. Brain Res. 967: 152-160.

Kropotov A, Sedova V, Ivanov V et al. 1999. A novel human DNA-binding protein with sequence similarity to a subfamily of redox proteins which is able to repress RNA-polymerase-III-driven transcription of the Alu-family retroposons in vitro. Eur. J. Biochem. 260: 336-346.

Kropotov A, Gogvadze V, Shupliakov O, Tomilin N, Serikov VB, Tomilin NV, Zhivotovsky B. 2006. Peroxiredoxin V is essential for protection against apoptosis in human lung carcinoma cells. Exp. Cell Res. 312: 2806-2815.

Kropotov A, Serikov V, Suh J, Smirnova A, Bashkirov V, Zhivotovsky B, Tomilin N. 2006. Constitutive expression of the human peroxiredoxin V gene contributes to protection of the genome from oxidative DNA lesions and to suppression of transcription of noncoding DNA. FEBS J. 273: 2607-2617.

Kropotov A, Usmanova N, Serikov V, Zhivotovsky B, Tomilin N. 2007. Mitochondrial targeting of human peroxiredoxin V protein and regulation of PRDX5 gene expression by nuclear transcription factors controlling biogenesis of mitochondria. FEBS J. 274: 5804-5814.

Kropotov AV, Grudinkin PS, Pleskach NM, Gavrilov BA, Tomilin NV, Zhivotovsky B. 2004. Downregulation of peroxiredoxin V stimulates formation of etoposide-induced double-strand DNA breaks. FEBS Lett. 572: 75-79.

Lambert AJ, Buckingham JA, Boysen HM, Brand MD. 2010. Low complex I content explains the low hydrogen peroxide production rate of heart mitochondria from the long-lived pigeon, Columba livia. Aging Cell 9: 78-91.

Larkin MA, Blackshields G, Brown NP et al. 2007. Clustal W and Clustal X version 2.0. Bioinformatics. 23: 2947-2948.

Larson, G., Cucchi, T., Dobney, K., 2011. Genetic aspects of pig domestication. In: Rothschild, M.F., Ruvinsky, A. (Eds.), The genetics of the pig, CAB International, pp. 14-37.

Lebovitz RM, Zhang H, Vogel H, Cartwright J, Jr., Dionne L, Lu N, Huang S, Matzuk MM. 1996. Neurodegeneration, myocardial injury, and perinatal death in mitochondrial superoxide dismutase-deficient mice. Proc. Natl. Acad. Sci. U. S. A 93: 9782-9787.

Lee KW, Lee DJ, Lee JY, Kang DH, Kwon J, Kang SW. 2011. Peroxiredoxin II restrains DNA damage-induced death in cancer cells by positively regulating JNK-dependent DNA repair. J. Biol. Chem. 286: 8394-8404.

Lee SP, Hwang YS, Kim YJ, Kwon KS, Kim HJ, Kim K, Chae HZ. 2001. Cyclophilin a binds to peroxiredoxins and activates its peroxidase activity. J. Biol. Chem. 276: 29826-29832.

Lee W, Choi KS, Riddell J, Ip C, Ghosh D, Park JH, Park YM. 2007. Human peroxiredoxin 1 and 2 are not duplicate proteins: the unique presence of CYS83 in Prx1 underscores the structural and functional differences between Prx1 and Prx2. J. Biol. Chem. 282: 22011-22022.

Legault J, Carrier C, Petrov P, Renard P, Remacle J, Mirault ME. 2000. Mitochondrial GPx1 decreases induced but not basal oxidative damage to mtDNA in T47D cells. Bioch. Biophys. Res. Comm. 272: 416-422.

Lei XG, Cheng WH, McClung JP. 2007. Metabolic regulation and function of glutathione peroxidase-1. Annu. Rev. Nutr. 27: 41-61.

Leonard JA, Wayne RK, Wheeler J, Valadez R, Guillen S, Vila C. 2002. Ancient DNA evidence for Old World origin of New World dogs. Science 298: 1613-1616.

Leyens G, Donnay I, Knoops B. 2003. Cloning of bovine peroxiredoxins - gene expression in bovine tissues and amino acid sequence comparison with rat, mouse and primate peroxiredoxins. Comp. Biochem. Physiol. B-Biochem. Mol. Biol. 136: 943-955.

Leyens G, Knoops B, Donnay I. 2004. Expression of peroxiredoxins in bovine oocytes and embryos produced in vitro. Mol. Reprod. Dev. 69: 243-251.

Li J, Li L, Zhang S, Zhang G. 2011. Cloning, genomic structure, and expression analysis of peroxiredoxin V from bay scallop Argopecten irradians. Fish. Shellfish. Immunol. 30: 309-316.

Li L, Shoji W, Takano H et al. 2007. Increased susceptibility of MER5 (peroxiredoxin III) knockout mice to LPS-induced oxidative stress. Biochem. Biophys. Res. Commun. 355: 715-721.

Li L, Shoji W, Oshima H, Obinata M, Fukumoto M, Kanno N. 2008. Crucial role of peroxiredoxin III in placental antioxidant defense of mice. FEBS Lett. 582: 2431-2434.

Li L, Kaifu T, Obinata M, Takai T. 2009. Peroxiredoxin III-deficiency sensitizes macrophages to oxidative stress. J. Biochem. 145: 425-427.

Li Y, Huang TT, Carlson EJ et al. 1995. Dilated cardiomyopathy and neonatal lethality in mutant mice lacking manganese superoxide dismutase. Nat. Genet. 11: 376-381.

Liang H, Yoo SE, Na R, Walter CA, Richardson A, Ran Q. 2009. Short form glutathione peroxidase 4 is the essential isoform required for survival and somatic mitochondrial functions. J. Biol. Chem. 284: 30836-30844.

Lindblad-Toh K, Wade CM, Mikkelsen TS et al. 2005. Genome sequence, comparative analysis and haplotype structure of the domestic dog. Nature 438: 803-819.

Link AJ, Robison K, Church GM. 1997. Comparing the predicted and observed properties of proteins encoded in the genome of Escherichia coli K-12. Electrophoresis 18: 1259-1313.

Lu JL, Vallat JM, Pollard JD, Knoops B, Ouvrier R. 2006. Expression of the antioxidant enzyme peroxiredoxin 5 in the human peripheral nervous system. J. Peripher. Nerv. Syst. 11: 318-324.

Lubos E, Loscalzo J, Handy DE. 2011. Glutathione peroxidase-1 in health and disease: from molecular mechanisms to therapeutic opportunities. Antioxid. Redox. Signal. 15: 1957-1997.

Manevich Y, Feinstein SI, Fisher AB. 2004. Activation of the antioxidant enzyme 1-CYS peroxiredoxin requires glutathionylation mediated by heterodimerization with pi GST. Proc. Natl. Acad. Sci. U. S. A 101: 3780-3785.

Marcot, J., 2007. Molecular phylogeny of terrestrial artiodactyls: conflicts and resolution. In: D.R.Prothero and S.E.Foss (Ed.), The evolution of artiodactyls, The Johns Hopkins University Press, Baltimore, pp. 4-18.

Marom M, Azem A, Mokranjac D. 2011. Understanding the molecular mechanism of protein translocation across the mitochondrial inner membrane: still a long way to go. Biochim. Biophys. Acta 1808: 990-1001.

Marques FZ, Campain AE, Tomaszewski M, Zukowska-Szczechowska E, Yang YH, Charchar FJ, Morris BJ. 2011. Gene expression profiling reveals renin mRNA overexpression in human hypertensive kidneys and a role for microRNAs. Hypertension 58: 1093-1098.

Matsushima S, Ide T, Yamato M et al. 2006. Overexpression of mitochondrial peroxiredoxin-3 prevents left ventricular remodeling and failure after myocardial infarction in mice. Circulation 113: 1779-1786.

McCormack JE, Faircloth BC, Crawford NG, Gowaty PA, Brumfield RT, Glenn TC. 2012. Ultraconserved elements are novel phylogenomic markers that resolve placental mammal phylogeny when combined with species-tree analysis. Genome Res. 22: 746-751

Melov S, Coskun P, Patel M et al. 1999. Mitochondrial disease in superoxide dismutase 2 mutant mice. Proc. Natl. Acad. Sci. U. S. A 96: 846-851.

Mirault ME, Tremblay A, Beaudoin N, Tremblay M. 1991. Overexpression of seleno-glutathione peroxidase by gene transfer enhances the resistance of T47D human breast cells to clastogenic oxidants. J. Biol. Chem. 266: 20752-20760.

Mokranjac D, Neupert W. 2009. Thirty years of protein translocation into mitochondria: unexpectedly complex and still puzzling. Biochim. Biophys. Acta 1793: 33-41.

Momose T, Ohshima C, Maeda M, Endo T. 2007. Structural basis of functional cooperation of Tim15/Zim17 with yeast mitochondrial Hsp70. EMBO Rep. 8: 664-670.

Monteiro G, Horta BB, Pimenta DC, Augusto O, Netto LE. 2007. Reduction of 1-Cys peroxiredoxins by ascorbate changes the thiol-specific antioxidant paradigm, revealing another function of vitamin C. Proc. Natl. Acad. Sci. U. S. A 104: 4886-4891.

Moon JC, Hah YS, Kim WY et al. 2005. Oxidative stress-dependent structural and functional switching of a human 2-Cys peroxiredoxin isotype II that enhances HeLa cell resistance to H2O2-induced cell death. J. Biol. Chem. 280: 28775-28784.

Mowbray AL, Kang DH, Rhee SG, Kang SW, Jo H. 2008. Laminar shear stress up-regulates peroxiredoxins (PRX) in endothelial cells: PRX 1 as a mechanosensitive antioxidant. J. Biol. Chem. 283: 1622-1627.

Mukhopadhyay SS, Leung KS, Hicks MJ, Hastings PJ, Youssoufian H, Plon SE. 2006. Defective mitochondrial peroxiredoxin-3 results in sensitivity to oxidative stress in Fanconi anemia. J. Cell Biol. 175: 225-235.

Murphy WJ, Pringle TH, Crider TA, Springer MS, Miller W. 2007. Using genomic data to unravel the root of the placental mammal phylogeny. Genome Res. 17: 413-421.

Murphy, W.J., Eizirik, E., 2009. Placental mammals (Eutheria). In: Hedges, S.B., Kumar, S. (Eds.), The Timetree of Life, Oxford University Press, pp. 471-474.

Musicco C, Capelli V, Pesce V, Timperio AM, Calvani M, Mosconi L, Zolla L, Cantatore P, Gadaleta MN. 2009. Accumulation of overoxidized Peroxiredoxin III in aged rat liver mitochondria. Biochim. Biophys Acta 1787: 890-896.

Myers, P., Espinosa, R., Parr, C.S., Jones, T., Hammond, G.S., Dewey, T.A., 2012. The Animal Diversity Web (University of Michigan Museum of Zoology). Accessed at http://animaldiversity.org.

Nakai K, Horton P. 1999. PSORT: a program for detecting sorting signals in proteins and predicting their subcellular localization. Trends Biochem. Sci. 24: 34-36.

Nauseef WM. 2007. How human neutrophils kill and degrade microbes: an integrated view. Immunol. Rev. 219: 88-102.

Nemoto Y, Yamamoto T, Takada S, Matsui Y, Obinata M. 1990. Antisense Rna of the Latent Period Gene (Mer5) Inhibits the Differentiation of Murine Erythroleukemia-Cells. Gene 91: 261-265.

Neupert W, Herrmann JM. 2007. Translocation of proteins into mitochondria. Annu. Rev. Biochem. 76: 723-749.

Neuspiel M, Schauss AC, Braschi E, Zunino R, Rippstein P, Rachubinski RA, Andrade-Navarro MA, McBride HM. 2008. Cargo-selected transport from the mitochondria to peroxisomes is mediated by vesicular carriers. Curr. Biol. 18: 102-108.

Nguyen-Nhu NT, Knoops B. 2003. Mitochondrial and cytosolic expression of human peroxiredoxin 5 in Saccharomyces cerevisiae protect yeast cells from oxidative stress induced by paraquat. FEBS Lett. 544: 148-152.

Nguyen-Nhu NT, Berck J, Clippe A et al. 2007. Human peroxiredoxin 5 gene organization, initial characterization of its promoter and identification of alternative forms of mRNA. Biochim. Biophys. Acta 1769: 472-483.

Nguyen Ba AN, Pogoutse A, Provart N, Moses AM. 2009. NLStradamus: a simple Hidden Markov Model for nuclear localization signal prediction. BMC. Bioinformatics. 10: 202.

Nielsen H, Engelbrecht J, Brunak S, von Heijne G. 1997. Identification of prokaryotic and eukaryotic signal peptides and prediction of their cleavage sites. Protein Eng 10: 1-6.

Nishihara H, Maruyama S, Okada N. 2009. Retroposon analysis and recent geological data suggest near-simultaneous divergence of the three superorders of mammals. Proc. Natl. Acad. Sci. U. S. A 106: 5235-5240.

Noh DY, Ahn SJ, Lee RA, Kim SW, Park IA, Chae HZ. 2001. Overexpression of peroxiredoxin in human breast cancer. Anticancer Res. 21: 2085-2090.

Noh YH, Baek JY, Jeong W, Rhee SG, Chang TS. 2009. Sulfiredoxin Translocation into Mitochondria Plays a Crucial Role in Reducing Hyperoxidized Peroxiredoxin III. J. Biol. Chem. 284: 8470-8477.

Nolden M, Ehses S, Koppen M, Bernacchia A, Rugarli EI, Langer T. 2005. The m-AAA protease defective in hereditary spastic paraplegia controls ribosome assembly in mitochondria. Cell 123: 277-289.

Nonn L, Berggren M, Powis G. 2003. Increased expression of mitochondrial peroxiredoxin-3 (thioredoxin peroxidase-2) protects cancer cells against hypoxia and drug-induced hydrogen peroxide-dependent apoptosis. Mol. Cancer Res. 1: 682-689.

O'Leary MA, Gatesy J. 2008. Impact of increased character sampling on the phylogeny of Cetartiodactyla (mammalia): combined analysis including fossils. Cladistics 24: 397-442.

Oberley TD, Verwiebe E, Zhong W, Kang SW, Rhee SG. 2001. Localization of the thioredoxin system in normal rat kidney. Free Radic. Biol. Med. 30: 412-424.

Olmos Y, Valle I, Borniquel S, Tierrez A, Soria E, Lamas S, Monsalve M. 2009. Mutual dependence of Foxo3a and PGC-1alpha in the induction of oxidative stress genes. J. Biol. Chem. 284: 14476-14484.

Orliac MJ, Pierre-Olivier A, Ducrocq S. 2010. Phylogenetic relationships of the Suidae (Mammalia, Cetartiodactyla): new insights on the relationships within Suoidea. Zool. Scr. 39: 315-330.

Ostrander EA, Wayne RK. 2005. The canine genome. Genome Res. 15: 1706-1716.

Pagliarini DJ, Calvo SE, Chang B et al. 2008. A mitochondrial protein compendium elucidates complex I disease biology. Cell 134: 112-123.

Pamplona R. 2011. Mitochondrial DNA damage and animal longevity: insights from comparative studies. J. Aging Res. 2011: 807108.

Panfili E, Sandri G, Ernster L. 1991. Distribution of glutathione peroxidases and glutathione reductase in rat brain mitochondria. FEBS Lett. 290: 35-37.

Park JH, Kim YS, Lee HL et al. 2006. Expression of peroxiredoxin and thioredoxin in human lung cancer and paired normal lung. Respirology 11: 269-275.

Park JW, Mieyal JJ, Rhee SG, Chock PB. 2009. Deglutathionylation of 2-Cys peroxiredoxin is specifically catalyzed by sulfiredoxin. J. Biol. Chem. 284: 23364-23374.

Park JP, Piszczek G, Rhee SG, Chock PB. 2011. Glutathionylation of Peroxiredoxin I Induces Decamer to Dimers Dissociation with Concomitant Loss of Chaperone Activity. Biochemistry 50: 3204-3210.

Parker HG, Shearin AL, Ostrander EA. 2010. Man's Best Friend Becomes Biology's Best in Show: Genome Analyses in the Domestic Dog. Annu. Rev. Genet. 44: 309-336.

Parmigiani RB, Xu WS, Venta-Perez G, Erdjument-Bromage H, Yaneva M, Tempst P, Marks PA. 2008. HDAC6 is a specific deacetylase of peroxiredoxins and is involved in redox regulation. Proc. Natl. Acad. Sci. U. S. A 105: 9633-9638.

Peng Y, Yang PH, Guo Y et al. 2004. Catalase and peroxiredoxin 5 protect Xenopus embryos against alcohol-induced ocular anomalies. Invest Ophthalmol. Vis. Sci. 45: 23-29.

Peng Y, Yang PH, Ng SS, Lum CT, Kung HF, Lin MC. 2004. Protection of Xenopus laevis embryos against alcohol-induced delayed gut maturation and growth retardation by peroxiredoxin 5 and catalase. J. Mol. Biol. 340: 819-827.

Peskin AV, Cox AG, Nagy P, Morgan PE, Hampton MB, Davies MJ, Winterbourn CC. 2010. Removal of amino acid, peptide and protein hydroperoxides by reaction with peroxiredoxins 2 and 3. Biochem. J. 432: 313-321.

Pfeifer H, Conrad M, Roethlein D, Kyriakopoulos A, Brielmeier M, Bornkamm GW, Behne D. 2001. Identification of a specific sperm nuclei selenoenzyme necessary for protamine thiol cross-linking during sperm maturation. FASEB J. 15: 1236-1238.

Plaisant F, Clippe A, Vander Stricht D, Knoops B, Gressens P. 2003. Recombinant peroxiredoxin 5 protects against excitotoxic brain lesions in newborn mice. Free Radical Biology and Medicine 34: 862-872.

Plishker GA, Chevalier D, Seinsoth L, Moore RB. 1992. Calcium-activated potassium transport and high molecular weight forms of calpromotin. J. Biol. Chem. 267: 21839-21843.

Poncin S, Gerard AC, Boucquey M, Senou M, Calderon PB, Knoops B, Lengele B, Many MC, Colin IM. 2008. Oxidative stress in the thyroid gland: from harmlessness to hazard depending on the iodine content. Endocrinology 149: 424-433.

Poole LB. 2007. The catalytic mechanism of peroxiredoxins. Subcell. Biochem. 44: 61-81.

Price SA, Bininda-Emonds OR, Gittleman JL. 2005. A complete phylogeny of the whales, dolphins and even-toed hoofed mammals (Cetartiodactyla). Biol. Rev. Camb. Philos. Soc. 80: 445-473.

Puglisi R, Maccari I, Pipolo S, Conrad M, Mangia F, Boitani C. 2012. The nuclear form of glutathione peroxidase 4 is associated with sperm nuclear matrix and is required for proper paternal chromatin decondensation at fertilization. J. Cell Physiol 227: 1420-1427.

Pushpa-Rekha TR, Burdsall AL, Oleksa LM, Chisolm GM, Driscoll DM. 1995. Rat phospholipid-hydroperoxide glutathione peroxidase. cDNA cloning and identification of multiple transcription and translation start sites. J. Biol. Chem. 270: 26993-26999.

Qian W, Zhang J. 2009. Protein subcellular relocalization in the evolution of yeast singleton and duplicate genes. Genome Biol. Evol. 1: 198-204.

Qiao B, Wang J, Xie J, Niu Y, Ye S, Wan Q, Ye Q. 2012. Detection and identification of peroxiredoxin 3 as a biomarker in hepatocellular carcinoma by a proteomic approach. Int. J. Mol. Med. 29: 832-840.

Qu D, Rashidian J, Mount MP et al. 2007. Role of Cdk5-mediated phosphorylation of Prx2 in MPTP toxicity and Parkinson's disease. Neuron 55: 37-52.

Radyuk SN, Michalak K, Klichko VI, Benes J, Rebrin I, Sohal RS, Orr WC. 2009. Peroxiredoxin 5 confers protection against oxidative stress and apoptosis and also promotes longevity in Drosophila. Biochem. J. 419: 437-445.

Radyuk SN, Michalak K, Klichko VI, Benes J, Orr WC. 2010. Peroxiredoxin 5 modulates immune response in Drosophila. Biochim. Biophys. Acta 1800: 1153-1163.

Ralat LA, Manevich Y, Fisher AB, Colman RF. 2006. Direct evidence for the formation of a complex between 1-cysteine peroxiredoxin and glutathione S-transferase pi with activity changes in both enzymes. Biochemistry 45: 360-372.

Ralat LA, Misquitta SA, Manevich Y, Fisher AB, Colman RF. 2008. Characterization of the complex of glutathione S-transferase pi and 1-cysteine peroxiredoxin. Arch. Biochem. Biophys. 474: 109-118.

Ran Q, Liang H, Gu M, Qi W, Walter CA, Roberts LJ, Herman B, Richardson A, Van RH. 2004. Transgenic mice overexpressing glutathione peroxidase 4 are protected against oxidative stress-induced apoptosis. J. Biol. Chem. 279: 55137-55146.

Rhee SG, Chae HZ, Kim K. 2005. Peroxiredoxins: a historical overview and speculative preview of novel mechanisms and emerging concepts in cell signaling. Free Radic. Biol. Med. 38: 1543-1552.

Rhee SG. 2006. Cell signaling. H2O2, a necessary evil for cell signaling. Science 312: 1882-1883.

Rhee SG, Woo HA. 2011. Multiple Functions of Peroxiredoxins: Peroxidases, Sensors and Regulators of the Intracellular Messenger H2O2, and Protein Chaperones. Antioxid. Redox Signal. 15: 781-94.

Rosso L, Marques AC, Reichert AS, Kaessmann H. 2008. Mitochondrial targeting adaptation of the hominoid-specific glutamate dehydrogenase driven by positive Darwinian selection. PLoS. Genet. 4: e1000150.

Rosso L, Marques AC, Weier M, Lambert N, Lambot MA, Vanderhaeghen P, Kaessmann H. 2008. Birth and rapid subcellular adaptation of a hominoid-specific CDC14 protein. PLoS. Biol. 6: e140.

Rucktaschel R, Girzalsky W, Erdmann R. 2011. Protein import machineries of peroxisomes. Biochim. Biophys. Acta 1808: 892-900.

Ruvinsky, A., Rothschild, M.F., Larson, G., Gongora, 2011. Systematics and evolution of the pig. In: Rothschild, M.F., Ruvinsky, A. (Eds.), The Genetics of the Pig, CAB International, pp. 1-13.

Saito Y, Nishio K, Ogawa Y, Kinumi T, Yoshida Y, Masuo Y, Niki E. 2007. Molecular mechanisms of 6-hydroxydopamine-induced cytotoxicity in PC12 cells: Involvement of hydrogen peroxide-dependent and -independent action. Free Radic. Biol. Med. 42: 675-685.

Savolainen P, Zhang YP, Luo J, Lundeberg J, Leitner T. 2002. Genetic evidence for an East Asian origin of domestic dogs. Science 298: 1610-1613.

Sayed AA, Williams DL. 2004. Biochemical characterization of 2-Cys peroxiredoxins from Schistosoma mansoni. J. Biol. Chem. 279: 26159-26166.

Schluter A, Real-Chicharro A, Gabaldon T, Sanchez-Jimenez F, Pujol A. 2010. PeroxisomeDB 2.0: an integrative view of the global peroxisomal metabolome. Nucleic Acids Res. 38: D800-D805.

Schmidt O, Pfanner N, Meisinger C. 2010. Mitochondrial protein import: from proteomics to functional mechanisms. Nat. Rev. Mol. Cell Biol. 11: 655-667.

Schmidt TR, Doan JW, Goodman M, Grossman LI. 2003. Retention of a duplicate gene through changes in subcellular targeting: an electron transport protein homologue localizes to the golgi. J. Mol. Evol. 57: 222-228.

Schneider M, Forster H, Boersma A et al. 2009. Mitochondrial glutathione peroxidase 4 disruption causes male infertility. FASEB J. 23: 3233-3242.

Schroder E, Eaton P. 2008. Hydrogen peroxide as an endogenous mediator and exogenous tool in cardiovascular research: issues and considerations. Curr. Opin. Pharmacol. 8: 153-159.

Schulz C, Lytovchenko O, Melin J et al. 2011. Tim50's presequence receptor domain is essential for signal driven transport across the TIM23 complex. J. Cell Biol. 195: 643-656.

Seiler A, Schneider M, Forster H et al. 2008. Glutathione peroxidase 4 senses and translates oxidative stress into 12/15-lipoxygenase dependent- and AIF-mediated cell death. Cell Metab. 8: 237-248.

Senou M, Khalifa C, Thimmesch M et al. 2010. A coherent organization of differentiation proteins is required to maintain an appropriate thyroid function in the Pendred thyroid. J. Clin. Endocrinol. Metab 95: 4021-4030.

Sensi M, Nicolini G, Zanon M, Colombo C, Molla A, Bersani I, Lupetti R, Parmiani G, Anichini A. 2005. Immunogenicity without immunoselection: a mutant but functional antioxidant enzyme retained in a human metastatic melanoma and targeted by CD8(+) T cells with a memory phenotype. Cancer Res. 65: 632-640.

Sensi M, Pietra G, Molla A et al. 2009. Peptides with dual binding specificity for HLA-A2 and HLA-E are encoded by alternatively spliced isoforms of the antioxidant enzyme peroxiredoxin 5. Int. Immunol. 21: 257-268.

Seo JH, Lim JC, Lee DY et al. 2009. Novel protective mechanism against irreversible hyperoxidation of peroxiredoxin: Nalpha-terminal acetylation of human peroxiredoxin II. J. Biol. Chem. 284: 13455-13465.

Seo MJ, Liu X, Chang M, Park JH. 2012. GATA-binding protein 1 is a novel transcription regulator of peroxiredoxin 5 in human breast cancer cells. Int. J. Oncol. 40: 655-664.

Seo MS, Kang SW, Kim K, Baines IC, Lee TH, Rhee SG. 2000. Identification of a new type of mammalian peroxiredoxin that forms an intramolecular disulfide as a reaction intermediate. J. Biol. Chem. 275: 20346-20354.

Serikov VB, Leutenegger C, Krutilina R, Kropotov A, Pleskach N, Suh JH, Tomilin NV. 2006. Cigarette smoke extract inhibits expression of peroxiredoxin V and increases airway epithelial permeability. Inhal. Toxicol. 18: 79-92.

Sevier CS, Kaiser CA. 2008. Ero1 and redox homeostasis in the endoplasmic reticulum. Biochim. Biophys. Acta 1783: 549-556.

Shichita T, Hasegawa E, Kimura A et al. 2012. Peroxiredoxin family proteins are key initiators of post-ischemic inflammation in the brain. Nat. Med. 18: 911-917.

Shih SF, Wu YH, Hung CH, Yang HY, Lin JY. 2001. Abrin triggers cell death by inactivating a thiol-specific antioxidant protein. J. Biol. Chem. 276: 21870-21877.

Silva JP, Shabalina IG, Dufour E et al. 2005. SOD2 overexpression: enhanced mitochondrial tolerance but absence of effect on UCP activity. EMBO J. 24: 4061-4070.

Singh AK, Dhaunsi GS, Gupta MP, Orak JK, Asayama K, Singh I. 1994. Demonstration of glutathione peroxidase in rat liver peroxisomes and its intraorganellar distribution. Arch. Biochem. Biophys. 315: 331-338.

Singha UK, Hamilton V, Duncan MR, Weems E, Tripathi MK, Chaudhuri M. 2012. Protein Translocase of Mitochondrial Inner Membrane in Trypanosoma brucei. J. Biol. Chem. 287: 14480-14493.

Sinha D, Joshi N, Chittoor B, Samji P, D'Silva P. 2010. Role of Magmas in protein transport and human mitochondria biogenesis. Hum. Mol. Genet. 19: 1248-1262.

Songe-Moller L, van den Born E, Leihne V, Vagbo CB, Kristoffersen T, Krokan HE, Kirpekar F, Falnes PO, Klungland A. 2010. Mammalian ALKBH8 possesses tRNA methyltransferase activity required for the biogenesis of multiple wobble uridine modifications implicated in translational decoding. Mol. Cell Biol. 30: 1814-1827.

Sorokina EM, Feinstein SI, Milovanova TN, Fisher AB. 2009. Identification of the amino acid sequence that targets peroxiredoxin 6 to lysosome-like structures of lung epithelial cells. Am. J. Physiol Lung Cell Mol. Physiol 297: L871-L880.

Sorokina EM, Feinstein SI, Zhou SP, Fisher AB. 2011. Intracellular targeting of peroxiredoxin 6 to lysosomal organelles requires MAPK activity and binding to 14-3-3 epsilon. Am. J. Physiol Cell Physiol 300: C1430-C1441.

Springer MS, Murphy WJ. 2007. Mammalian evolution and biomedicine: new views from phylogeny. Biol. Rev. Camb. Philos. Soc. 82: 375-392.

Stewart M. 2007. Molecular mechanism of the nuclear protein import cycle. Nat. Rev. Mol. Cell Biol. 8: 195-208.

Sullivan DM, Wehr NB, Fergusson MM, Levine RL, Finkel T. 2000. Identification of oxidant-sensitive proteins: TNF-alpha induces protein glutathiolation. Biochemistry 39: 11121-11128.

Sun HN, Kim SU, Huang SM et al. 2010. Microglial peroxiredoxin V acts as an inducible anti-inflammatory antioxidant through cooperation with redox signaling cascades. J. Neurochem. 114: 39-50.

Sutton A, Khoury H, Prip-Buus C, Cepanec C, Pessayre D, Degoul F. 2003. The Ala16Val genetic dimorphism modulates the import of human manganese superoxide dismutase into rat liver mitochondria. Pharmacogenetics 13: 145-157.

Szklarczyk R, Huynen MA. 2009. Expansion of the human mitochondrial proteome by intra- and inter-compartmental protein duplication. Genome Biol. 10: R135.

Tavender TJ, Sheppard AM, Bulleid NJ. 2008. Peroxiredoxin IV is an endoplasmic reticulum-localized enzyme forming oligomeric complexes in human cells. Biochem. J. 411: 191-199.

Tavender TJ, Springate JJ, Bulleid NJ. 2010. Recycling of peroxiredoxin IV provides a novel pathway for disulphide formation in the endoplasmic reticulum. EMBO J. 29: 4185-4197.

Taylor SD, Davenport LD, Speranza MJ, Mullenbach GT, Lynch RE. 1993. Glutathione peroxidase protects cultured mammalian cells from the toxicity of adriamycin and paraquat. Arch. Biochem. Biophys. 305: 600-605.

Toppo S, Flohe L, Ursini F, Vanin S, Maiorino M. 2009. Catalytic mechanisms and specificities of glutathione peroxidases: variations of a basic scheme. Biochim. Biophys. Acta 1790: 1486-1500.

Touriol C, Bornes S, Bonnal S, Audigier S, Prats H, Prats AC, Vagner S. 2003. Generation of protein isoform diversity by alternative initiation of translation at non-AUG codons. Biol. Cell 95: 169-178.

Trujillo M, Clippe A, Manta B, Ferrer-Sueta G, Smeets A, Declercq JP, Knoops B, Radi R. 2007. Pre-steady state kinetic characterization of human peroxiredoxin 5: taking advantage of Trp84 fluorescence increase upon oxidation. Arch. Biochem. Biophys. 467: 95-106.

Uittenbogaard M, Chiaramello A. 2002. Expression of the bHLH transcription factor Tcf12 (ME1) gene is linked to the expansion of precursor cell populations during neurogenesis. Brain Res. Gene Expr. Patterns. 1: 115-121.

Ursini F, Heim S, Kiess M, Maiorino M, Roveri A, Wissing J, Flohe L. 1999. Dual function of the selenoprotein PHGPx during sperm maturation. Science 285: 1393-1396.

Usmanova N, Tomilin N, Zhivotovsky B, Kropotov A. 2011. Transcription factor GABP/NRF-2 controlling biogenesis of mitochondria regulates basal expression of peroxiredoxin V but the mitochondrial function of peroxiredoxin V is dispensable in the dog. Biochimie 93: 306-313.

Utsunomiya H, Komatsu N, Yoshimura S, Tsutsumi Y, Watanabe K. 1991. Exact ultrastructural localization of glutathione peroxidase in normal rat hepatocytes: advantages of microwave fixation. J. Histochem. Cytochem. 39: 1167-1174.

Valko M, Leibfritz D, Moncol J, Cronin MT, Mazur M, Telser J. 2007. Free radicals and antioxidants in normal physiological functions and human disease. Int. J. Biochem. Cell Biol. 39: 44-84.

Van der Eecken V, Clippe A, Van Veldhoven PP, Knoops B. 2011. Mitochondrial targeting of peroxiredoxin 5 is preserved from annelids to mammals but is absent in pig Sus scrofa domesticus. Mitochondrion. 11: 973-81.

Van Der Heyden MAG, Kok B, Kouwenhoven EN, Toien O, Barnes BM, Fedorov VG, Efimov IR, Opthof T. 2007. Cloning, sequence analysis and phylogeny of connexin43 isolated from American black bear heart. Dna Sequence 18: 380-384.

van der Laan M, Hutu DP, Rehling P. 2010. On the mechanism of preprotein import by the mitochondrial presequence translocase. Biochim. Biophys. Acta 1803: 732-739.

Van Remmen H, Williams MD, Guo Z, Estlack L, Yang H, Carlson EJ, Epstein CJ, Huang TT, Richardson A. 2001. Knockout mice heterozygous for Sod2 show alterations in cardiac mitochondrial function and apoptosis. Am. J. Physiol Heart Circ. Physiol 281: H1422-H1432.

Van Remmen H, Ikeno Y, Hamilton M et al. 2003. Life-long reduction in MnSOD activity results in increased DNA damage and higher incidence of cancer but does not accelerate aging. Physiol Genomics 16: 29-37.

Van Valkenburgh B, Wayne RK. 2010. Carnivores. Current Biology 20: R915-919.

Van Veldhoven PP, Croes K, Asselberghs S, Herdewijn P, Mannaerts GP. 1996. Peroxisomal beta-oxidation of 2-methyl-branched acyl-CoA esters: stereospecific recognition of the 2S-methyl compounds by trihydroxycoprostanoyl-CoA oxidase and pristanoyl-CoA oxidase. FEBS Lett. 388: 80-84.

Vila C, Seddon J, Ellegren H. 2005. Genes of domestic mammals augmented by backcrossing with wild ancestors. Trends Genet. 21: 214-218.

Vogtle FN, Wortelkamp S, Zahedi RP et al. 2009. Global analysis of the mitochondrial N-proteome identifies a processing peptidase critical for protein stability. Cell 139: 428-439.

Wang MX, Wei A, Yuan J, Clippe A, Bernard A, Knoops B, Murrell GA. 2001. Antioxidant enzyme peroxiredoxin 5 is upregulated in degenerative human tendon. Biochem. Biophys. Res. Commun. 284: 667-673.

Wang X, Huang Y, Lavrov DV, Gu X. 2009. Comparative study of human mitochondrial proteome reveals extensive protein subcellular relocalization after gene duplications. BMC. Evol. Biol. 9: 275.

Watabe S, Kohno H, Kouyama H, Hiroi T, Yago N, Nakazawa T. 1994. Purification and characterization of a substrate protein for mitochondrial ATP-dependent protease in bovine adrenal cortex. J. Biochem. 115: 648-654.

Wattiez R, Hermans C, Bernard A, Lesur O, Falmagne P. 1999. Human bronchoalveolar lavage fluid: two-dimensional gel electrophoresis, amino acid microsequencing and identification of major proteins. Electrophoresis 20: 1634-1645.

Wayne RK, Ostrander EA. 2007. Lessons learned from the dog genome. Trends Genet. 23: 557-567.

Wildman DE, Uddin M, Opazo JC et al. 2007. Genomics, biogeography, and the diversification of placental mammals. Proc. Natl. Acad. Sci. U. S. A 104: 14395-14400.

Williams MD, Van RH, Conrad CC, Huang TT, Epstein CJ, Richardson A. 1998. Increased oxidative damage is correlated to altered mitochondrial function in heterozygous manganese superoxide dismutase knockout mice. J. Biol. Chem. 273: 28510-28515.

Wonsey DR, Zeller KI, Dang CV. 2002. The c-Myc target gene PRDX3 is required mitochondrial homeostasis and neoplastic transformation. Proc. Natl. Acad. Sci. USA. 99: 6649-6654.

Woo HA, Kang SW, Kim HK, Yang KS, Chae HZ, Rhee SG. 2003. Reversible oxidation of the active site cysteine of peroxiredoxins to cysteine sulfinic acid - Immunoblot detection with antibodies specific for the hyperoxidized cysteine-containing sequence. J. Biol. Chem. 278: 47361-47364.

Woo HA, Chae HZ, Hwang SC, Yang KS, Kang SW, Kim K, Rhee SG. 2003. Reversing the inactivation of peroxiredoxins caused by cysteine sulfinic acid formation. Science 300: 653-656.

Woo HA, Jeong W, Chang TS, Park KJ, Park SJ, Yang JS, Rhee SG. 2005. Reduction of cysteine sulfinic acid by sulfiredoxin is specific to 2-cys peroxiredoxins. J. Biol. Chem. 280: 3125-3128.

Woo HA, Yim SH, Shin DH, Kang D, Yu DY, Rhee SG. 2010. Inactivation of peroxiredoxin I by phosphorylation allows localized H(2)O(2) accumulation for cell signaling. Cell 140: 517-528.

Woo, H.A., Rhee, S.G., 2010. Immunoblot detection of proteins that contain cysteine sulfinic or sulfonic acids with antibodies specific for the hyperoxidized cysteine-sequence sequence. In: Das DK (Ed.), Methods in Redox Signaling, Mary Ann Liebert, New Rochelle, NY, pp. 19-23.

Wood-Allum CA, Barber SC, Kirby J et al. 2006. Impairment of mitochondrial anti-oxidant defence in SOD1-related motor neuron injury and amelioration by ebselen. Brain 129: 1693-1709.

Wood ZA, Schroder E, Robin HJ, Poole LB. 2003. Structure, mechanism and regulation of peroxiredoxins. Trends Biochem. Sci. 28: 32-40.

Wu C, Liu T, Chen W et al. 2010. Redox regulatory mechanism of transnitrosylation by thioredoxin. Mol. Cell Proteomics. 9: 2262-2275.

Wu YZ, Manevich Y, Baldwin JL, Dodia C, Yu K, Feinstein SI, Fisher AB. 2006. Interaction of surfactant protein A with peroxiredoxin 6 regulates phospholipase A2 activity. J. Biol. Chem. 281: 7515-7525.

Yagi K, Komura S, Kojima H, Sun Q, Nagata N, Ohishi N, Nishikimi M. 1996. Expression of human phospholipid hydroperoxide glutathione peroxidase gene for protection of host cells from lipid hydroperoxide-mediated injury. Biochem. Biophys. Res. Commun. 219: 486-491.

Yamamoto H, Fukui K, Takahashi H et al. 2009. Roles of Tom70 in import of presequence-containing mitochondrial proteins. J. Biol. Chem. 284: 31635-31646.

Yamamoto T, Matsui Y, Natori S, Obinata M. 1989. Cloning of A Housekeeping-Type Gene (Mer5) Preferentially Expressed in Murine Erythroleukemia-Cells. Gene 80: 337-343.

Yamashita H, Avraham S, Jiang S, London R, Van Veldhoven PP, Subramani S, Rogers RA, Avraham H. 1999. Characterization of human and murine PMP20 peroxisomal proteins that exhibit antioxidant activity in vitro. J. Biol. Chem. 274: 29897-29904.

Yang HY, Kwon J, Cho EJ et al. 2010. Proteomic analysis of protein expression affected by peroxiredoxin V knock-down in hypoxic kidney. J. Proteome. Res. 9: 4003-4015.

Yant LJ, Ran Q, Rao L, Van RH, Shibatani T, Belter JG, Motta L, Richardson A, Prolla TA. 2003. The selenoprotein GPX4 is essential for mouse development and protects from radiation and oxidative damage insults. Free Radic. Biol. Med. 34: 496-502.

Yim SH, Kim YJ, Oh SY, Fujii J, Zhang Y, Gladyshev VN, Rhee SG. 2011. Identification and characterization of an alternatively transcribed form of peroxiredoxin IV that is specifically expressed in spermatids of the postpubertal mouse testis. J. Biol. Chem. 286: 39002-39012.

Yogev O, Pines O. 2011. Dual targeting of mitochondrial proteins: mechanism, regulation and function. Biochim. Biophys. Acta 1808: 1012-1020.

Yoo SE, Chen L, Na R, Liu Y, Rios C, Van RH, Richardson A, Ran Q. 2012. Gpx4 ablation in adult mice results in a lethal phenotype accompanied by neuronal loss in brain. Free Radic. Biol. Med. 52: 1820-1827.

Young JC, Hoogenraad NJ, Hartl FU. 2003. Molecular chaperones Hsp90 and Hsp70 deliver preproteins to the mitochondrial import receptor Tom70. Cell 112: 41-50.

Yuan J, Murrell GA, Trickett A, Landtmeters M, Knoops B, Wang MX. 2004. Overexpression of antioxidant enzyme peroxiredoxin 5 protects human tendon cells against apoptosis and loss of cellular function during oxidative stress. Biochim. Biophys. Acta 1693: 37-45.

Zhang S, Liu Z, Yuan J, Lin M, Sawant MS, Xu A. 2003. Cloning and characterization of AmphiPrxV, a new member of peroxiredoxin family from the amphioxus Branchiostoma belcheri tsingtauense. Curr. Sci. 84: 213-218.

Zhou X, Xu S, Xu J, Chen B, Zhou K, Yang G. 2011. Phylogenomic analysis resolves the interordinal relationships and rapid diversification of the Laurasiatherian mammals. Syst. Biol. 61: 150-164.

Zhou Y, Kok KH, Chun ACS, Wong CM, Wu HW, Lin MCM, Fung PCW, Kung HF, Jin DY. 2000. Mouse peroxiredoxin V is a thioredoxin peroxidase that inhibits p53-induced apoptosis. Bioch. Biophysi. Res. Comm. 268: 921-927.

Zito E, Melo EP, Yang Y, Wahlander A, Neubert TA, Ron D. 2010. Oxidative protein folding by an endoplasmic reticulum-localized peroxiredoxin. Mol. Cell 40: 787-797.

Zitzler J, Link D, Schafer R, Liebetrau W, Kazinski M, Bonin-Debs A, Behl C, Buckel P, Brinkmann U. 2004. High-throughput functional genomics identifies genes that ameliorate toxicity due to oxidative stress in neuronal HT-22 cells. Mol. Cell. Proteom. 3: 834-840.

VI. Annexes

Annex 1: Amino acid sequence alignment of human PRDX5 and mammalian orthologs

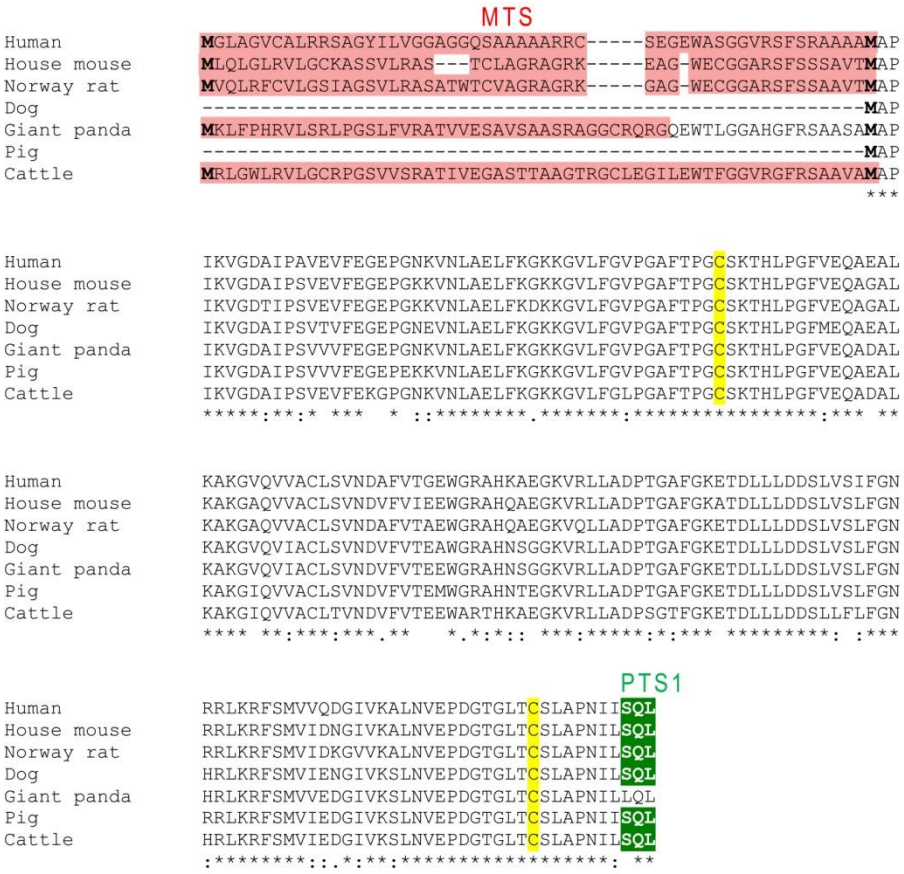

Supplementary figure 1. ClustalX 2.0.7 amino acid sequence alignment of human PRDX5 and mammalian orthologs. Dots (.) and double dots (:) indicate conservative substitutions, asterisks (*) indicate identities. Conservative cysteines, peroxisomal targeting sequences (PTS1) and TargetP v1.1 predicted MTS are highlighted in yellow, green and red respectively. Methionines (bold) encoded by the two alternative initiation codons are indicated. GenBank accession numbers are as follows: NP_036226 (Human, *Homo sapiens*); NP_036151 (House mouse, *Mus musculus*); NP_446062 (Norway rat, *Rattus norvegicus*); XP_533241 (Dog, *Canis lupus familiaris*); XM_002916664 (Giant panda, *Ailuropoda melanoleuca*); NP_999309 (Pig, *Sus scrofa*); NP_777174 (Cattle, *Bos taurus*).

Annex 2: Subcellular fractionation of pig liver by differential centrifugation

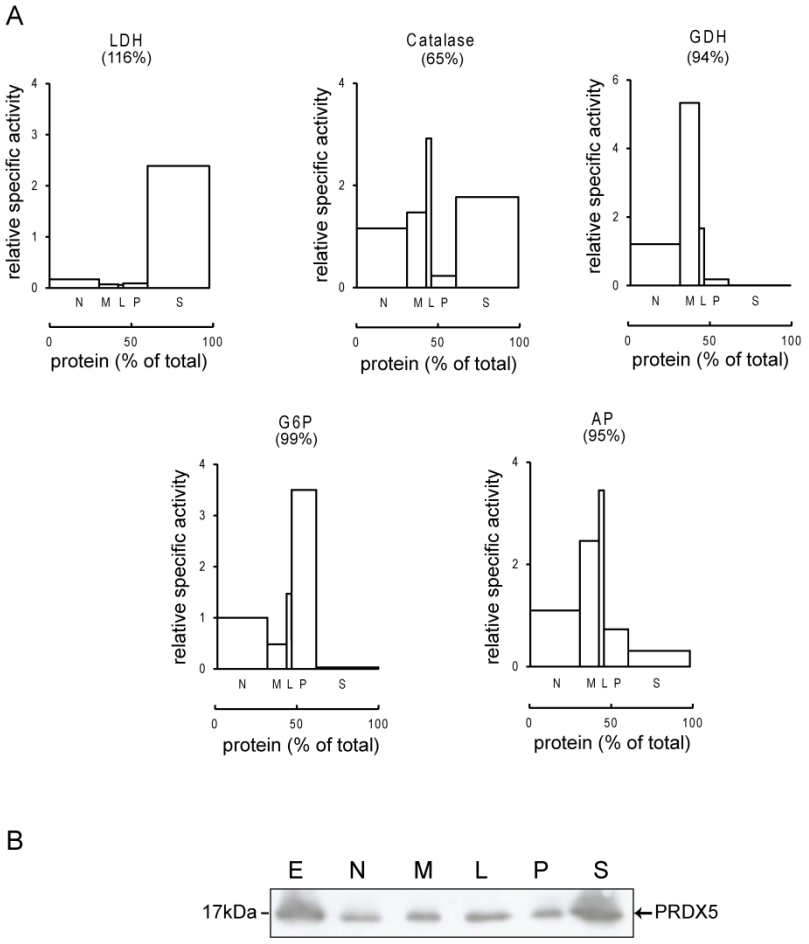

Supplementary figure 2. Pig liver homogenate was differentially centrifuged to obtain a post-nuclear fraction (E), a nuclear fraction (N), a heavy mitochondrial fraction (M), a light mitochondrial fraction (L), a microsomal fraction (P) and a cytosolic fraction (S). **(A)** Pig crude fractions were analyzed for enzyme markers. LDH, catalase, GDH, G6P and AP were cytosol, peroxisomes, mitochondria, endoplasmic reticulum and lysosome markers respectively. Enzymatic activities are expressed as relative specific activities, defined as the % of total enzymatic activity/ the % of total protein. Recoveries for the marker enzymes are indicated under brackets at the top of the graphic. **(B)** Immunoblot analysis of PRDX5 in pig crude fractions was performed with polyclonal antibodies directed against human PRDX5. 40μg of protein from each fraction were loaded. GDH: glutamate dehydrogenase; LDH: lactate dehydrogenase; G6P: glucose-6-phosphatase; AP: acid phosphatase.

Annex 3: Subcellular fractionation of dog liver by differential centrifugation

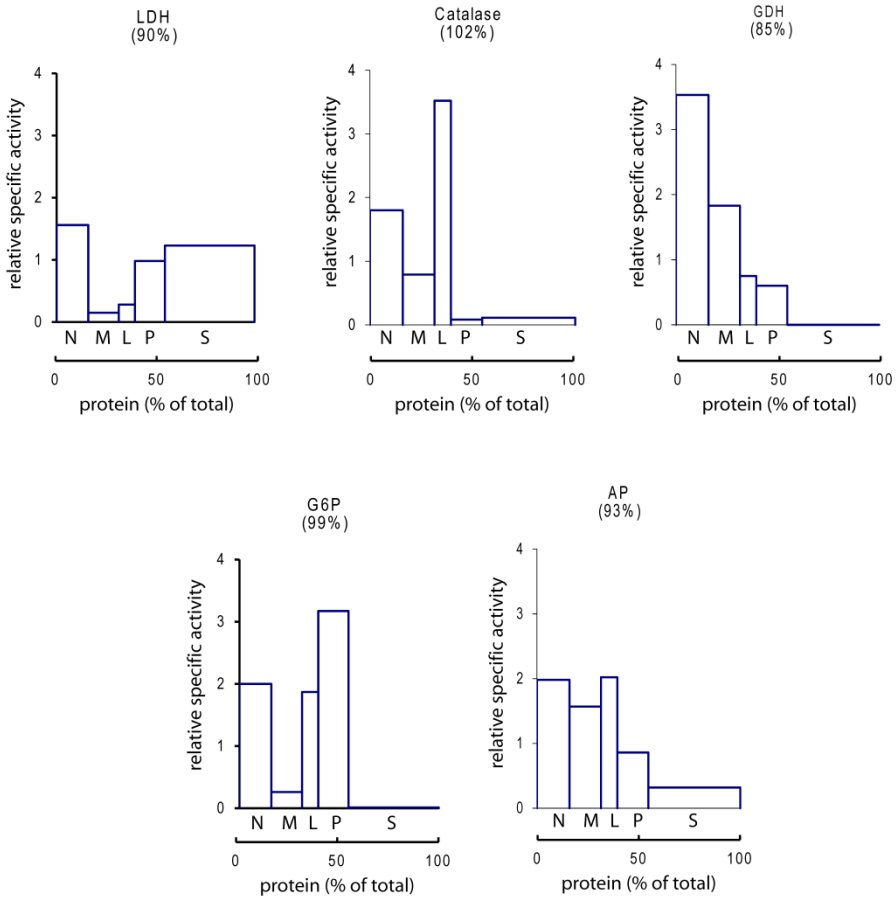

Supplementary figure 3. Dog liver homogenate was differentially centrifuged to obtain a post-nuclear fraction (E), a nuclear fraction (N), a heavy mitochondrial fraction (M), a light mitochondrial fraction (L), a microsomal fraction (P) and a cytosolic fraction (S). Dog crude fractions were analyzed for enzyme markers. LDH, catalase, GDH, G6P and AP were cytosol, peroxisomes, mitochondria, endoplasmic reticulum and lysosome markers respectively. Enzymatic activities are expressed as relative specific activities, defined as the % of total enzymatic activity/ the % of total protein. Recoveries for the marker enzymes are indicated under brackets at the top of the graphic.

Annex 4: Analysis of enzyme markers in dog Percoll fractions

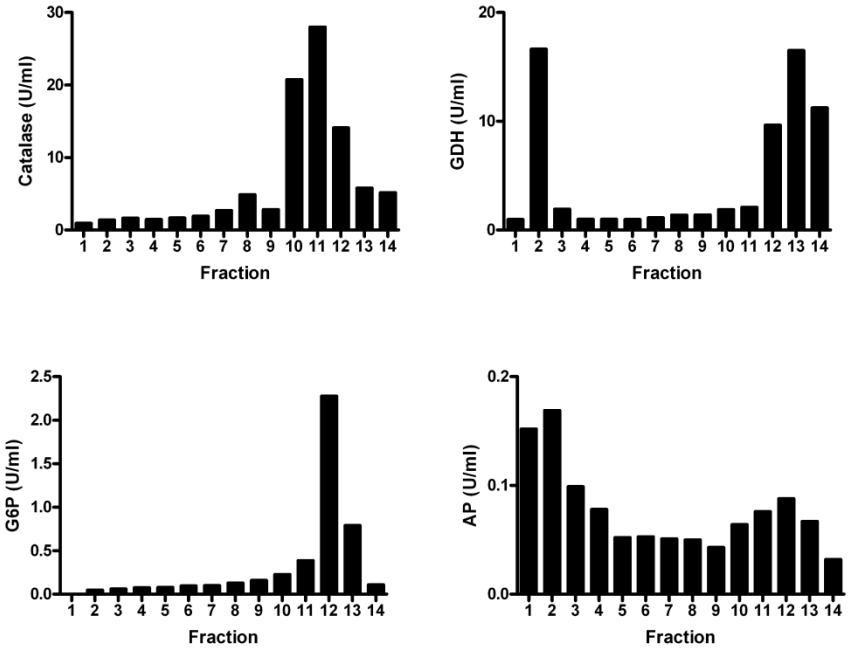

Supplementary figure 4. Dog liver homogenate was differentially centrifuged to obtain a post-nuclear fraction (E), a nuclear fraction (N), a heavy mitochondrial fraction (M), a light mitochondrial fraction (L), a microsomal fraction (P) and a cytosolic fraction (S). L-fraction was further separated by centrifugation through a Percoll gradient. Percoll fractions were analyzed for enzyme markers. Catalase, GDH, G6P and AP were peroxisomes, mitochondria, endoplasmic reticulum and lysosome markers respectively. Based on enzyme marker distribution, fractions 2 and 10 were chosen to represent mitochondrial and peroxisomal fractions, respectively.

Annex 5: PRDX5 may be absent in peroxisomes of human cells

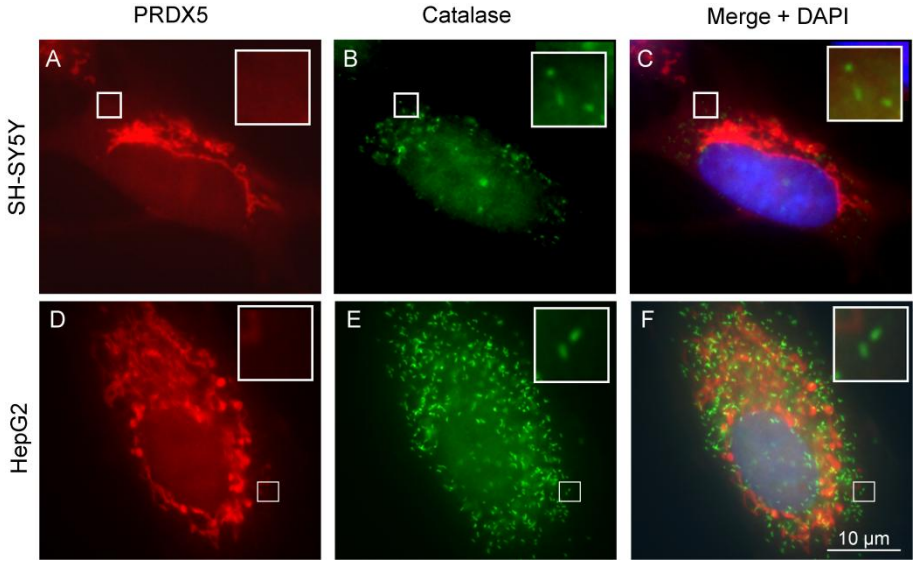

Supplementary figure 5. Detection of PRDX5 (A and D) and peroxisomal catalase (B and E) by immunofluorescence in human SH-SY5Y (A-C) and HepG2 cells (D-F). Nuclei were labelled with DAPI. Insets on the right corner represent magnification of outlined areas.

Annex 6: Kozak consensus in mouse and rat *PRDX5*

A. Kozak consensus sequence

B. House mouse PRDX5 mRNA (5′ region)

```
cgggugggcugcggcagcggggcgggu AUG cuacagcuggggcuucgaguccugggcugc
                            M  L  Q  L  G  L  R  V  L  G  C
aaagccaguucugugcuccgugcaucgacgugcuuggcaggcagagcaggccggaaagaa
 K  A  S  S  V  L  R  A  S  T  C  L  A  G  R  A  G  R  K  E
gcagguugggaguguggcggagcccgcagcuucagcagcuccgcggugacc AUG gccccg
 A  G  W  E  C  G  G  A  R  S  F  S  S  S  A  V  T  M  A  P
```

Norway rat PRDX5 mRNA (5′ region)

```
ugcggcggcggggcgggc AUG guccagcugagguuuugcguccuaggcagcauagccgga
                   M  V  Q  L  R  F  C  V  L  G  S  I  A  G
ucggugcuccgugcaucggcuacuuggacgugcguggcaggcagagcaggccggaaagga
 S  V  L  R  A  S  A  T  W  T  C  V  A  G  R  A  G  R  K  G
gcagguugggaguguggugggcccgcagcuucagcagugccgcggugacu AUG gccccg
 A  G  W  E  C  G  G  A  R  S  F  S  S  A  A  V  U  M  A  P
```

Supplementary figure 6. Kozak consensus in mouse and rat PRDX5. (A) Kozak consensus sequence (Kozak, 1978)[From (Iacono et al. 2005)]. **(B)** 5′ sequence of house mouse and Norway rat PRDX5 mRNA. Alternative translation initiation codons are indicated in bold and are underlined. Nucleotides matching the Kozak consensus sequence are highlighted in grey. Genbank accession numbers are NM_012021 and NM_053610 for house mouse and Norway rat respectively.

Annex 7: Abolition of PRDX5 mitochondrial targeting sequence in pig

Supplementary figure 7. ClustalX 2.0.7 nucleotidic sequence alignment of pig and bovine PRDX5 exon I. Asterisks (*) indicate identities. Translation initiation codons, sequences encoding MTS and encoding the mature part of PRDX5 are highlighted in black, red and blue respectively. Gaps are boxed. Genbank accession numbers for pig and bovine are Gene ID: 397273 and Gene ID: 282885, respectively. MTS: mitochondrial targeting sequence; UTR: untranslated region. Pig, *Sus scrofa*; Bovine, *Bos taurus*.